SIMPLIFIED NUMERICAL MODELS FOR THE GENERATION OF SYNTHETIC REFLECTION PROFILING SEISMOGRAMS AND SYNTHETIC REFLECTION/REFRACTION SEISMOGRAMS

by

Charles David Lodge

United States
Naval Postgraduate School

THESIS

SIMPLIFIED NUMERICAL MODELS FOR THE GENERATION OF SYNTHETIC REFLECTION PROFILING SEISMOGRAMS AND SYNTHETIC REFLECTION/REFRACTION SEISMOGRAMS

by

Charles David Lodge

April 1970

Simplified Numerical Models for the Generation of Synthetic Reflection Profiling Seismograms and Synthetic Reflection/Refraction Seismograms

by

Charles David Lodge
Lieutenant Commander, United States Navy
B.A., Rice University, 1962

Submitted in partial fulfillment of the
requirements for the degree of

MASTER OF SCIENCE IN OCEANOGRAPHY

from the
NAVAL POSTGRADUATE SCHOOL
April 1970

ABSTRACT

Two numerical models were developed which generate synthetic seismograms in formats similar to those of records obtained in field exploration. The models solve the hyperbolic wave equations in one and two dimensions by finite difference approximations in initially undeformed solution domains of transversely-isotropic layered media subjected to a time varying, dilatational forcing stress applied at the surface. A velocity attenuation term was included in the models to inhibit strong boundary reflections.

The one-dimensional model produces synthetic reflection profiling seismograms for arbitrary horizontal or dipping layers. The two-dimensional model generates synthetic reflection/refraction seismograms for horizontal layered media with arbitrary distribution of wave velocities, Poisson's ratio and density. Several sample records were produced for some representative velocity structures. The synthetic seismograms were interpreted and gross correlation was carried out as if they were actual field records.

TABLE OF CONTENTS

LIST OF TABLES

LIST OF FIGURES

ACKNOWLEDGEMENTS

The author wishes to extend his sincere appreciation to Professor Robert S. Andrews who provided invaluable assistance in delimiting the scope of the problem and in interpretation of the results. Appreciation is also extended to the staff of the Naval Postgraduate School Computer Facility, especially Mr. David F. Norman, for assistance in running and debugging the programs. Particular thanks are due to the author's wife, Diana, whose moral support and secretarial skills aided the project immeasurably.

I. INTRODUCTION

A major problem in exploration geology is the determination of structural relationships for areas in which the rocks cannot be directly examined. This is usually a subjective process, involving the extrapolation of lithologic facies from a region where control is available, such as surface outcrops, mines or wells, across an unknown or inaccessible area to another point with known structure. Indications of subsurface structure, including magnetic, seismic and gravity measurements as well as interpretation of surface morphological features, are frequently relied upon to aid this process.

The problem becomes particularly acute in oceanic regions where the only available control may be continental outcrops several hundreds of miles away, a few bottom grab samples and shallow sediment cores and a rough bottom topography. Remote measurements may then become the only method of initial structure determination.

Frequent use is made of the manner in which the ocean bottom and sub-bottom rocks reflect and transmit acoustic or seismic energy, not only for the correlation of near-shore with on shore structures, but also for initial determination of sub-bottom structures. When conducting seismic exploratory operations, the information obtained is usually presented as a two-dimensional graph (seismogram) on which three variables are shown. These variables are: horizontal distance, time and intensity of energy received. Depth information may be inferred from the time scale with a known or assumed vertical distribution of sonic velocity. A high level of intensity is usually assumed to represent a point or surface at which the physical

parameters of the media change more or less abruptly, reflecting energy or providing a surface along which energy might be propagated.

Interpretation of the seismograms and the development of a subsurface structure can be aided by the use of a mathematical model of the supposed structure which would produce a synthetic seismogram. The synthetic seismogram could be compared with the field record for correlation.

This paper presents the development of two numerical models which produce synthetic seismograms for layered media subjected to an initial time varying, compressional (dilatational) stress input applied at the surface. The models were designed to have fairly wide variability while remaining simple enough to preclude the use of inordinate computer time and storage requirements. The one-dimensional model produces a reflection profiling seismogram. It is applicable to the case of vertically incident dilatational waves reflected and transmitted by arbitrary bottom profile and sub-bottom layered structure of horizontal or dipping interfaces. The two-dimensional model yields a set of seismograms applicable to a reflection/refraction problem where the receivers are distributed in a horizontal array. Both dilatational and shear stresses are treated. The region modeled is one of horizontal layered media with arbitrary distribution of shear and dilatational wave velocities and of density.

No attempt was made here to include the wide variability of possible media which is an integral part of the large SLAM (Stress waves in LAyered Media) code model developed at the Illinois Institute of Technology (IIT) [Constantino 1969] primarily to treat the neighborhood of high energy (nuclear) explosively generated ground shocks.

The IIT model has the capability of simulating a wide variety of conditions but requires a large amount of computing time and space in order to produce a single trace. It is felt that the two models presented here have a greater applicability to marine and terrestrial seismic exploration problems.

These models were developed on the basis of numerical approximations to the solutions of the wave equations in one and two dimensions by finite difference methods. The computer programs were written in the FORTRAN IV language and were run on a dual IBM 360/67 system. The plotting subroutines used to drive a CALCOMP 765 plotter were prepared by the staff of the United States Naval Postgraduate School Computer Facility [1969].

II. THE SEISMIC REFLECTION PROFILING MODEL

The problem of synthetic seismic profile generation was approached as one of repeated transmission of normally incident longitudinal (dilatational) disturbances through transversely-isotropic media. The seismogram was developed by changing the velocity structure in the solution domain between pulse transmissions, corresponding to a change in position of the shot point as the profiling vessel moves across an area of changing water depth and sub-bottom structure. The solutions are presented as successive traces as though from a pressure hydrophone located at any depth below the shot point.

A. THE MATHEMATICAL MODEL

It was assumed that the wave velocity (C) is continuous throughout the domain and either varies linearly with depth (x) or is constant. Additionally, it was assumed that in transition zones, where the wave velocity does change, density remains constant. Under these assumptions, the equation of motion in one dimension for dilatational waves can be written (modified from Wolf [1937]):

$$E: \quad \frac{\partial^2 u}{\partial t^2} = \frac{\partial}{\partial x}\left(C^2 \frac{\partial u}{\partial x}\right) + A \frac{\partial u}{\partial t}, \tag{1}$$

where u is longitudinal particle displacement and A is a velocity attenuation parameter which is a function of x. Carrying out the indicated differentiation of the right side of equation (1) yields:

$$E: \quad \frac{\partial^2 u}{\partial t^2} = C^2 \frac{\partial^2 u}{\partial x^2} + 2C \frac{\partial C}{\partial x} \frac{\partial u}{\partial x} + A \frac{\partial u}{\partial t}. \tag{2}$$

Four collateral conditions are required in order to complete a well-posed problem. The following conditions were selected:

initial conditions:

I1: $$u(x,0) = 0 \,, \tag{3}$$

I2: $$u_t(x,0) = 0 \,, \tag{4}$$

boundary conditions:

B1: $$u(L,t) = 0 \,. \tag{5}$$

B2: $$u_x(0,t) = F(t) \,, \quad t \leq t_1 \,, \tag{6a}$$

$$u_x(0,t) = 0 \,, \quad t > t_1 \,, \tag{6b}$$

where L is the distance to the lower boundary.

The initial conditions allow the solution domain to be initially undeformed and at rest. The first boundary condition requires that displacements are zero for all time at the lower boundary, which then becomes perfectly reflective. The second boundary condition allows a variable stress to be applied to the upper boundary for $t \leq t_1$. For $t > t_1$, normal stresses are not transmitted across this boundary. It then becomes a free surface.

The second term on the right side of equation (1), $A\frac{\partial u}{\partial t}$, represesents an attenuation factor, dependent on depth and particle velocity, which was used to reduce the magnitude of the disturbance in the lower regions of the domain so that reflections from the lower boundary would not mask late arriving multiple reflections from points nearer to the surface. The function A(x) is assumed to be zero in the region from which reflections are to be studied.

B. THE SOLUTION DOMAIN

The solution domain (Fig. 1) is divided by N equally spaced mesh points into N-1 subintervals each of length δx. A sample wave velocity distribution is shown in the figure. The upper boundary (x = 0) is shown on the left. In the region $0 \leqslant x \leqslant x_1$, the wave velocity is constant and equal to C1. For $x_2 \leqslant x \leqslant L$, the velocity is equal to C2. In the transition zone, $x_1 < x < x_2$, the velocity varies linearly from C1 to C2.

The time-depth mesh is an array of N by M mesh points. Each rectangular mesh area is then of size δx by δt. This mesh is the full solution domain and the objective of the model is to find a solution of equation (2) at each mesh point under the collateral conditions, equations (3) through (6).

C. THE DIFFERENCE EQUATIONS

A central difference form for each of the partial derivatives in equation (2) can be written in terms of the (i,j) mesh point [Smith 1965] . Figure 2 shows the (i,j) and neighboring mesh points. The required derivatives, in central difference form, become:

$$\frac{\partial v}{\partial t} \doteq \frac{v_{i,j+1} - v_{i,j-1}}{2\delta t} \quad ; \qquad \frac{\partial^2 v}{\partial t^2} \doteq \frac{v_{i,j+1} - 2v_{i,j} + v_{i,j-1}}{\delta t^2} \quad ;$$

$$\frac{\partial v}{\partial x} \doteq \frac{v_{i+1,j} - v_{i-1,j}}{2\delta x} \quad ; \qquad \frac{\partial^2 v}{\partial x^2} \doteq \frac{v_{i+1,j} - 2v_{i,j} + v_{i-1,j}}{\delta x^2} \quad ;$$

$$\frac{\partial c}{\partial x} \doteq \frac{c_{i+1} - c_{i-1}}{2\delta x} \quad .$$

Figure 1. The solution domain

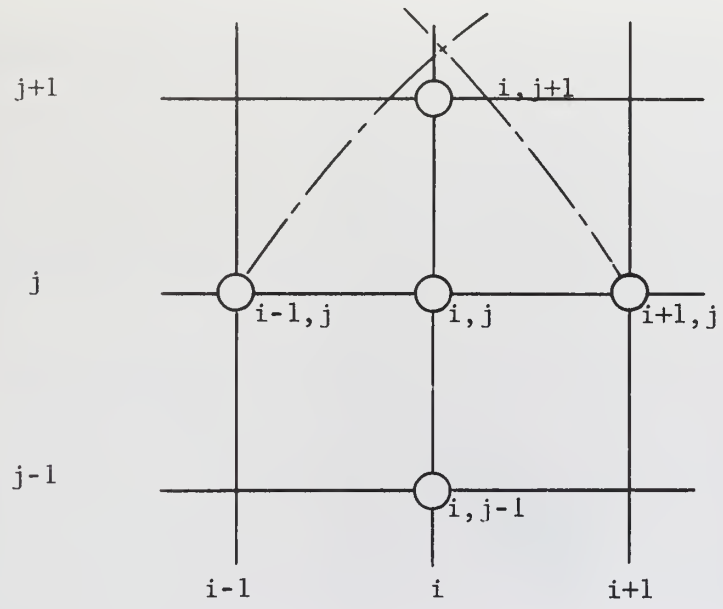

Figure 2. Mesh detail.

Substituting these into equation (2) gives the difference equation of motion for the (i,j) mesh point:

$$\frac{u_{i,j+1} - 2u_{i,j} + u_{i,j-1}}{\delta t^2} = c_i^2 \left(\frac{u_{i+1,j} - 2u_{i,j} + u_{i-1,j}}{\delta x^2} \right)$$

$$+ 2c_i \left(\frac{c_{i+1} - c_{i-1}}{2\delta x} \right) \left(\frac{u_{i+1,j} - u_{i-1,j}}{2\delta x} \right) + A_i \left(\frac{u_{i,j+1} - u_{i,j-1}}{2\delta t} \right) . \qquad (7)$$

The collateral conditions become:

I1: $$u_{i,1} = 0 , \qquad (8)$$

I2: $$\frac{u_{i,2} - u_{i,0}}{2\delta t} = 0 . \qquad (9)$$

B1: $$u_{N,j} = 0 . \qquad (10)$$

B2: $$\frac{u_{2,j} - u_{0,j}}{2\delta x} = F_j . \qquad (11)$$

where $F_j = F(t)$, $0 \leqslant t \leqslant t_1$,

$F_j = 0$, $t > t_1$.

Solving equation (7) for $u_{i,j+1}$ gives:

E: $$u_{i,j+1} = \left[2u_{i,j} \left(1 - c_i^2 R^2 \right) + u_{i+1,j} \left(c_i^2 R^2 + \tfrac{1}{2} c_i (c_{i+1} - c_{i-1}) R^2 \right) \right.$$

$$+ u_{i-1,j} \left(c_i^2 R^2 - \tfrac{1}{2} c_i (c_{i+1} - c_{i-1}) R^2 \right)$$

$$\left. - u_{i,j-1} \left(1 + \tfrac{1}{2} A_i \delta t \right) \right] / \left[1 - \tfrac{1}{2} A_i \delta t \right] , \qquad (12)$$

where: $$R^2 = \left(\frac{\delta t}{\delta x} \right)^2 .$$

Writing equation (12) for j=1 and substituting $u_{i,0}$ from equation (9) yields the initial conditions:

I1: $$u_{i,1} = 0 . \qquad (8)$$

I2: $$u_{i,2} = 0 . \qquad (13)$$

Writing equation (12) for i=1 and substituting $u_{o,j}$ from equation (11) yields the boundary conditions:

B1: $$u_{N,j+1} = 0 \quad , \tag{10a}$$

B2: $$u_{1,j+1} = \left[2u_{1,j}\left(1 - C_1^2R^2\right) + 2u_{2,j}\left(C_1^2R^2\right)\right.$$

$$\left. - u_{1,j-1}\left(1 + \tfrac{1}{2}A_1\delta t\right) + F_j\delta t^2\left(\frac{C_1^2}{\delta x}\right)\right] \Big/ \left[1 - \tfrac{1}{2}A_1\delta t\right] \quad . \tag{14}$$

The equations (12), (8), (13), (10a) and (14) then form a well-posed problem for numerical solution. Initially, the j=1 and j=2 rows are set to zero following equations (8) and (13). The j+1 row can then be solved utilizing equation (10a) for the lower boundary (i=N), (14) for the upper boundary (i=1) and (12) for the interior points. Note that the value of u anywhere along the interior of the j+1 row is dependent only on the values of u at three points along the j row and one on the j-1 row (shown as circles in Fig. 2).

D. STABILITY AND CONVERGENCE

1. Stability

Because of the large number of arithmetic operations involved (approximately 10^9 for the solution spaces used), it is necessary to insure that there is a stable decay of errors introduced in the various computations. Studies of the stability of the centered difference formulation of the basic wave equation:

$$\frac{\partial^2 u}{\partial t^2} = C^2\frac{\partial^2 u}{\partial x^2} \quad , \tag{15}$$

have been carried out by several investigators [Smith 1965] . Smith investigated the stability by the Fourier series method and showed

that the centered difference formulation is stable for the mesh ratio:

$$\frac{\delta t}{\delta x} \leq \frac{1}{C} . \tag{16}$$

The addition of the velocity gradient and velocity attenuation terms in equation (2) alters the stability conditions somewhat. A large velocity gradient, approaching discontinuous velocity change, generates instability in the gradient region. Investigation of the stability conditions showed that if the condition:

$$\Delta C_i = C_{i+1} - C_{i-1} \leq C_i , \tag{17}$$

were imposed on the gradient regions, the requirement on the mesh ratio [equation (16)] becomes:

$$\frac{\delta t}{\delta x} \leq \frac{0.89}{C} . \tag{18}$$

The addition of a negative attenuation term tends to decrease the right side of equation (18). This would lead to a more stringent requirement on the mesh ratio. This effect was found to be quite small for the values of A(x) necessary to damp lower boundary reflections. Empirically, it was found that stability would be assured by requiring that:

$$\frac{\delta t}{\delta x} \leq \frac{0.95}{C} . \tag{19}$$

2. Convergence

A finite difference scheme is said to be convergent if the exact solution of the difference equations approaches the exact solution of the partial differential equations as δx and δt

approach zero together. Forsythe and Wasow [1967] have shown that convergence of a finite difference scheme such as equation (12) with boundary conditions such as equations (8), (13), (10a) and (14) is convergent as long as the mesh ratio is such that the (i, j+1) mesh point lies within the intersection of the characteristics through the (i-1, j) and (i+1, j) mesh points (see Fig. 2). The equation defining the characteristics for equation (2) is:

$$\left(\frac{dx}{dt}\right)^2 = C^2 \quad . \tag{20}$$

This leads to:

$$\frac{dx}{dt} = \pm C \quad . \tag{21}$$

Convergence is then assured for:

$$\frac{\delta t}{\delta x} \leq \frac{1}{C} \quad . \tag{16}$$

It is apparent then that as long as equation (19) holds, the finite difference formulation will be both stable and convergent.

E. DESCRIPTION OF THE PROGRAM

The program requires 140K bytes of main core storage. An average run with a 251x1800 mesh grid with 41 shot points requires approximately 13 min of main run time exclusive of output time required for the plotting subroutines.

1. Distribution parameters

The advantage of this model lies in the wide variability of the conditions which may be easily simulated. The primary parameters used to model various conditions are the distribution parameters. They are:

a. wave velocity distribution, C(x,t),

b. forcing function, F(t),

c. attenuation parameter, A(x).

The forcing function and the attenuation parameter are put into the model as single-valued, continuous, polygonal line functions of the indicated dependent variable. The wave velocity is put into the model as a two-dimensional array of points which describe the depths to isovelocity layers at successive horizontal stations. Figure 3 shows a sample distribution of isovelocity horizons with horizontal stations and shot points indicated. Horizontal station distances and the velocity defining array for this sample are shown in Tables I and II. At each shot point, the wave velocity is a single-valued, continuous polygonal line function of depth. An example of wave velocity distribution at a single shot point is shown in Fig. 4 along with a sample attenuation parameter and forcing function. The polygons for A(x) and F(t) are defined in Tables III and IV.

2. Numerical parameters

The numerical parameters, which remain constant throughout the problem, are used to control the computation of the distribution parameters and to set the arrangement and size of the solution domain. They are:

a. mesh size in the x direction, (DX),

b. mesh size in the t direction, (DT),

c. horizontal distance between successive solution stations (shot point spacing), (DK),

d. number of total x mesh points, (N),

e. number of total t mesh points, (M),

f. number of solution stations, (KK),

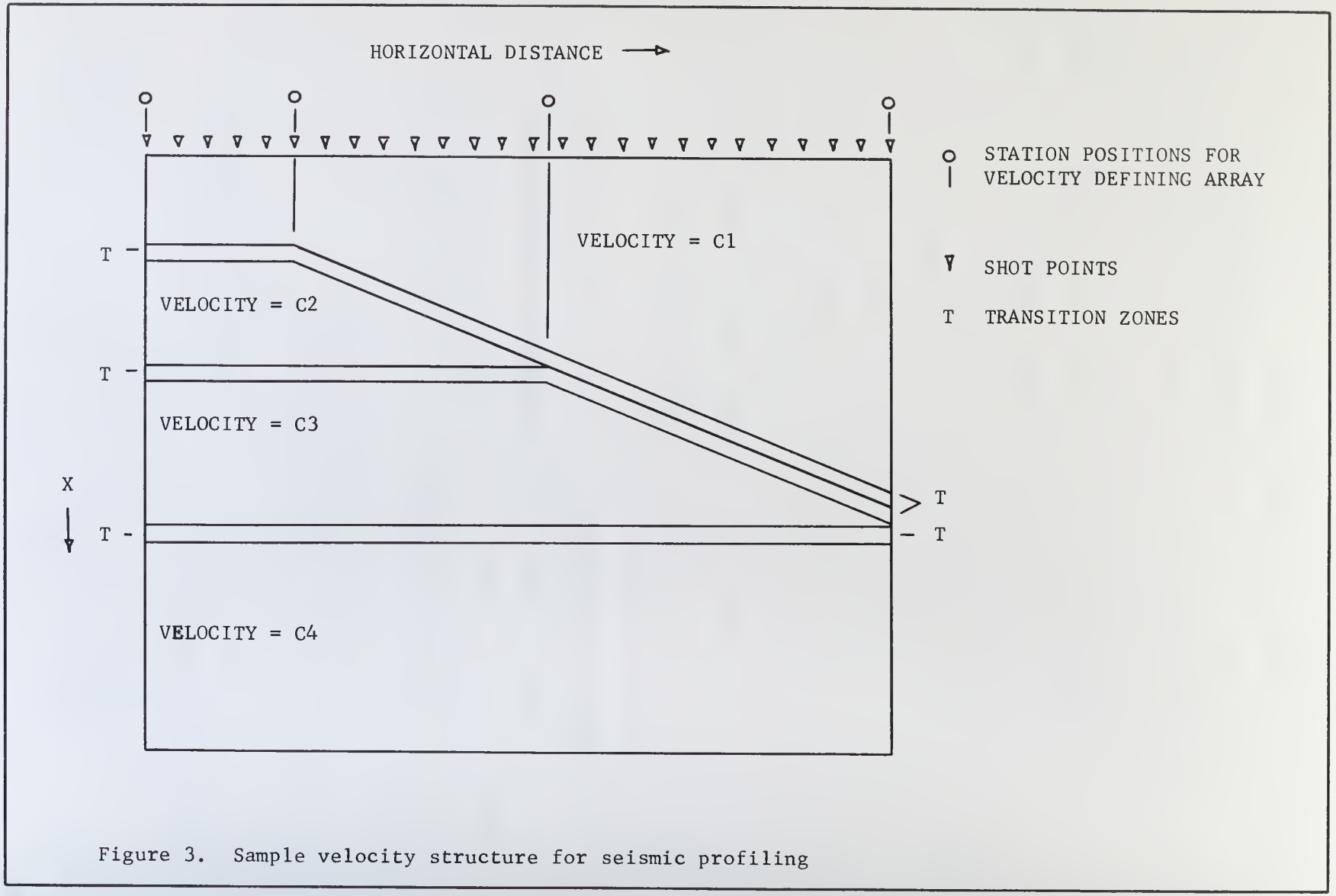

Figure 3. Sample velocity structure for seismic profiling

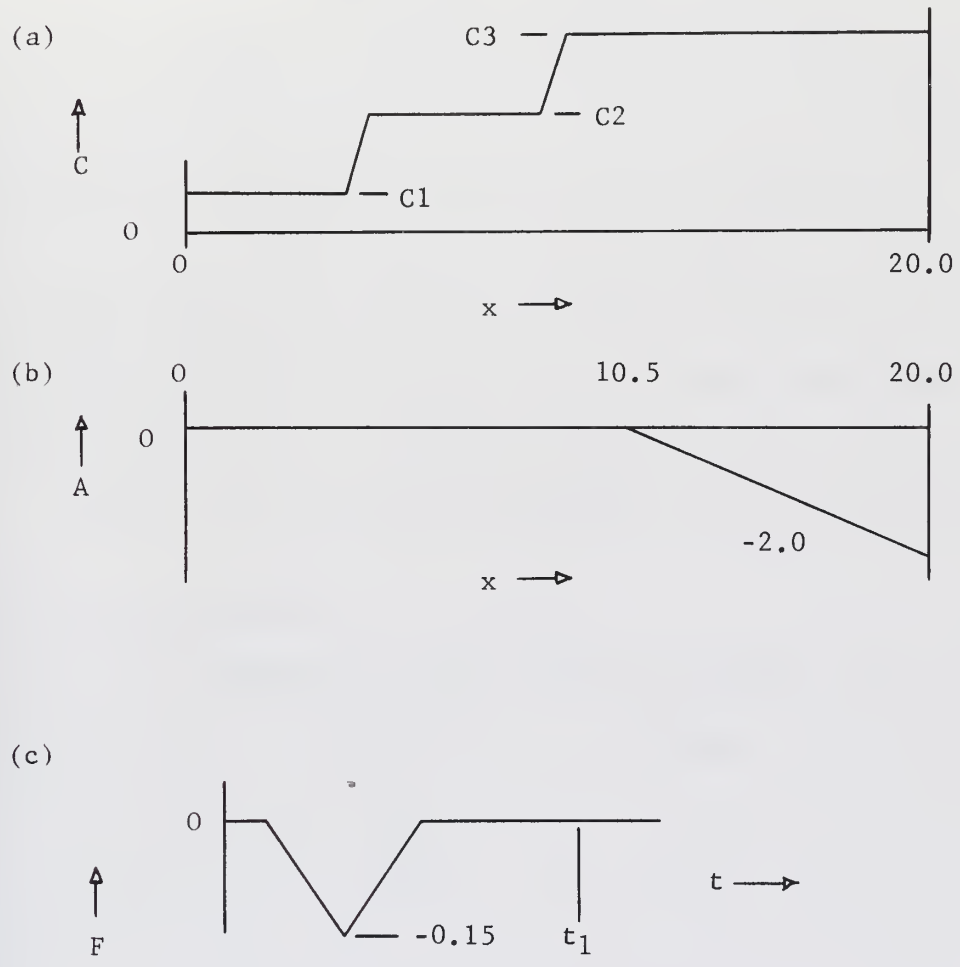

Figure 4. Sample distribution parameters

(a) Wave velocity at one shot point.
(b) Attenuation parameter.
(c) Forcing function.

g. number of points defining the distribution parameter polygons:

(1) wave velocity polygon, (NC),

(2) attenuation parameter polygon, (NA),

(3) forcing function polygon, (NF),

h. number of horizontal stations in the velocity defining array, (NG),

i. mesh point at which the output stress is to be measured, (IP),

j. horizontal distance to the first shot point, (EEE).

Additional numerical parameters are put into the program which control the size, scale and arrangement of the output traces. For details of their use see the explanatory notes in the program.

Table I.

Sample horizontal station distances

Station	Distance
1	0.0
2	2.0
3	10.5
4	20.0

Table II.

Sample velocity defining array

	Station Numbers 1	2	3	4	Velocity
Depth to isovelocity horizons	0.0	0.0	0.0	0.0	C1
	2.0	2.0	4.5	9.8	C1
	2.2	2.2	4.7	10.0	C2
	4.7	4.7	4.7	10.0	C2
	4.9	4.9	4.9	10.2	C3
	20.0	20.0	20.0	20.0	C3

Table III.

Sample attenuation parameter polygon

Depth	A(x)
0.0	0.0
10.5	0.0
20.0	-2.0

Table IV

Sample forcing function polygon

Time	F(t)
0.0	0.0
0.10	0.0
0.40	-0.15
0.70	0.0
2.0	0.0

F. SCALING THE PROBLEM

All wave velocities and depths were put into the model in non-dimensional form. The wave velocity in the upper layer and the depth to the first transition zone were chosen as the definitive values for non-dimensionalizing the problem. Non-dimensional time was then determined by these values through the mesh ratio. Practically, the scale of the problem is determined by the wave velocity values and one of the mesh sizes. In general, the wave velocity is entered as C distance units per time unit. For a mesh ratio of:

$$\frac{\delta t}{\delta x} = \frac{0.025}{0.10} = \frac{1}{4} \quad . \tag{22}$$

the stability condition [equation (19)] allows the wave velocity to vary from 0.0 to 3.4 distance units per time unit. If a value of C of 0.8 is to represent dilatational wave velocity in water (1.5 km/sec),

then the scale of the problem would depend on a choice of either time or depth mesh size, chosen in view of the definition desired. Table V shows some scales where the time mesh size was specified.

Table V.

Scales available for C = 0.8 = 1.5 km/sec

Numerical parameters: N = 251, M = 2000

Mesh Size x (m)	Mesh Size t (sec)	Distance Unit (m)	Time Unit (sec)	Seismogram Length (sec)	Depth to Lower Boundary (m)
187.5	.025	1875	1.0	50	46800
75	.010	750	0.4	20	18750
18.75	.0025	187.5	0.1	5	4680
7.5	.001	75	0.04	2	1875
1.875	.00025	18.75	0.01	0.5	468
0.75	.0001	7.5	0.004	0.2	187.5

III. THE REFLECTION/REFRACTION MODEL

Synthetic reflection/refraction seismogram generation requires solution of the wave equation in at least two dimensions. A rectangular solution space was chosen with three rigid, reflective boundaries and one free boundary corresponding to the air-water or air-ground interface. In order to produce a model with wide variability as well as one that may be easily manipulated without inordinate computer time and storage requirements, it was assumed that the media in the solution space is horizontally isotropic. The y-derivatives of density and Lamé's constants (and hence of shear and dilatational wave velocities) will then be zero.

A. THE MATHEMATICAL MODEL

It was assumed that density, ρ, and Lame's constants, λ and μ, are continuous throughout the solution domain. Further, it was assumed that density and the dilatational and shear wave velocities, C and S, are either constant or vary linearly with depth. Under these assumptions, the equations of motion in two dimensions for the propagation of shear and dilatational disturbances can be written (modified from Officer [1958] and Takeuchi [1966]):

E1:
$$\rho\frac{\partial^2 u}{\partial t^2} = \frac{\partial}{\partial x}\left[\lambda\left(\frac{\partial u}{\partial x}+\frac{\partial v}{\partial y}\right)+2\mu\frac{\partial u}{\partial x}\right] + \frac{\partial}{\partial y}\left[\mu\left(\frac{\partial v}{\partial x}+\frac{\partial u}{\partial y}\right)\right] + B\frac{\partial u}{\partial t}\ , \tag{23}$$

E2:
$$\rho\frac{\partial^2 v}{\partial t^2} = \frac{\partial}{\partial y}\left[\lambda\left(\frac{\partial u}{\partial x}+\frac{\partial v}{\partial y}\right)+2\mu\frac{\partial v}{\partial y}\right] + \frac{\partial}{\partial x}\left[\mu\left(\frac{\partial v}{\partial x}+\frac{\partial u}{\partial y}\right)\right] + B\frac{\partial u}{\partial t}\ , \tag{24}$$

where u and v are the particle displacements in the x and y directions and B is a velocity attenuation factor. The stresses are:

Dilatational stress: $\lambda\left(\frac{\partial u}{\partial x} + \frac{\partial v}{\partial y}\right)$.

Shear stress: $\mu\left(\frac{\partial v}{\partial x} + \frac{\partial u}{\partial y}\right)$.

These stresses are computed in the program and are used, in addition to displacements, to form the seismograms.

Carrying out the indicated differentiation on the right side of equations (23) and (24) and collecting terms yields:

E1: $$\frac{\partial^2 u}{\partial t^2} = \left(\frac{\lambda+2\mu}{\rho}\right)\frac{\partial^2 u}{\partial x^2} + \left(\frac{\lambda+\mu}{\rho}\right)\frac{\partial^2 v}{\partial x \partial y} + \frac{\mu}{\rho}\frac{\partial^2 u}{\partial y^2}$$

$$+ \frac{1}{\rho}\frac{\partial \lambda}{\partial x}\left(\frac{\partial u}{\partial x} + \frac{\partial v}{\partial y}\right) + \frac{2}{\rho}\frac{\partial \mu}{\partial x}\frac{\partial u}{\partial x} + \frac{B}{\rho}\frac{\partial u}{\partial t} \quad , \tag{25}$$

E2: $$\frac{\partial^2 v}{\partial t^2} = \left(\frac{\lambda+2\mu}{\rho}\right)\frac{\partial^2 v}{\partial y^2} + \left(\frac{\lambda+\mu}{\rho}\right)\frac{\partial^2 u}{\partial x \partial y} + \frac{\mu}{\rho}\frac{\partial^2 v}{\partial x^2}$$

$$+ \frac{1}{\rho}\frac{\partial \mu}{\partial x}\left(\frac{\partial v}{\partial x} + \frac{\partial u}{\partial y}\right) + \frac{B}{\rho}\frac{\partial u}{\partial t} \quad , \tag{26}$$

where it has been assumed that:

$$\frac{\partial \lambda}{\partial y} = \frac{\partial \mu}{\partial y} = 0 \quad ,$$

$$\frac{\partial^2 u}{\partial x \partial y} = \frac{\partial^2 u}{\partial y \partial x} \quad , \qquad \frac{\partial^2 v}{\partial x \partial y} = \frac{\partial^2 v}{\partial y \partial x} \quad .$$

The eight collateral conditions chosen to complete a well-posed problem were:

initial conditions:

I1: $$u(x,y,0) = 0 \quad , \tag{27}$$

I2: $$v(x,y,0) = 0 \quad , \tag{28}$$

I3: $$u_t(x,y,0) = 0 \quad , \tag{29}$$

I4: $$v_t(x,y,0) = 0 \quad , \tag{30}$$

boundary conditions:

B1: $$\begin{aligned} u(x,0,t) &= 0 \quad , \\ u(L,y,t) &= 0 \quad , \\ u(x,M,t) &= 0 \quad , \end{aligned} \tag{31}$$

B2: $$\begin{aligned} v(x,0,t) &= 0 \quad , \\ v(L,y,t) &= 0 \quad , \\ v(x,M,t) &= 0 \quad , \end{aligned} \tag{32}$$

B3: $$u_x(0,y,t) + v_y(0,y,t) = F(y,t) \quad , \tag{33}$$

where: $F(y,t) = 0$ for $t > t_1$

B4: $$u_y(0,y,t) + v_x(0,y,t) = 0 \quad . \tag{34}$$

The initial conditions allow the solution space to be initially undeformed and at rest. The first two boundary conditions (B1 and B2) require that displacements are zero for all time at the subsurface boundaries, which then become perfectly reflective. The other boundary conditions (B3 and B4) allow the x=0 boundary to become a free surface. Shear and dilatational stresses are not transmitted across the surface for all time except for an externally applied, time-varying dilatational stress, applied at a point or combination of points for $t < t_1$.

As in the one-dimensional model, an attenuation term was included in the equations of motion (E1 and E2) in order to keep boundary

reflections from masking multiple reflections in the central regions. The function B(x,y) is non-zero only in the vicinity of the three rigid boundaries and is zero in areas where disturbances are to be studied.

B. THE SOLUTION DOMAIN

The solution domain is a three-dimensional rectangular array of L by M by N mesh points dividing the domain into (L-1) by (M-1) by (N-1) equal subdivisions, each of size δx by δy by δt. Figure 5 shows the x-y solution space. The total solution domain is formed from N successive solution spaces or planes. A detail of the distance-depth-time mesh in the vicinity of mesh point (i,j,k) is shown in Fig. 6.

C. THE DIFFERENCE EQUATIONS

As in the one-dimensional model, a centered difference form for each partial derivative in equations (25) and (26) can be written. Making use of the definitions for wave velocities:

$$c^2 = \frac{\lambda + 2\mu}{\rho} \quad , \tag{35}$$

$$s^2 = \frac{\mu}{\rho} \quad , \tag{36}$$

finite difference forms of equations (25) and (26) may be written in terms of wave velocities and their derivatives. Carrying out this substitution and solving for the time leading (i,j,k+1) term for u and v yields:

E1: $$U_{i,j,k+1} = \Big[2U_{i,j,k}\left(1-C_i^2 RA - S_i^2 RC\right) + U_{(i+1),j,k}\left(C_i^2 + \frac{DL}{4} + \frac{DM}{2}\right)RA$$

$$+ U_{(i-1),j,k}\left(C_i^2 - \frac{DL}{4} - \frac{DM}{2}\right)RA + \left(U_{i,j+1,k} + U_{i,j-1,k}\right)S_i^2 RC + VA\left(C_i^2 - S_i^2\right)RB \tag{37}$$

$$+ \left(V_{(i+1),j,k} - V_{(i-1),j,k}\right)RE\,DL - U_{i,j,k-1}\left(1 + \frac{E_{ij}}{2\rho_i}\delta t\right)\Big] \Big/ \left[1 - \frac{B_{ij}}{2\rho_i}\delta t\right] \quad ,$$

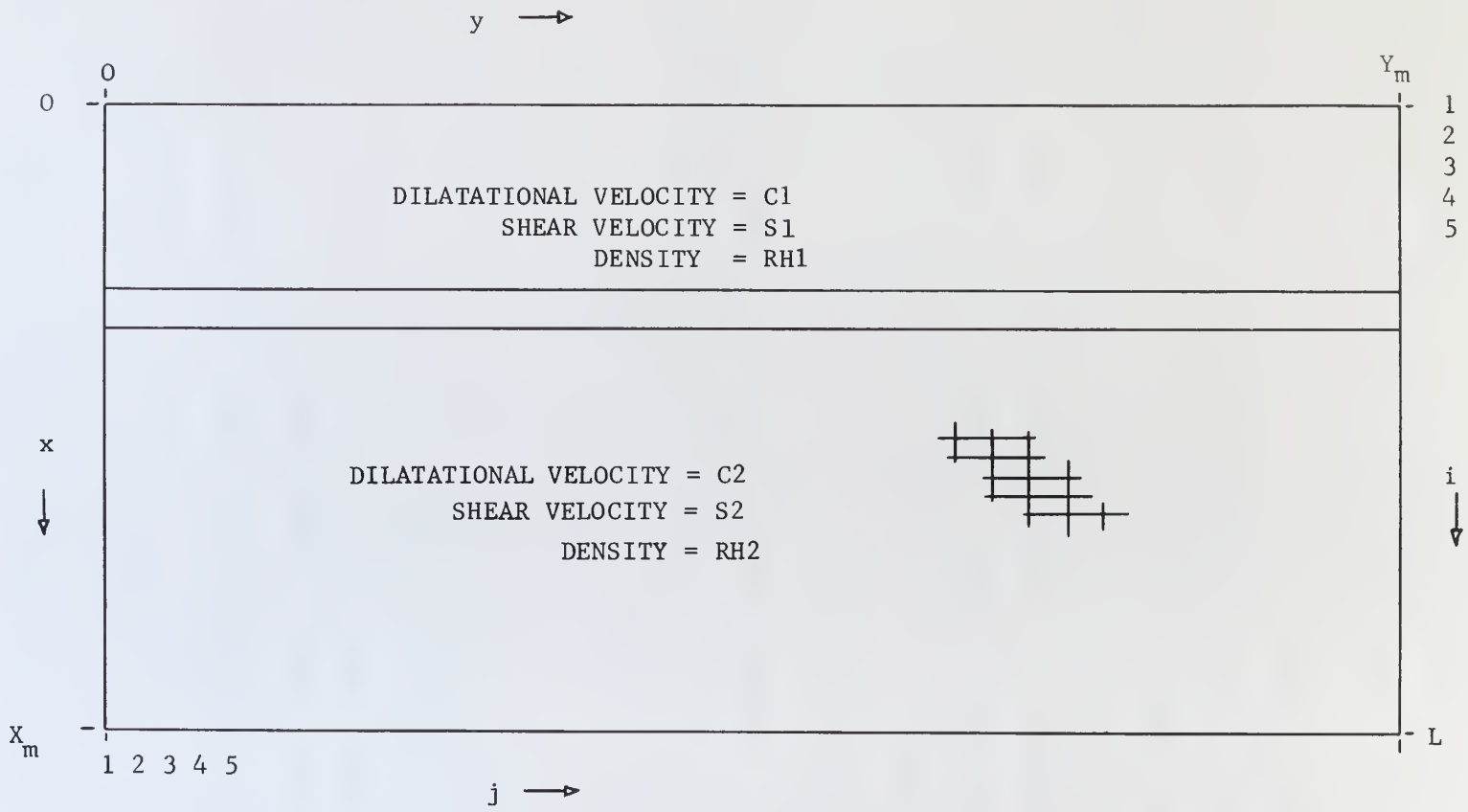

Figure 5. The x-y solution space.

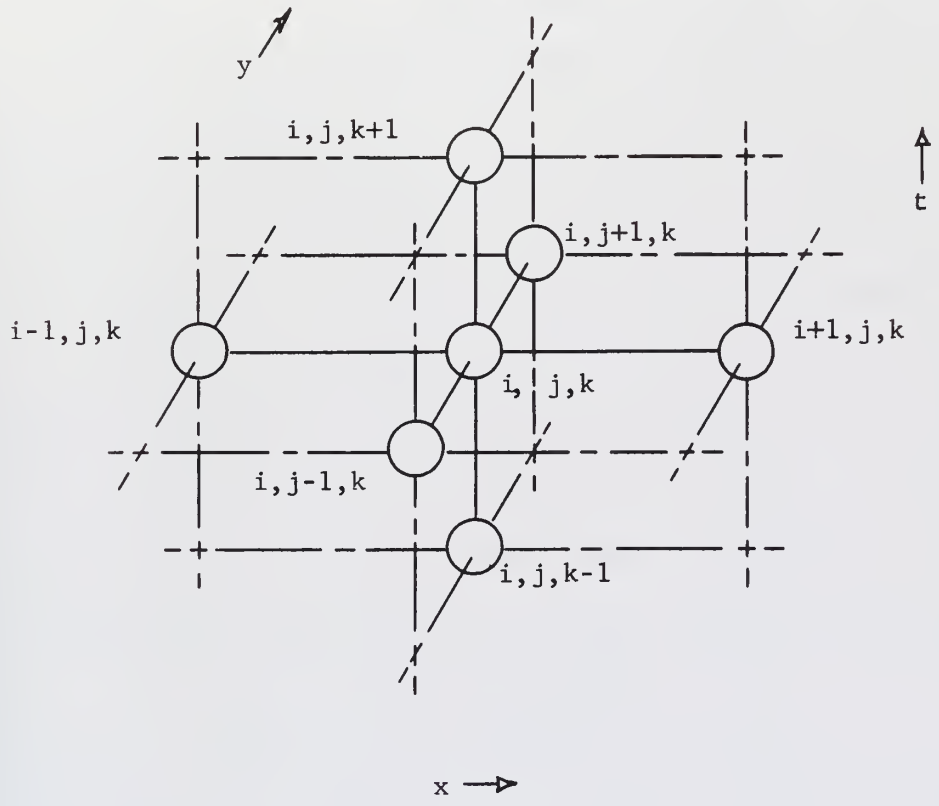

Figure 6. Isometric detail of three-dimensional mesh.

$$E2: \quad V_{i,j,k+1} = \Big[2V_{i,j,k}\left(1 - C_i^2 RC - S_i^2 RA\right) + V_{i+1,j,k}\left(S_i^2 + \frac{DM}{4}\right)RA$$
$$+ V_{i-1,j,k}\left(S_i^2 - \frac{DM}{4}\right)RA + \left(V_{i,j+1,k} + V_{i,j-1,k}\right)C_i RC + UA\left(C_i^2 - S_i^2\right)RB$$
$$+ \left(U_{i,j+1,k} - U_{i,j-1,k}\right)RB\,DM - V_{i,j,k-1}\left(1 + \frac{B_{ij}}{2\rho_i}\delta t\right)\Big] \Big/ \left[1 - \frac{B_{ij}}{2\rho_i}\delta t\right] , \tag{38}$$

where: $RA = \left(\frac{\delta t}{\delta x}\right)^2$, $RB = \frac{\delta t^2}{4\,\delta x\,\delta y}$, $RC = \left(\frac{\delta t}{\delta y}\right)^2$,

$DL = \frac{1}{\rho_i}\left(\lambda_{i+1} - \lambda_{i-1}\right)$, $DM = \frac{1}{\rho_i}\left(\mu_{i+1} - \mu_{i-1}\right)$,

$VA = V_{i+1,j+1,k} + V_{i-1,j-1,k} - V_{i+1,j-1,k} - V_{i-1,j+1,k}$,

$UA = U_{i+1,j+1,k} + U_{i-1,j-1,k} - U_{i+1,j-1,k} - U_{i-1,j-1,k}$.

The collateral conditions become:

$$I1: \quad U_{i,j,1} = 0 , \tag{39}$$

$$I2: \quad V_{i,j,1} = 0 , \tag{40}$$

$$I3: \quad U_{i,j,2} = 0 , \tag{41}$$

$$I4: \quad V_{i,j,2} = 0 , \tag{42}$$

$$B1: \quad U_{i,1,k} = 0 , \quad U_{L,j,k} = 0 , \quad U_{i,M,k} = 0 , \tag{43}$$

$$B2: \quad V_{i,1,k} = 0 , \quad V_{L,j,k} = 0 , \quad V_{i,M,k} = 0 , \tag{44}$$

$$B3: \quad U_{1,j,k+1} = \Big[2U_{1,j,k}\left(1 - C_1^2 RA - S_1^2 RC\right) + U_{2,j,k}\left(2C_1 RA\right)$$
$$+ \left(U_{1,j+1,k} + U_{1,j-1,k}\right)S_1^2 RC + \left(V_{1,j+1,k} - V_{1,j-1,k}\right)DL\,RB$$
$$- \left(C_1^2 RA - \frac{DL}{4} - \frac{DM}{2}\right)\left(2\delta x F_{j,k}\right) - U_{1,j,k-1}\left(1 + \frac{B_{1j}}{2\rho_1}\delta t\right)\Big] \Big/ \left[1 - \frac{B_{1j}}{2\rho_1}\delta t\right] , \tag{45}$$

$$B4: \quad V_{1,j,k+1} = \Big[2V_{1,j,k}\left(1 - C_1^2 RC - S_1^2 RA\right) + V_{2,j,k}\left(2S_1^2 RA\right)$$
$$+ \left(V_{1,j+1,k} + V_{1,j-1,k}\right)C_1^2 RC + \left(U_{1,j+1,k} - U_{1,j-1,k}\right)DM\,RB$$
$$+ \left(C_1^2 - S_1^2\right)\left(F_{j+1,k} - F_{j-1,k}\right)\left(2\delta x\,RB\right) - V_{1,j,k-1}\left(1 + \frac{B_{1j}}{2\rho_1}\delta t\right)\Big] \Big/ \left[1 - \frac{B_{1j}}{2\rho_1}\delta t\right] . \tag{46}$$

A well-posed problem for numerical solution is then formed by equations (37) and (38) with collateral conditions (39) through (46). Initially, the k=1 and k=2 planes are set to zero following equations (39) through (42). The k+1 plane can then be solved using equations (43) through (46) for the boundaries and equations (37) and (38) for the interior mesh points.

D. STABILITY AND CONVERGENCE

1. Stability

Under the conditions that the attenuation and velocity gradient terms are zero and that $\delta x = \delta y$, the difference equations (37) and (38) reduce to those for which a stability analysis was carried out by Alterman and Karal [1968], and Alterman and Rotenberg [1969]. The former paper showed that the stability criterion is given by:

$$\frac{\delta t}{\delta x} < \frac{1}{C}\left[1 + \left(\frac{S}{C}\right)^2\right]^{-\frac{1}{2}} . \tag{47}$$

In the latter paper, the authors indicated that stability was guaranteed under the condition that:

$$\frac{\delta t}{\delta x} < 0.86 , \tag{48}$$

with the assumption that S/C = 0.55, corresponding to a Poisson's ratio of 0.28. Poisson's ratio is defined in terms of wave velocities as:

$$\sigma = \frac{\frac{1}{2}\left(\frac{C}{S}\right)^2 - 1}{\left(\frac{C}{S}\right)^2 - 1} . \tag{49}$$

Empirically, it was found that the addition of attenuation and velocity gradient terms reduced the right side of equation (47), while

an increase in δy ($\delta y > \delta x$) reduced the left side. An approximate stability criterion was established, given by:

$$\frac{\delta t^2}{\delta x \delta y} < \frac{0.75}{C^2}\left[1+\left(\frac{S}{C}\right)^2\right]^{-1} , \qquad (50)$$

under the condition that the restrictions on velocity gradients (for C and S) given by equation (17) apply.

2. Convergence

Following the methods of Forsythe and Wasow [1967] and of Fox et al. [1962] , it was assumed that convergence would be assured as long as the mesh ratios were sufficiently small to insure that the (i,j,k+1) mesh point lies within the characteristic surfaces through adjacent mesh points in the k plane. Fox equated the characteristic surfaces with successive positions of a wave front. The most restrictive condition on convergence is then given by the maximum dilatational wave velocity in the solution space. This would give a less stringent mesh ratio condition than the stability condition. Therefore, as long as equation (49) holds, the method will be convergent as well as stable.

E. DESCRIPTION OF THE PROGRAM

The program produces a set of four seismograms: shear and dilatational stress and vertical and horizontal displacement. The data is written on a temporary storage device (tape, disk or drum). A second program then reads the data and plots the seismograms. An average run with a 71x81 grid, 800 time mesh points and 25 detectors requires 278K bytes of main core storage and a run time of 18 min. The output requires 325K bytes of temporary storage space. The primary limiting

factor on a given problem is the time required for input/output to and from the temporary storage device.

1. Distribution Parameters

As in the one-dimensional model, the distribution parameters are used to model the physical conditions in the solution space. They are:

a. dilatational wave velocity, C(x),

b. shear wave velocity, S(x),

c. density, RH(x),

d. forcing function, F(y,t),

e. attenuation parameter, B(x,y).

Wave velocities and density are put in the program as single-valued, continuous, polygonal line functions of depth. The forcing function is put in as was done in the one-dimensional model along with horizontal stations at which F is to be applied. The attenuation parameter is put into the program as two single-valued, continuous, polygonal parameters. They are:

e1. vertical attenuation parameter, BA(x),

e2. horizontal attenuation parameter, BB(y).

The full attenuation parameter, B(x,y), is then computed as follows:

$$B(x,y) = MAX[BA(x), BB(y)] \quad . \tag{51}$$

Tables VI through VIII give sample numerical input used to describe the various distribution parameters. Their distributions in the solution domain are shown graphically in Fig. 7 through 9.

Table VI.

Sample wave velocity and density polygons

Depth	C(x)	S(x)	RH(x)
0.0	0.6	0.0	1.0
3.0	0.6	0.0	1.0
3.3	1.2	0.82	2.1
7.0	1.2	0.82	2.1

Table VII.

Sample forcing function polygon

Time	F(t)
0.0	0.0
0.1	0.0
0.7	-0.15
1.30	0.0
2.50	0.0

Table VIII.

Sample attenuation parameter polygons

Depth	BA(x)	Distance	BB(y)
0.0	0.0	0.0	-2.5
4.0	0.0	1.0	-1.0
7.0	-2.5	2.0	0.0
		10.0	0.0
		11.0	-1.0
		12.0	-2.5

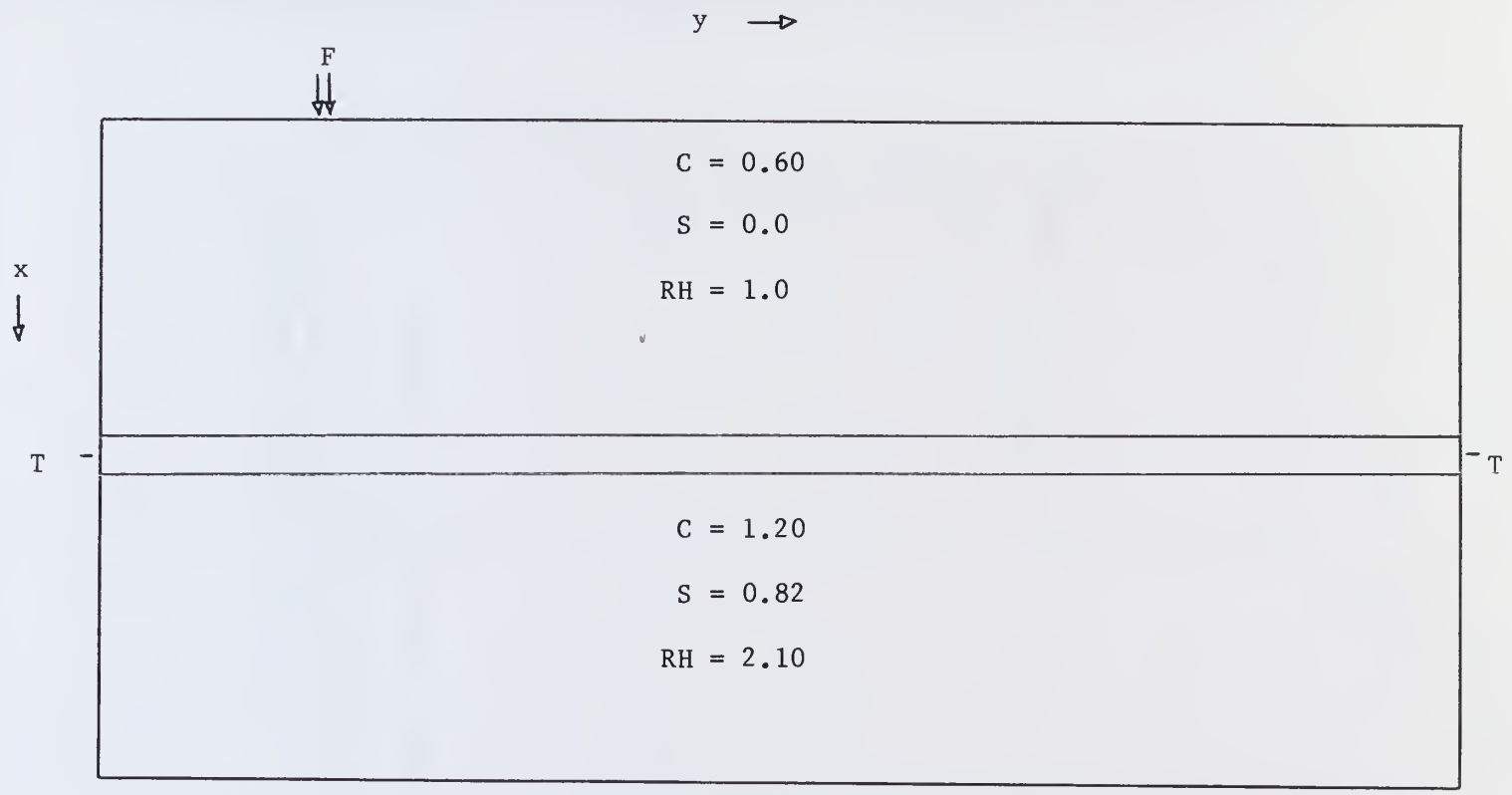

Figure 7. Sample distribution of wave velocities and density.

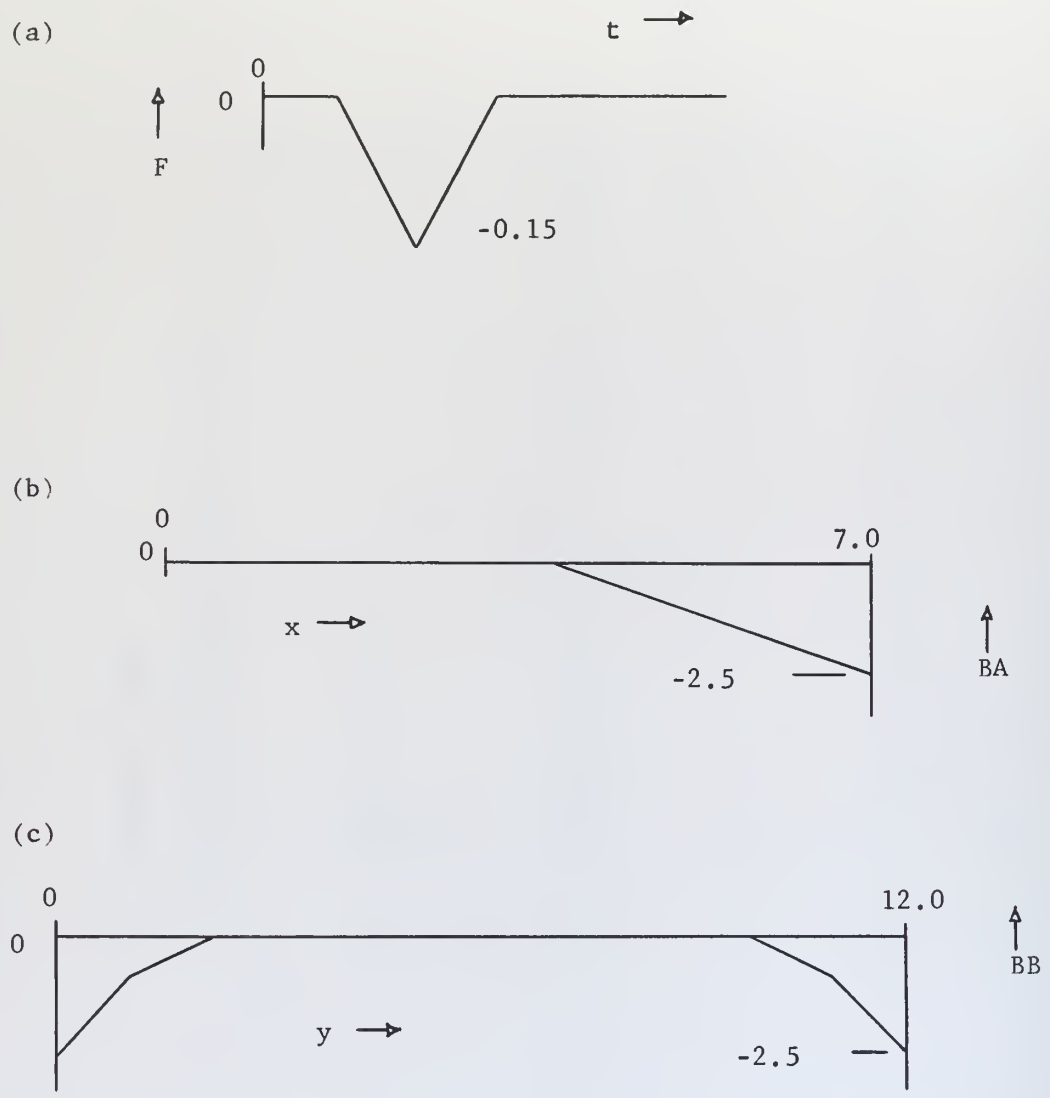

Figure 8. Sample distribution parameters.

(a) Forcing function
(b) Vertical attenuation parameter
(c) Horizontal attenuation parameter

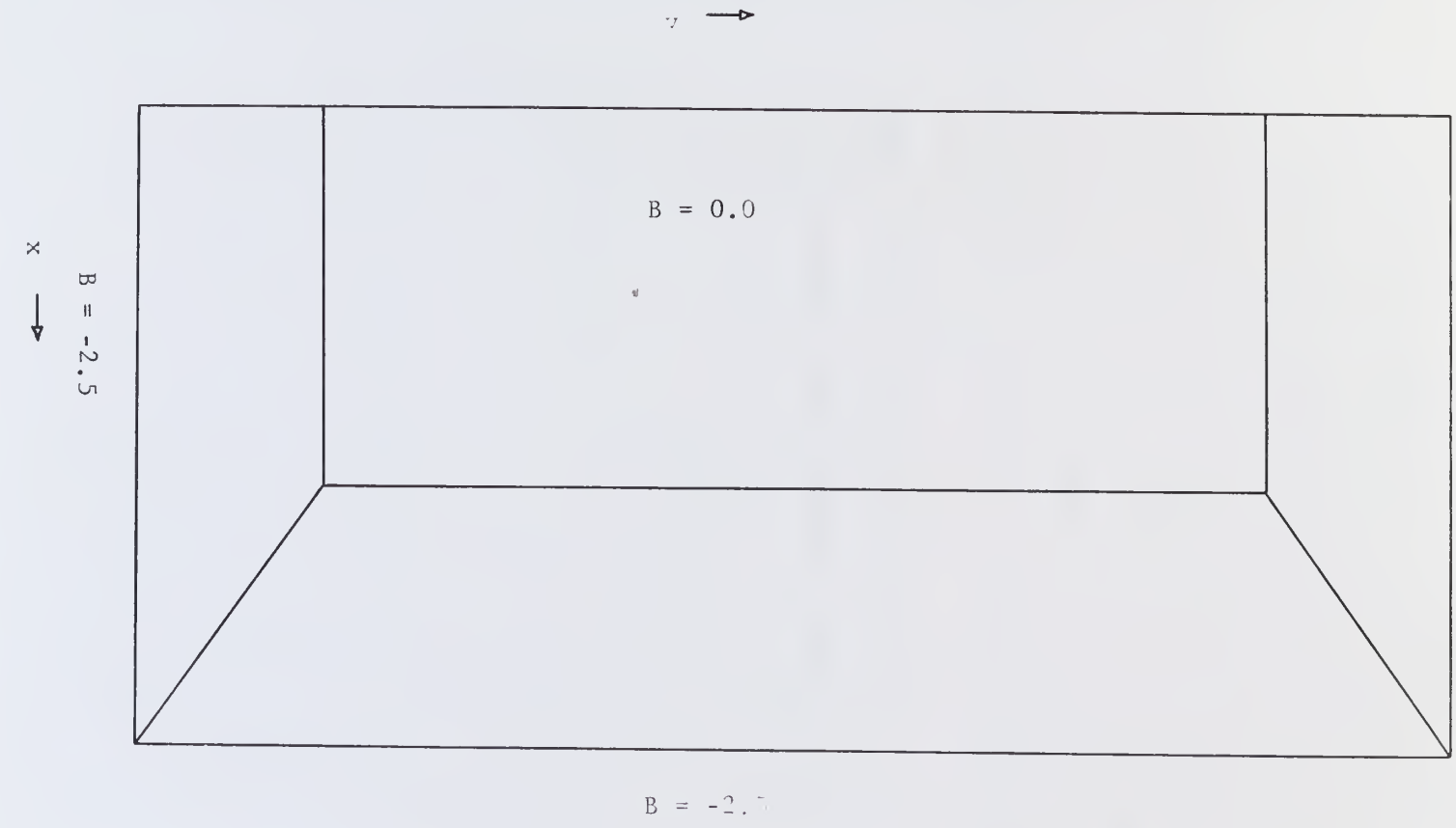

Figure 9. Sample distribution of the attenuation parameter.

2. Numerical Parameters

These parameters are used to control the computation of the distribution parameters and to set the arrangement and size of the solution domain. They are:

a. mesh size in the x direction, (DX),

b. mesh size in the y direction, (DY),

c. mesh size in the t direction, (DT),

d. number of total x mesh points, (L),

e. number of total y mesh points, (M),

f. number of total t mesh points, (N),

g. number of points defining the distribution parameter polygons:

(1) wave velocity and density polygons, (NC),

(2) forcing function polygon, (NF),

(3) attenuation parameter polygons:

(a) vertical, (NBA),

(b) horizontal, (NBB),

h. x mesh point at which the output is measured:

(1) stress, (IA),

(2) displacement, (ID),

i. number of horizontal output stations, (KK),

j. y index of the first output station, (JB),

k. mesh increment between output stations, (JJ),

l. shot point or area location:

(1) first shot mesh point, (MA),

(2) last shot mesh point, (MB),

m. last time mesh point at which F(y,t) is to be applied, (LL).

F. SCALING THE PROBLEM

The scale of the problem is determined by choices of wave velocity values and either δt or δx and δy. For mesh ratios of:

$$\frac{\delta t}{\delta x} = \frac{0.05}{0.10} = \frac{1}{2} \quad , \tag{52a}$$

$$\frac{\delta t}{\delta y} = \frac{0.05}{0.15} = \frac{1}{3} \quad , \tag{52b}$$

and under the condition on shear velocity that $S = C/\sqrt{3}$ ($\sigma = 0.25$), the dilatational wave velocity may vary from 0.0 to 1.86 distance units per time unit, and shear wave velocity may not exceed 1.07 distance units per time unit. If a value of $C = 0.60$ is to represent dilatational wave velocity in water of 1.5 km/sec, then the scale of the problem would depend upon a choice of either time or distance mesh size. Table IX shows scales available for various distance mesh sizes specified.

Table IX.

Scales available for C = 0.60 = 1.5 km/sec

Numerical parameters: L = 71; M = 81; N = 800

Mesh sizes			Units			Seismogram Length (sec)	Solution Space Size	
			Distance		Time			
x (m)	y (m)	t (sec)	x (m)	y (m)	t (sec)		x (m)	y (m)
100	150	.02	1000	1500	.4	16	7000	12000
10	15	.002	100	150	.04	1.6	700	1200
1	1.5	.0002	10	15	.004	.16	70	120

IV. INTERPRETATION

The synthetic seismic records produced by the two models presented in this paper were interpreted first in the manner of actual field records without direct reference to the structural profiles used. Extensive use was made of gross seismic interpretation techniques presented by Grant and West [1965] , Dobrin [1960] , and Bullen [1959] . Interpretation of the reflection and transmission of incident pulses was aided by the results of Alterman and Karal [1968] , Alterman and Rotenberg [1969] , Gupta [1966a and 1966b] , Sengbush, Lawrence and McDonal [1961] and Tooley, Spencer and Sagoci [1965] .

A. THE REFLECTION PROFILING SEISMOGRAMS

Each reflection profile produced by the model is designated by an alpha-numeric sequence. For example, C3H F7 A14 identifies the exact structure (C3H), forcing function (F7) and attenuation parameter (A14) used.

Six profiles were developed using three basic structures. The structures, shown in Fig. 10 through 15, can be described in terms of marine geology as follows:

(1) Shelf break with horizontal layers.

  (a) Increasing velocity in each successive layer (C3H).

  (b) With one low velocity layer (C4D).

(2) Flat bottom with double wedge.

  (a) High velocity wedge (C5A).

  (b) Low velocity wedge (C6C).

(3) Flat bottom, horizontal layering, penetrated unconformably by a dipping bed.

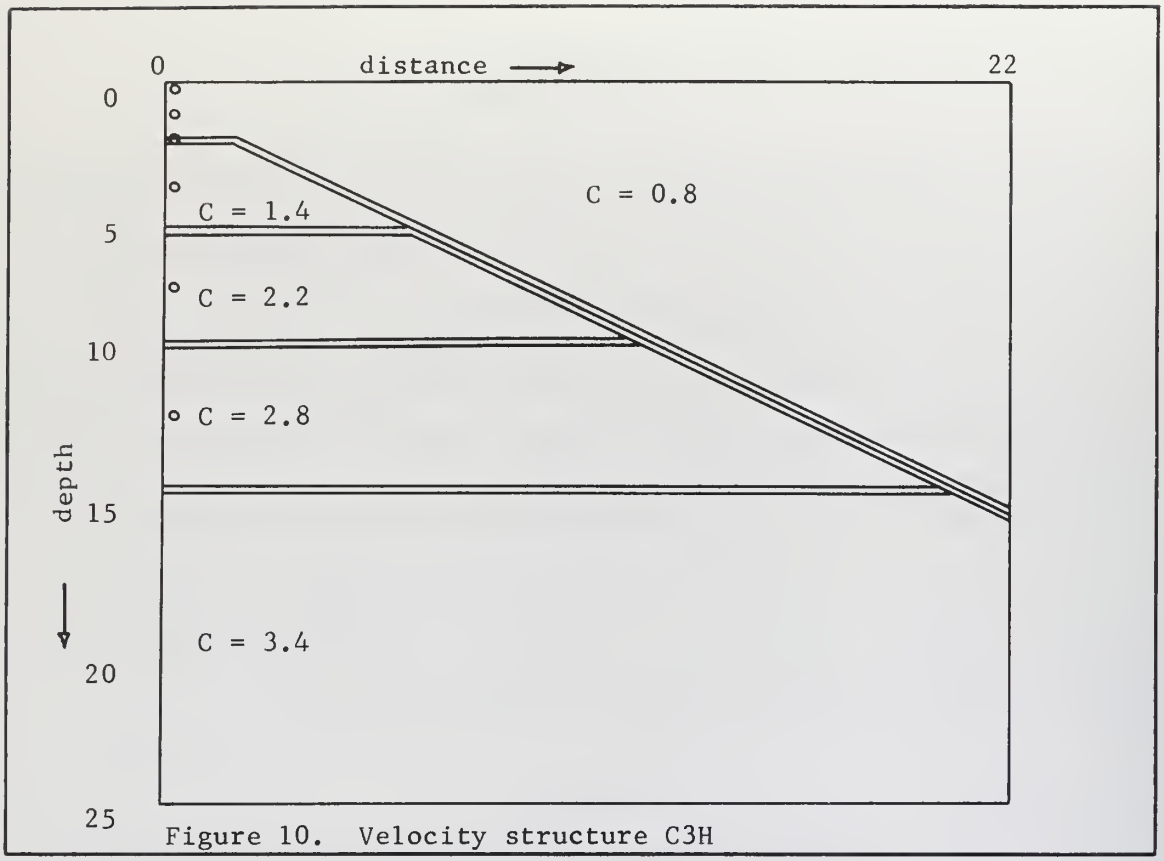

Figure 10. Velocity structure C3H

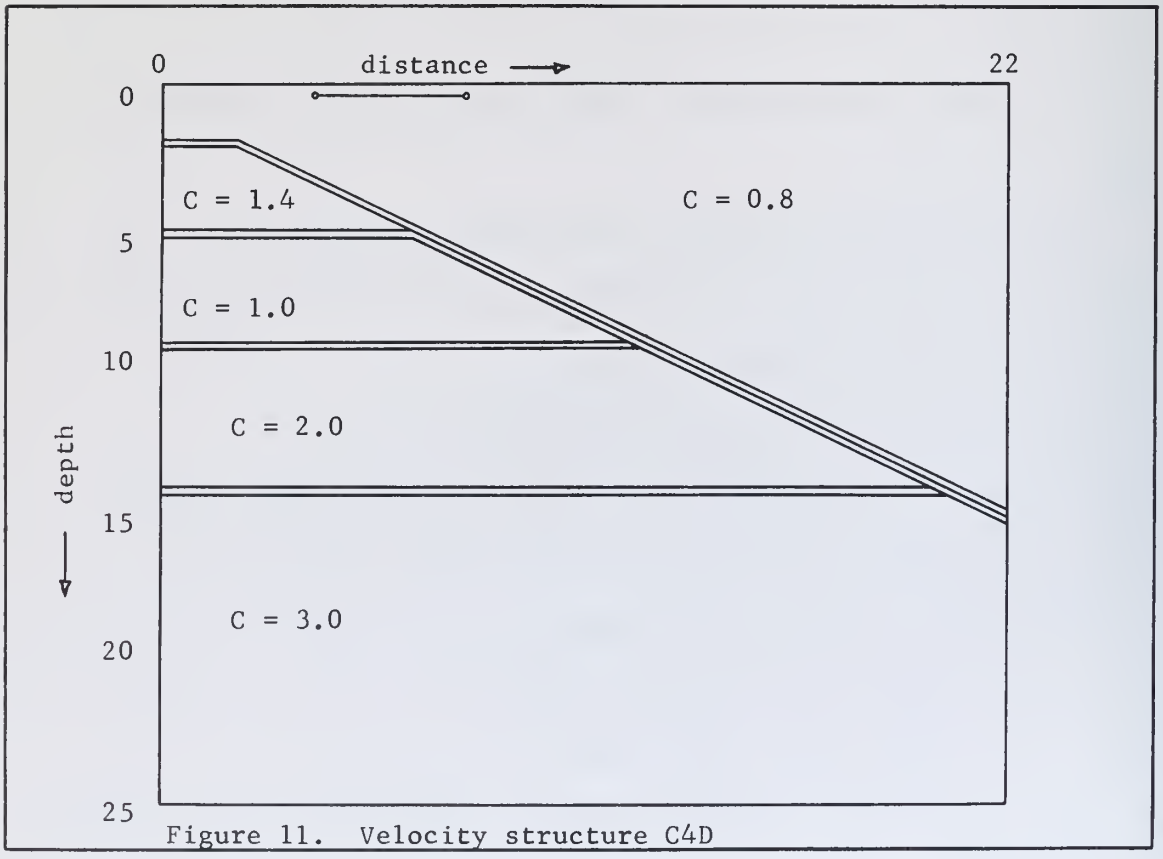

Figure 11. Velocity structure C4D

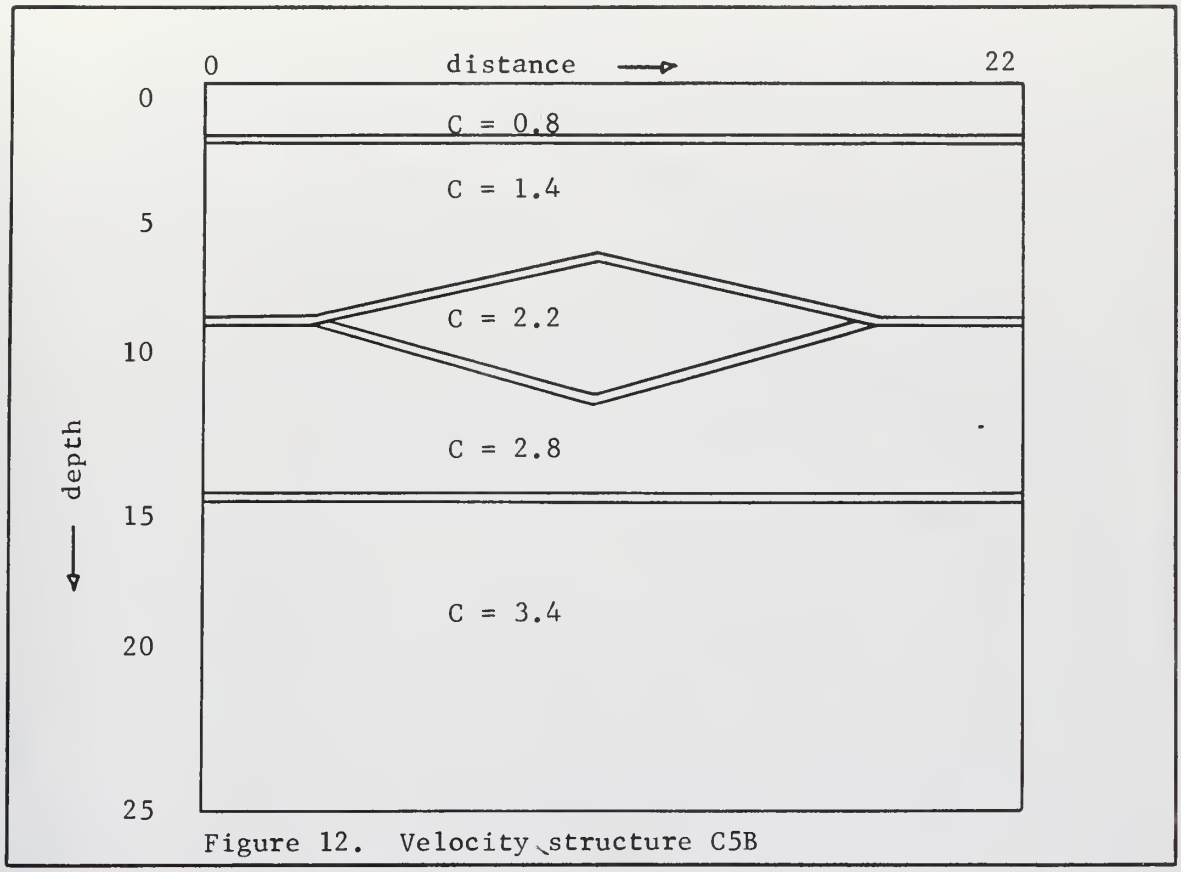

Figure 12. Velocity structure C5B

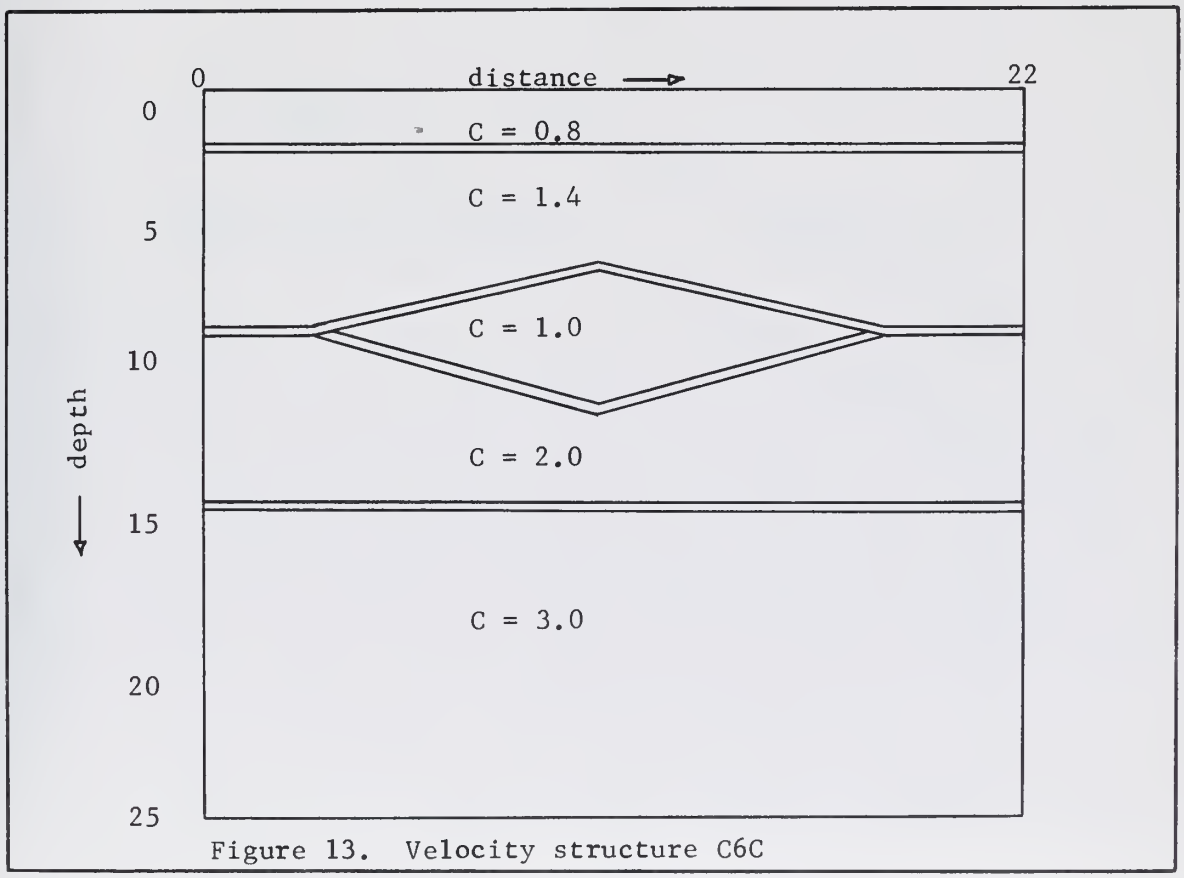

Figure 13. Velocity structure C6C

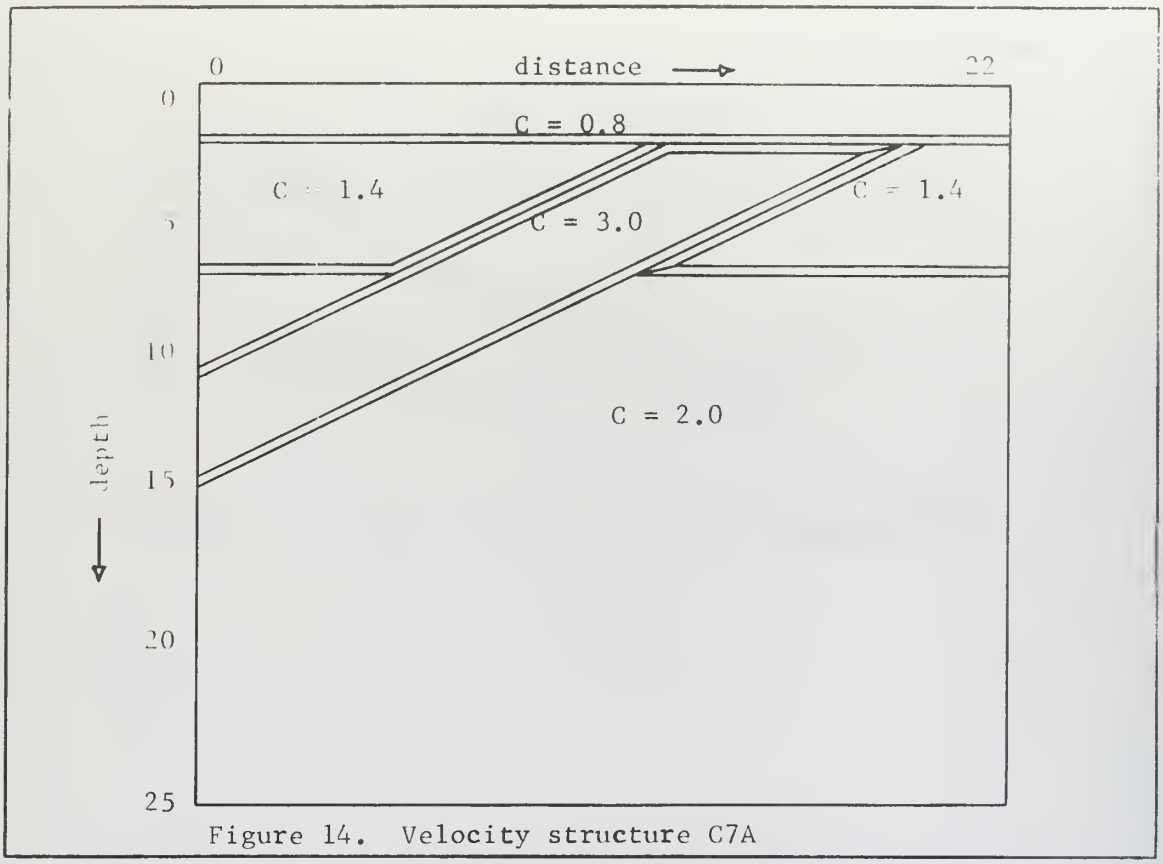

Figure 14. Velocity structure C7A

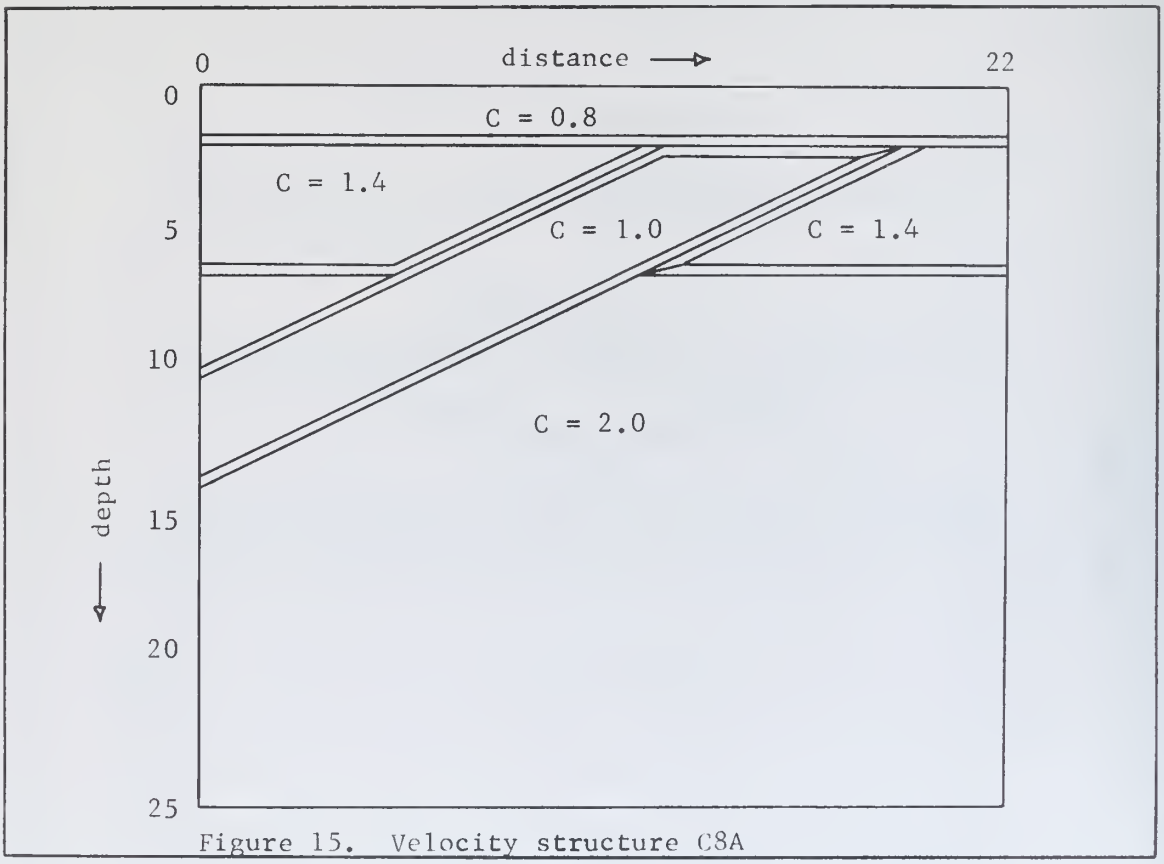

Figure 15. Velocity structure C8A

(a) High velocity bed (C7A).

(b) Low velocity bed (C8A).

All traces utilized forcing function F7 (Fig. 16) and attenuation parameter A14 (Fig. 17).

1. Variable Depth Records

As an aid to interpretation, several single traces were developed with a single velocity structure, where the depth of the detection point was varied between traces. The traces are shown in Fig. 18 along with the mesh point at which each was computed. These various detection points are shown as circles in Fig. 10. The traces were generated using a source located at a horizontal distance of 0.5 units for the problem designated C3H F7 A14. The first disturbance in each trace, designated d, is the direct wave. P_1 and P_2 designate the reflected pulses from the first and second transition zones, while the first primary multiple (P_1 reflected from the free surface) is shown by P_1P_s. Other multiples are marked in a similar manner.

These traces show clearly the development of a train of alternating negative and positive pulses behind the main pulse. The change in pulse shape is also quite evident. As the pulse progresses, the amplitude decreases and the pulse width increases. Additionally, the base and tip of the pulse form tends to become more rounded. These are primarily mesh effects and are dependent on mesh size (DX). When one particle is unloaded as the pulse passes by, the adjacent particle is still under stress, causing a reverse stress between the particles. In gradient zones, where the derivative of C is non-zero, there is also an elastic rebound effect which reinforces the pulse train.

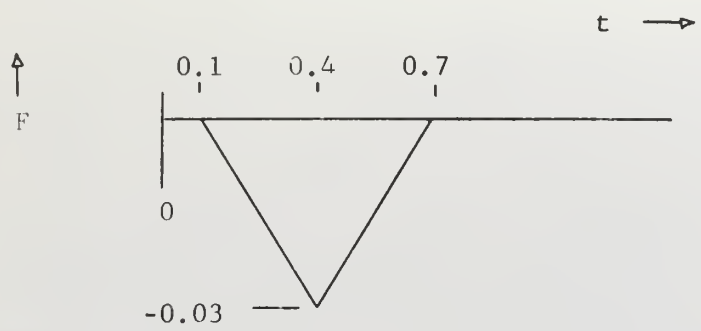

Figure 16. Forcing function F7

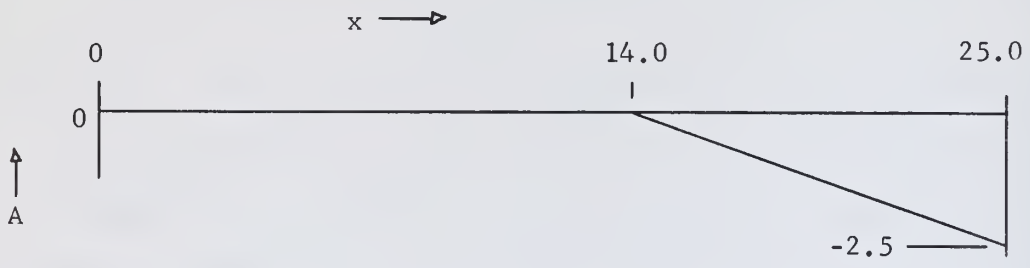

Figure 17. Attenuation parameter A14

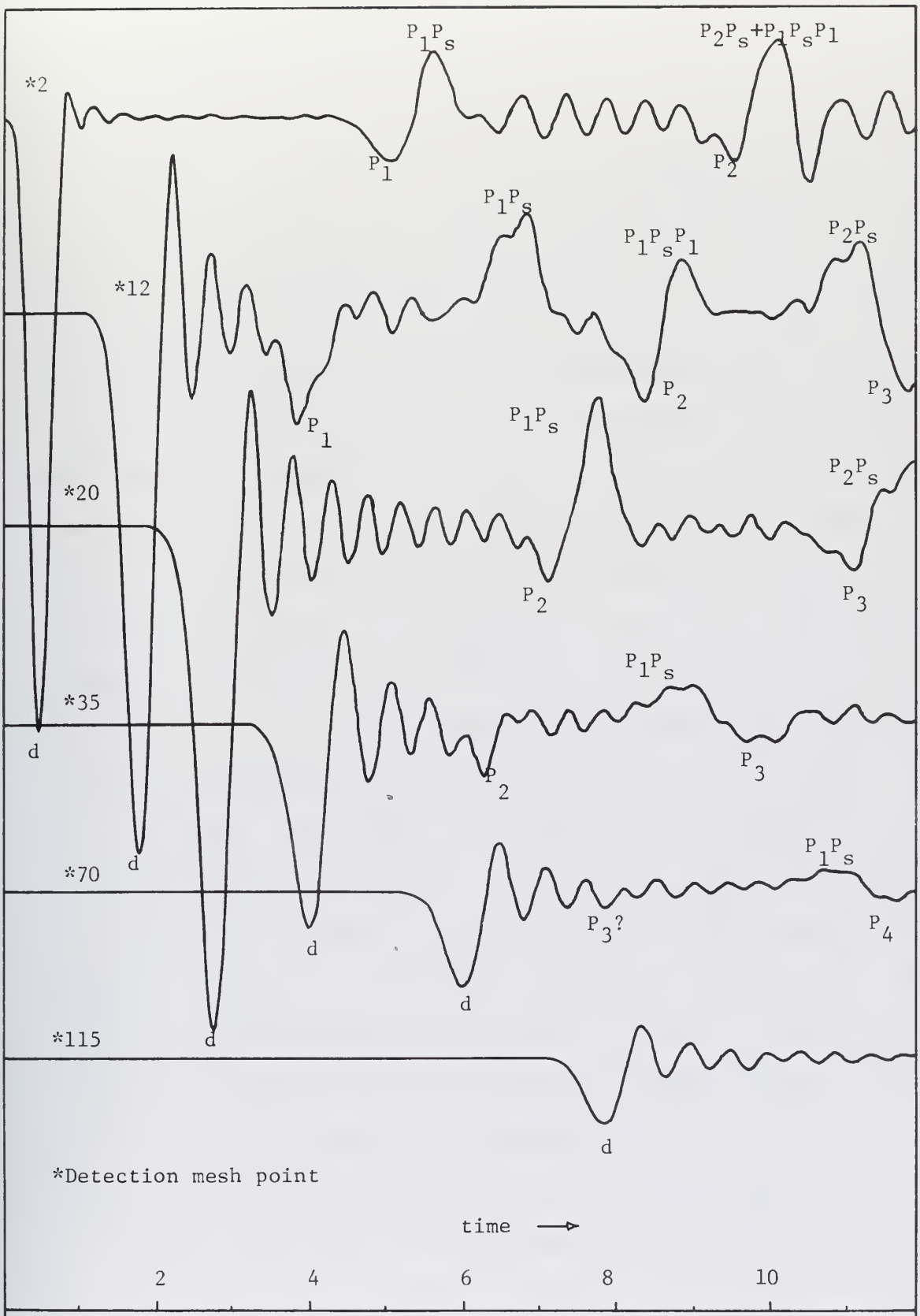

Figure 18. Stress versus time at various depths

2. The reflection profiling seismograms

Synthetic reflection profiling seismograms are shown in Fig. 19 through 26. Figure 19 is an uncorrelated version of Fig. 20, included so that lineations may be observed without the influence of correlation lines shown on the remaining figures. Solid lines on the seismograms mark lineations which were correlated with first reflections from a particular horizon. Dashed lines indicate multiple reflections which, if used as primary reflections, might lead to erroneous interpretations of structure. For each correlation, a particular phase was chosen and followed laterally through successive traces. Figures 20 and 21 show clearly the false dips introduced by the sloping bottom, increasing the pulse travel time in the lower velocity upper layer. The bottom slope causes a change in thickness of the top two layers (water and the first subbottom layer). The false dip introduced is a function of the bottom slope and the ratio of velocities involved. Note that there is a change in dip at each point where a layer pinches out.

Figures 22 and 23 show similar false dips and horizons introduced by variations in the thickness of a single layer. The high velocity wedge causes a doming up to be introduced into a horizontal transition zone below, while the low velocity wedge has the reverse effect. The most obvious feature of the records for velocity structures C7A and C8A (Fig. 24 and 25) is the relatively high amplitudes in the records in the areas where the dipping beds pinch out against the flat bottom. This is caused by a combination of factors. In velocity structure C7A (Fig. 24), there is a sharp change in velocity contrast across the bottom as the dipping bed outcrops. The steeper gradient then reflects more energy, causing an increase in amplitude in both

Figure 19

Uncorrelated reflection profile C3H F7 A14

DX: 0.10 DT: 0025 DK: 0.50

N: 251 M: 1800 IP: 2

Horizontal distance (d)

versus

time (t)

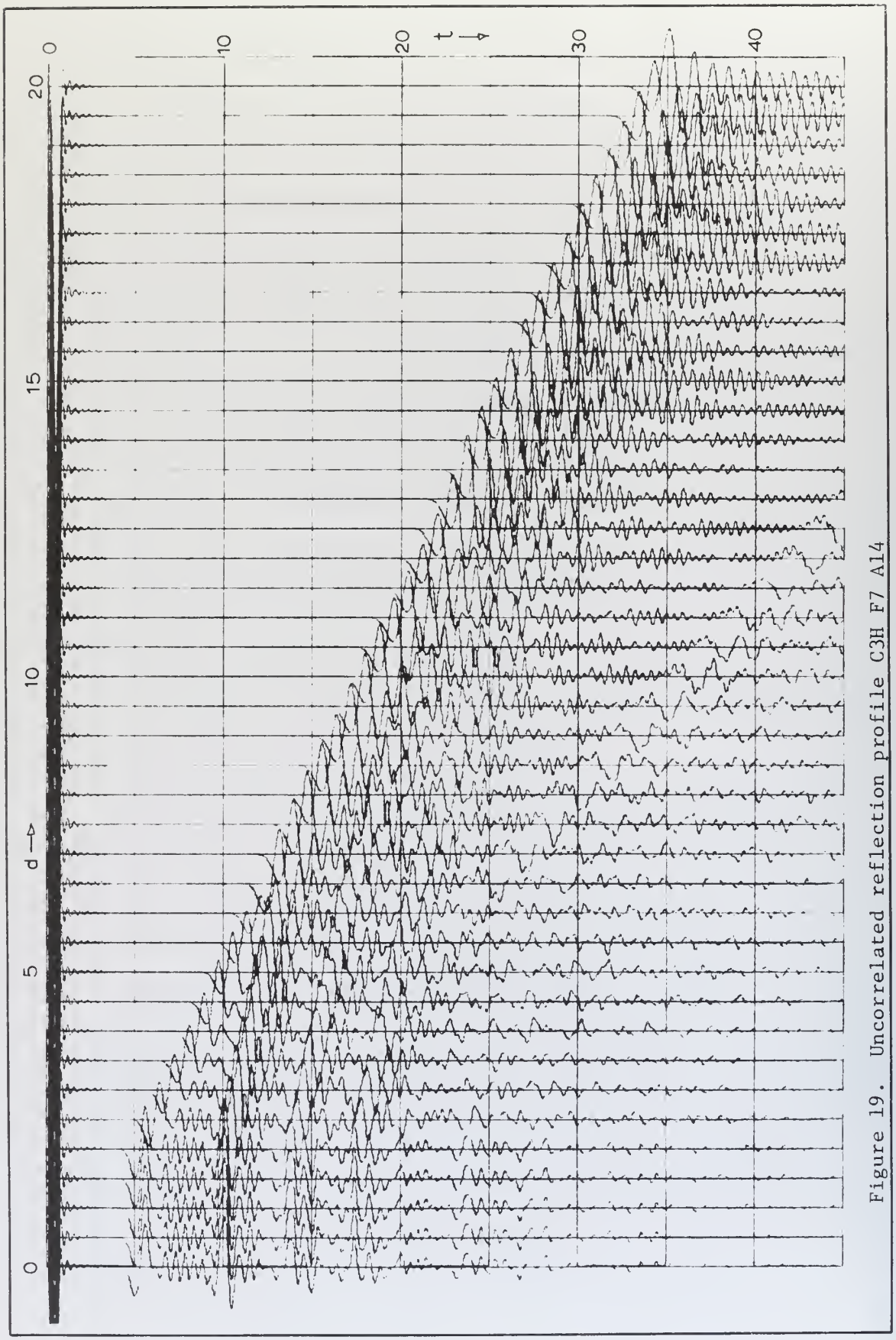

Figure 19. Uncorrelated reflection profile C3H F7 A14

Figure 20

Reflection profile C3H F7 A14

DX: 0.10 DT: 0.025 DK: 0.50

N: 251 M: 1800 IP: 2

Horizontal distance (d)

versus

time (t)

———— First reflections

— — — — Multiple reflections

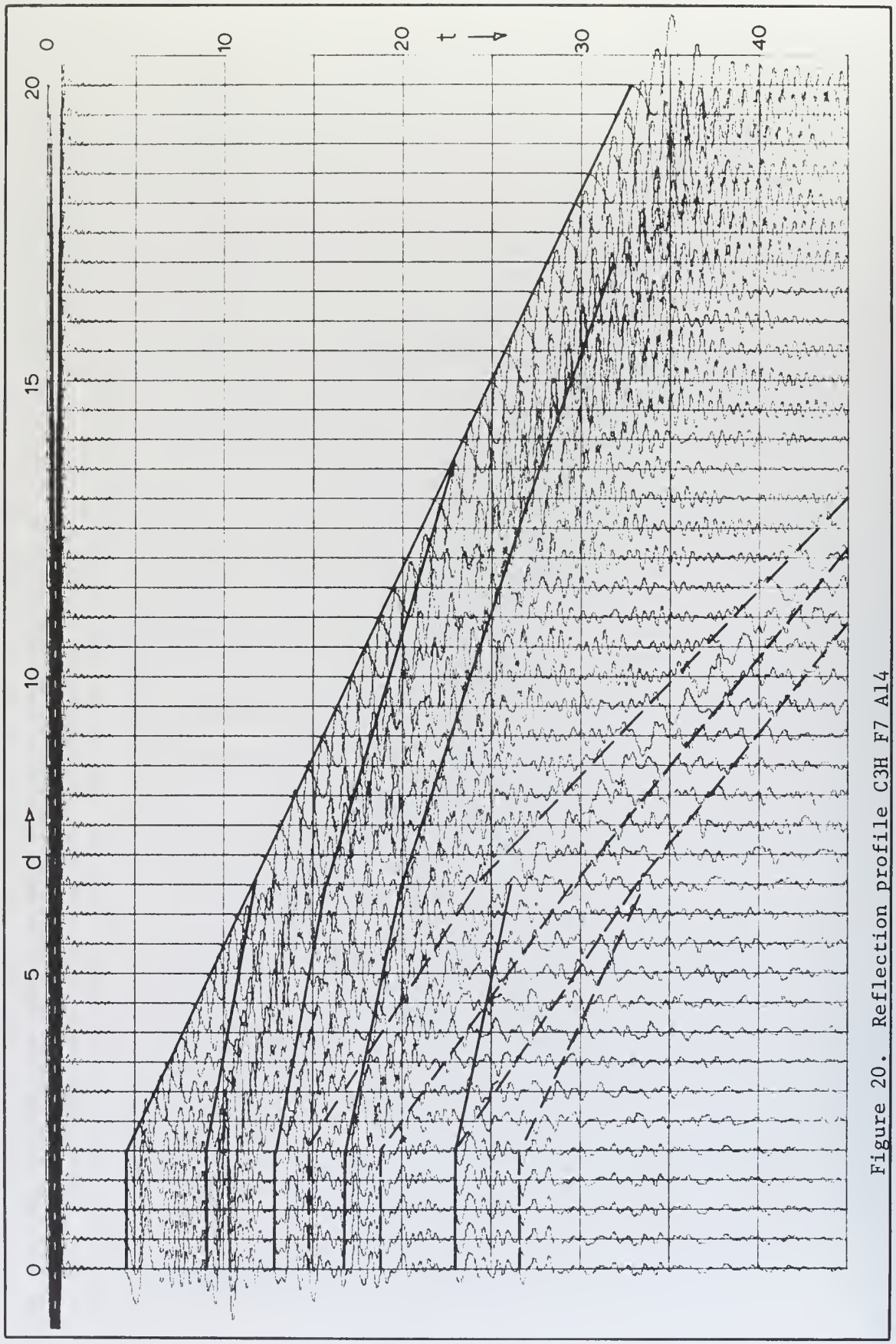

Figure 20. Reflection profile C3H F7 A14

Figure 21

Reflection profile C4D F7 A14

DX: 0.10 DT: 0.025 DK: 0.50

N: 251 M: 1800 IP: 2

Horizontal distance (d)

versus

time (t)

———— First reflections

— — — — Multiple reflections

•————• Location of precision trace (Fig. 26)

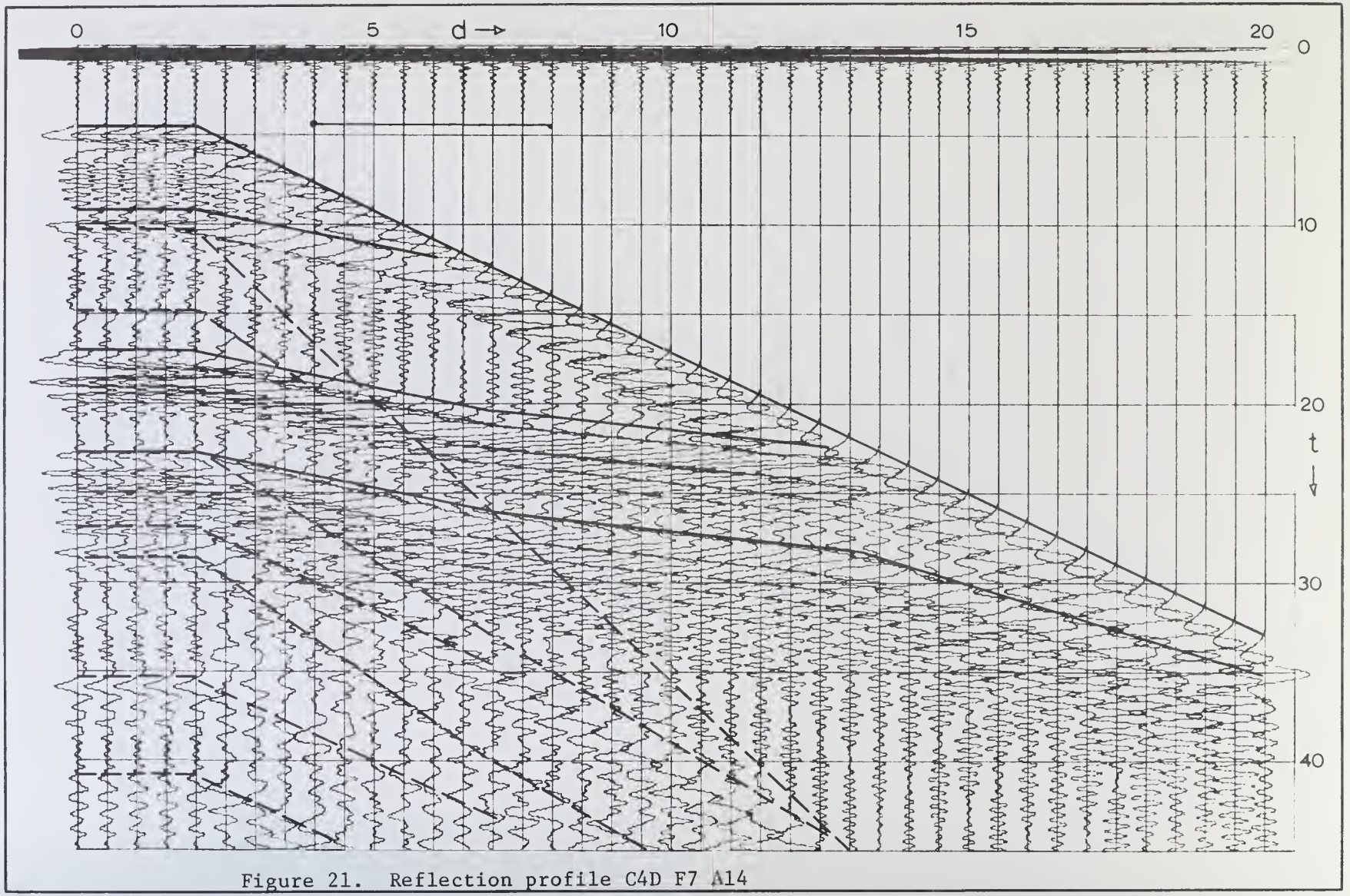

Figure 21. Reflection profile C4D F7 A14

Figure 22

Reflection profile C5B F7 A14

DX: 0.10 DT: 0.025 DK: 0.50

N: 251 M: 1800 IP: 2

Horizontal distance (d)

versus

time (t)

———— First reflections

— — — — Multiple reflections

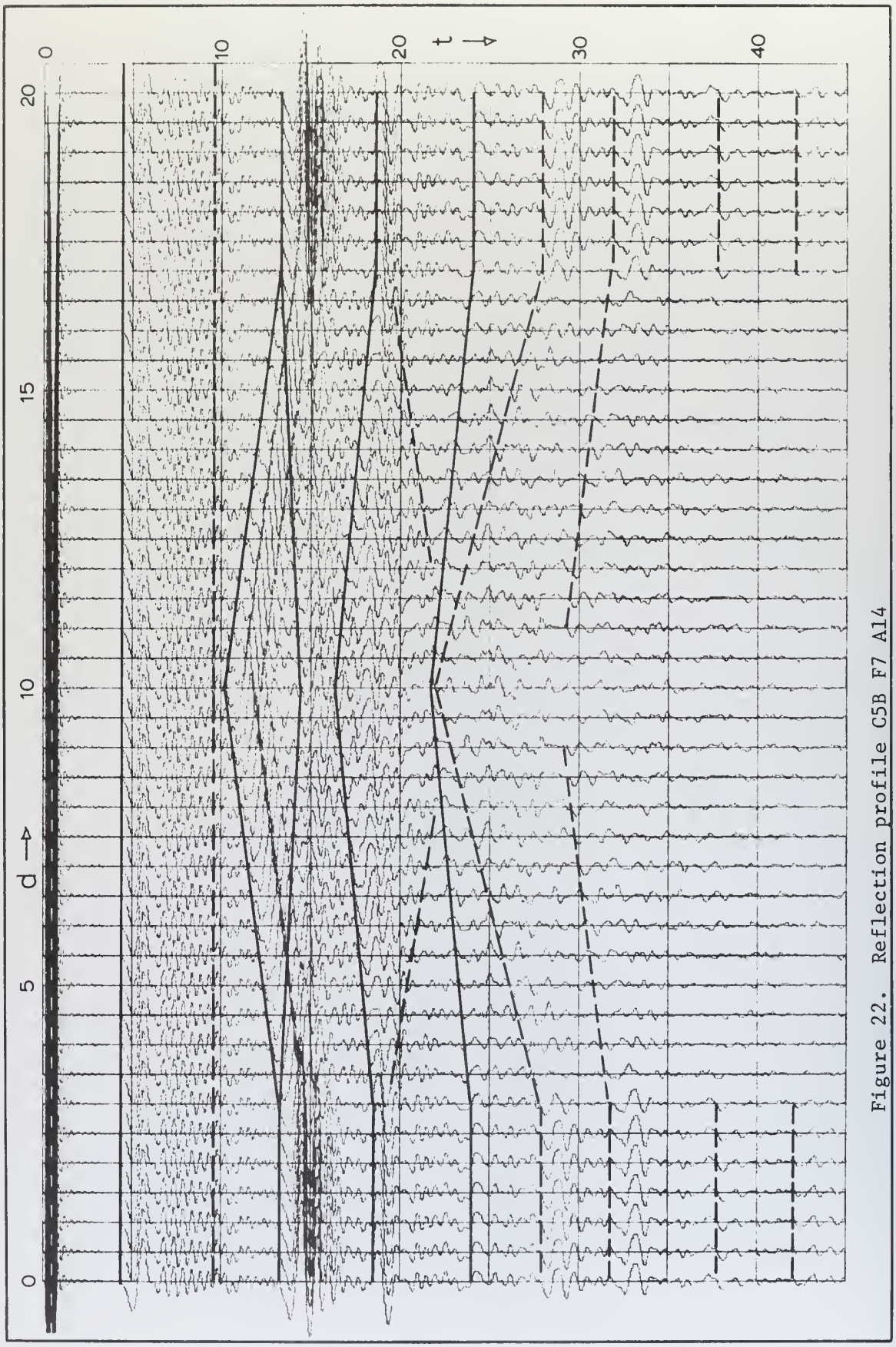

Figure 22. Reflection profile C5B F7 A14

Figure 23

Reflection profile C6C F7 A14

DX: 0.10 DT: 0.025 DK: 0.50

N: 251 M: 1800 IP: 2

Horizontal distance (d)

versus

time (t)

———— First reflections

— — — Multiple reflections

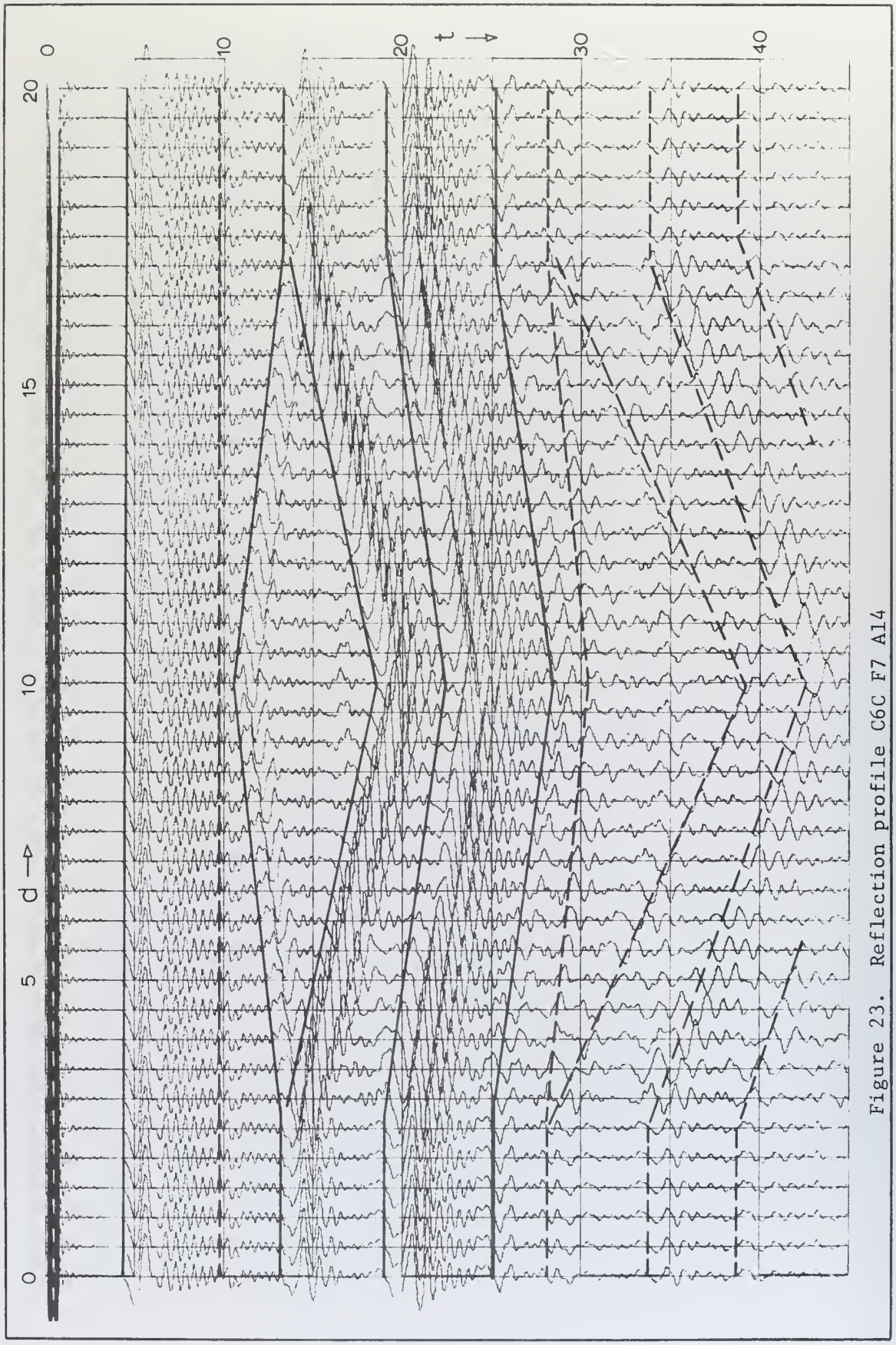

Figure 23. Reflection profile C6C F7 A14

Figure 24

Reflection profile C7A F7 A14

DX: 0.10 DT: 0.025 DK: 0.50

N: 251 M: 1800 IP: 2

Horizontal distance (d)

versus

time (t)

———— First reflections

— — — Multiple reflections

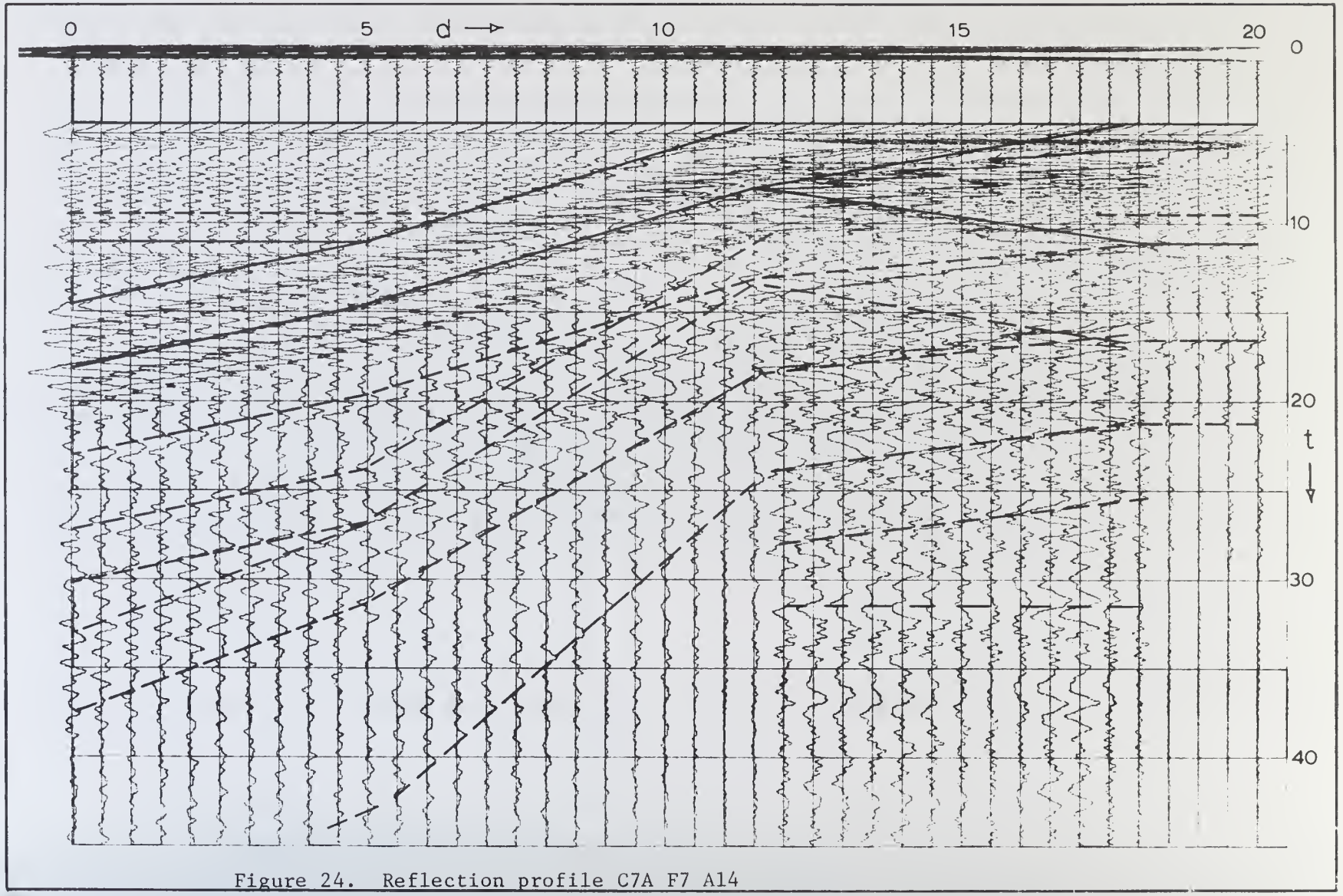

Figure 24. Reflection profile C7A F7 A14

Figure 25

Reflection profile C8A F7 A14

DX: 0.10 DT: 0.025 DK: 0.50

N: 251 M: 1800 IP: 2

Horizontal distance (d)

versus

time (t)

———— First reflections

— — — Multiple reflections

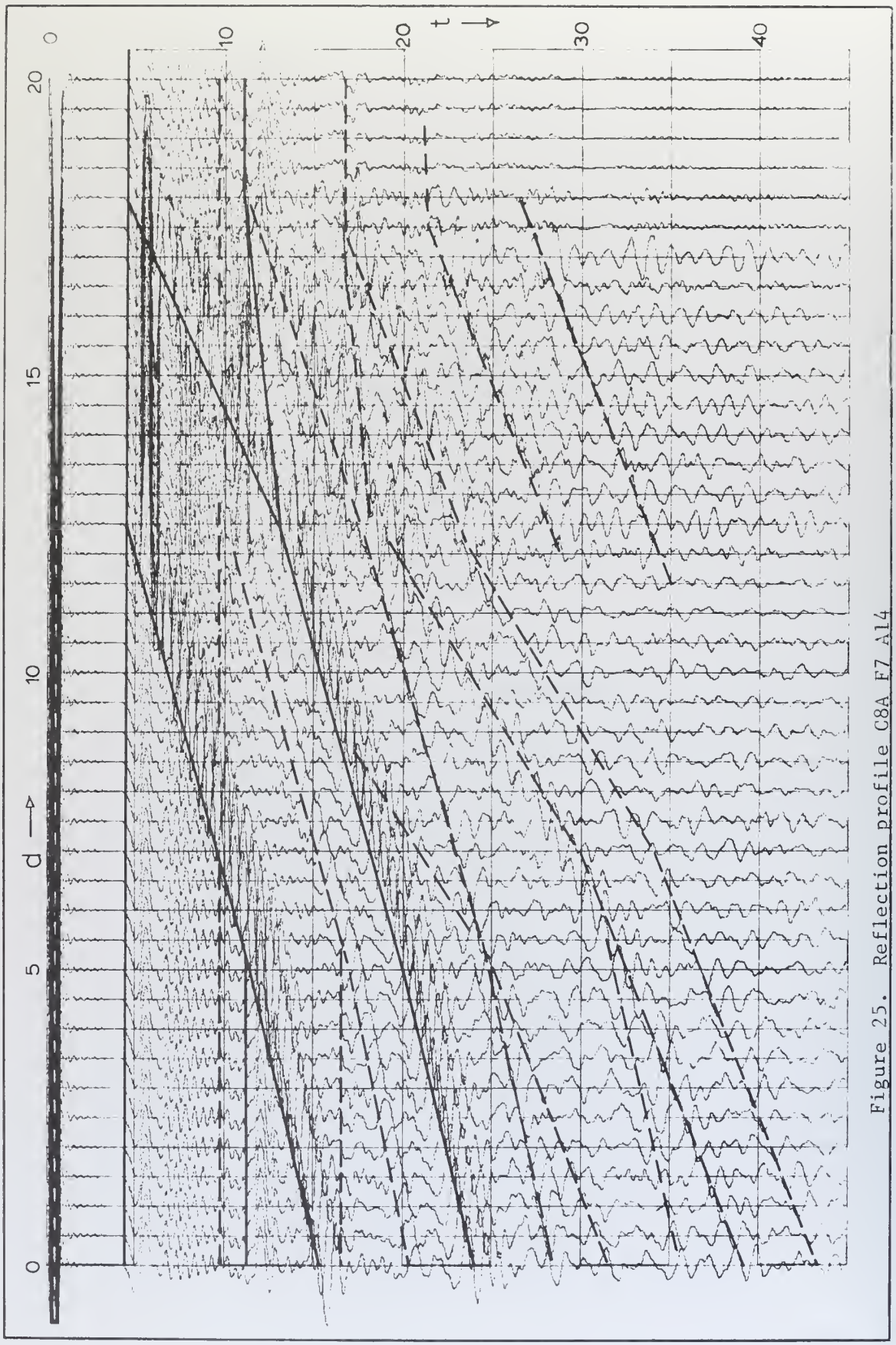

Figure 25. Reflection profile C8A F7 A14

Figure 26

Precision reflection profile C4D F7 A14

DX: 0.10 DT: 0.025 DK: 0.10 EEE: 4.0

N: 251 M: 1800 IP: 2

Horizontal distance (d)

versus

time (t)

———— First reflections

— — — Multiple reflections

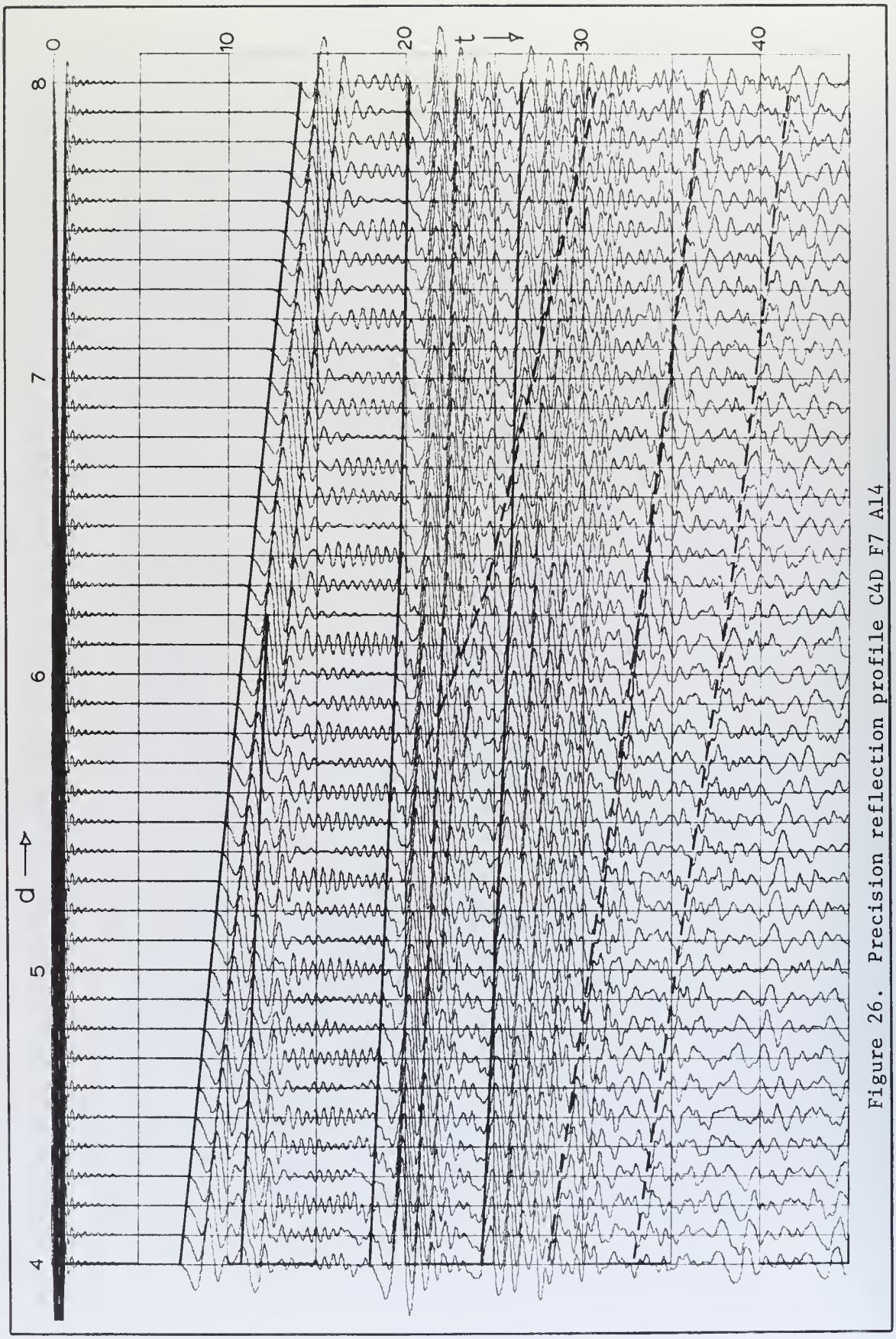

Figure 26. Precision reflection profile C4D F7 A14

first reflections and multiples. Additionally, there is a resonance effect of the large number of multiples being generated. This resonance effect is also present in velocity structure C8A (Fig. 25). There is also a tuning effect due to the relationship between the thickness of the transition zone and the primary period of the incident pulse [Sengbush, Lawrence and McDonal 1961] which would lead to high amplitude reflected pulses. The possibility that instabilities were introduced in these high gradient areas was considered. All parameters, however, are well within stability criteria established in Section II.

Figure 26 is an example of a "precision trace" that may be produced by the model. This seismogram presents a section of a record obtained with the same velocity structure as that shown in Fig. 21 (C4D F7 A14) with an expanded horizontal scale. The horizontal distance covered includes the region where the first sub-bottom layer pinches out. This area (from 4.0 to 8.0) is marked on Fig. 21 with a horizontal line in the record. The "precision trace" was obtained by reducing the shot point spacing (DK).

B. THE REFLECTION/REFRACTION SEISMOGRAMS

Each set of synthetic seismograms developed by the model is designated by a letter-number sequence similar to that used in the reflection profiling model. CA F5A B3 L2 identifies the exact wave velocity and density structure (CA), forcing function (F5A), attenuation parameter (B3) and shot point location (L2) used to generate the records. The seismograms presented in this section were developed using the following velocity structures (Fig. 27 through 29):

(1) Two elastic layers, (CA).

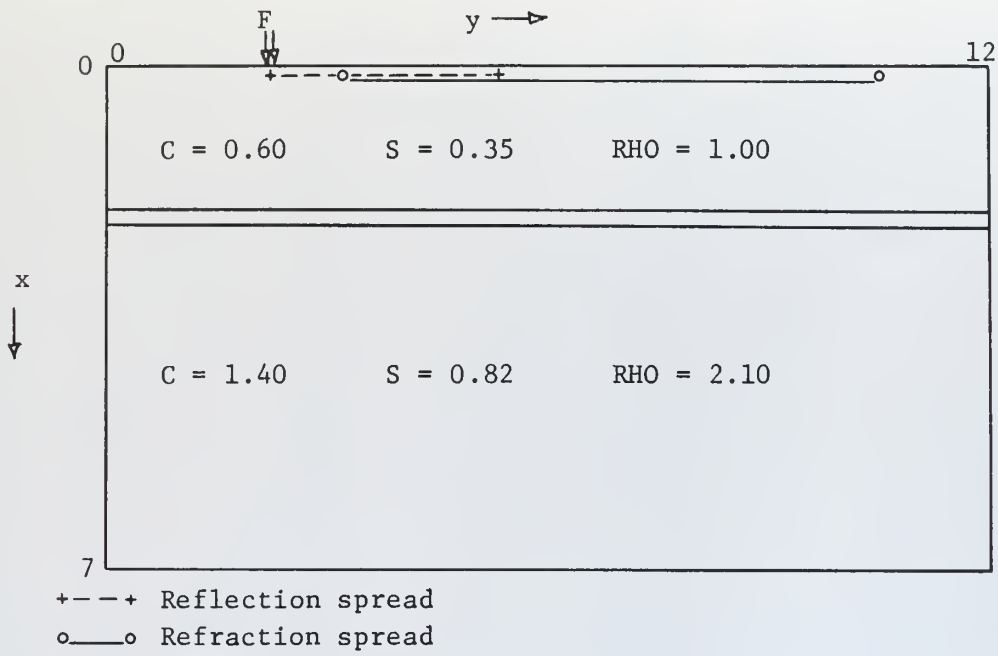

Figure 27. Velocity structure CA

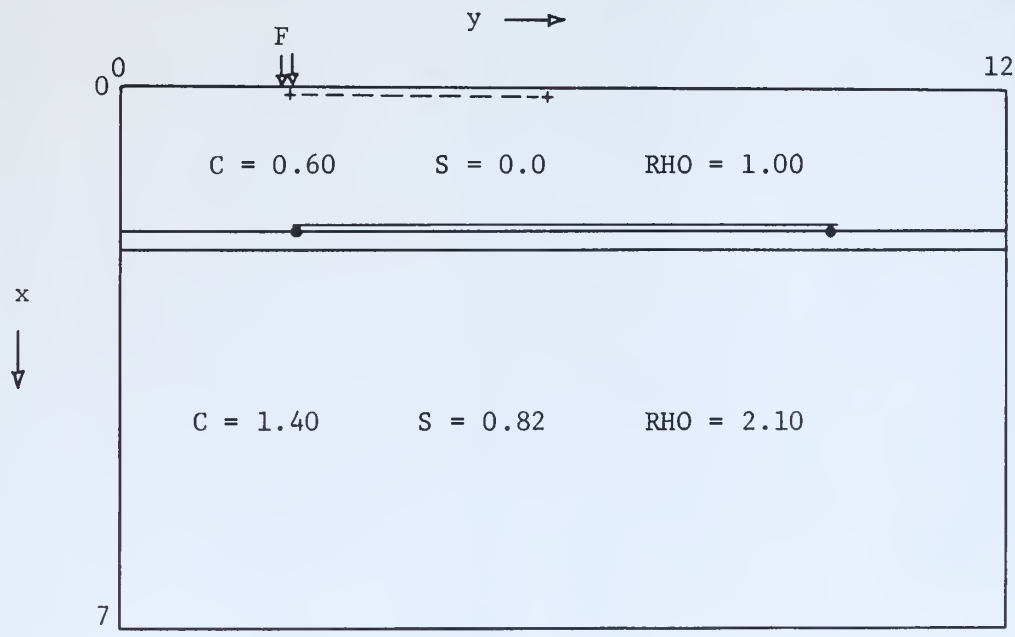

Figure 28. Velocity structure CB

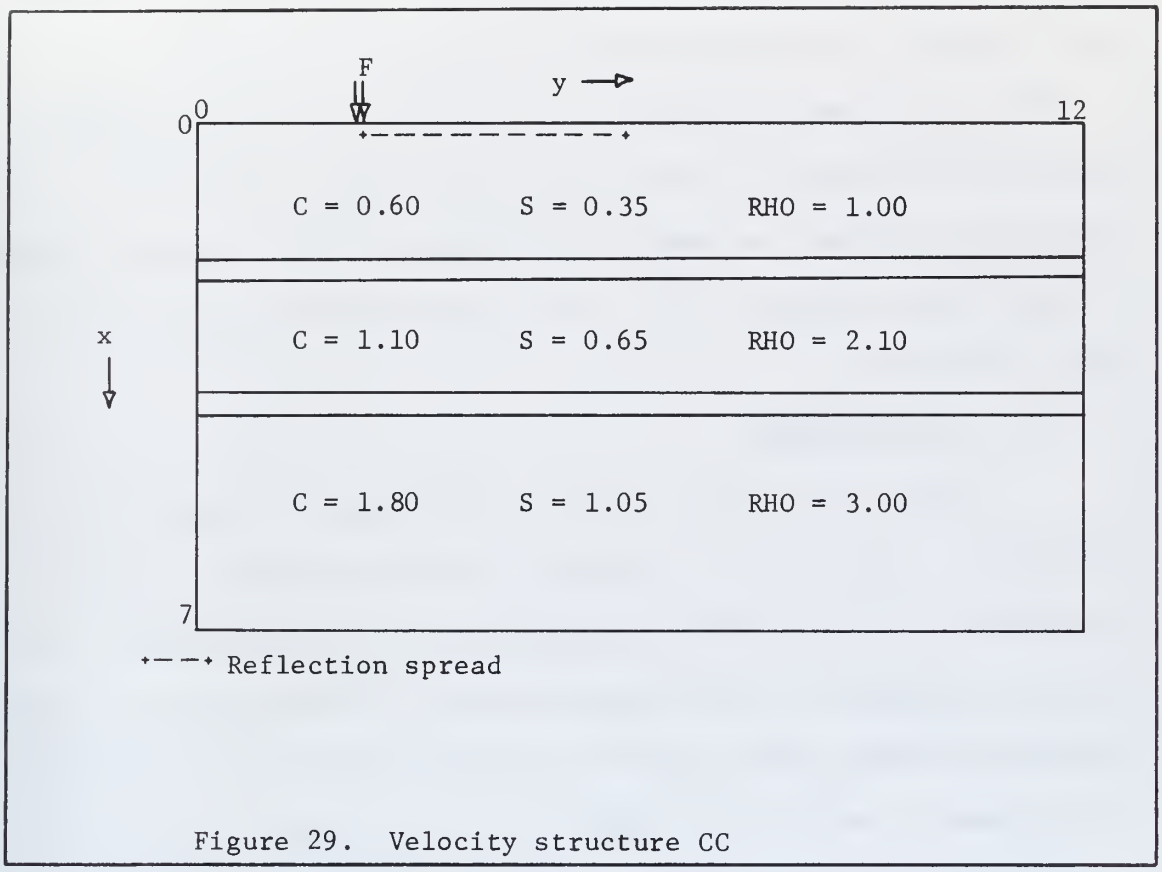

Figure 29. Velocity structure CC

(2) Water layer over elastic layer, (CB).

(3) Three elastic layers, (CC).

With the exception of the water layer in CB, all velocity structures were designed with Poisson's ratio of 0.25.

All traces were produced utilizing forcing function F5A (Fig.30), attenuation parameter B3 (Fig. 31) and shot point location L2. At this shot point location, the surface dilatational forcing stress is applied at mesh points j=15 and j=16. This is marked by the letter "F" in Fig. 27 through 29.

1. The Seismograms

Selected correlated synthetic seismograms are shown in Fig. 32 through 36. Figure 32 is a complete set of four synthetic seismic records for a close (reflection) spread of 25 surface detectors for velocity structure CA. The detector spread is shown in Fig. 27. Comparison of these records shows the interdependence of the displacements and stresses. Actual land field records would include only vertical and/or horizontal displacements, or particle velocity, while marine records would only consist of the dilatational (pressure) record. The additional synthetic seismograms enable the proper phase arrivals to be quickly identified. A set of theoretical time-distance curves was developed for velocity structures CA and CB (Fig. 37), where it was assumed that the width of the transition zone was zero. There is good agreement between these theoretical arrival times and correlated lineations on the synthetic records.

The first trace on the dilatation record corresponds to a normally incident wave. It bears a very close resemblance to traces obtained with the one-dimensional model for similar velocity structures.

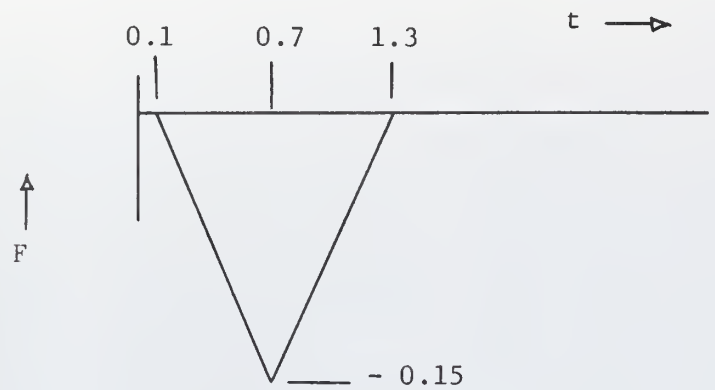

Figure 30. Forcing function F5A

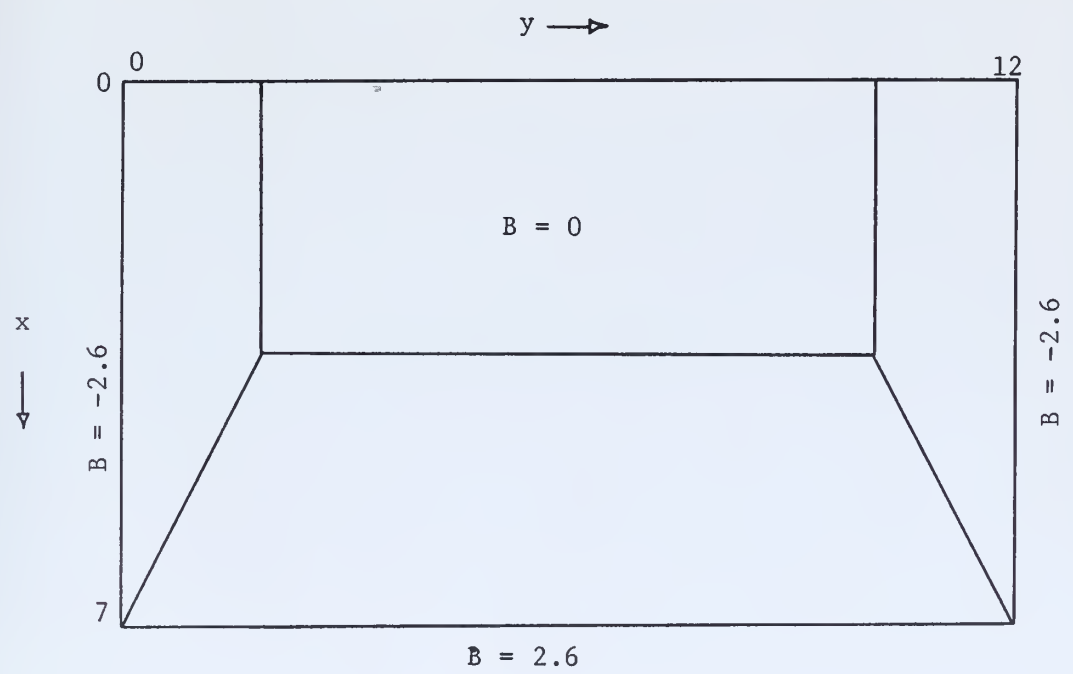

Figure 31. Attenuation parameter B3

Figure 32

Reflection seismogram CA F5A B3 L2

A: Dilatational stress

B: Shear stress

C: Vertical displacement

D: Horizontal displacement

DX: 0.10 DY: 0.15 DT: 0.05

L: 71 M: 81 N: 800

IA: 2 ID: 1 JB: 16 JJ: 1

Horizontal distance (d)

versus

time (t)

————o Direct wave arrivals

———— First reflections

— — — Multiple reflections

———– – —– Shear-dilatation conversion wave

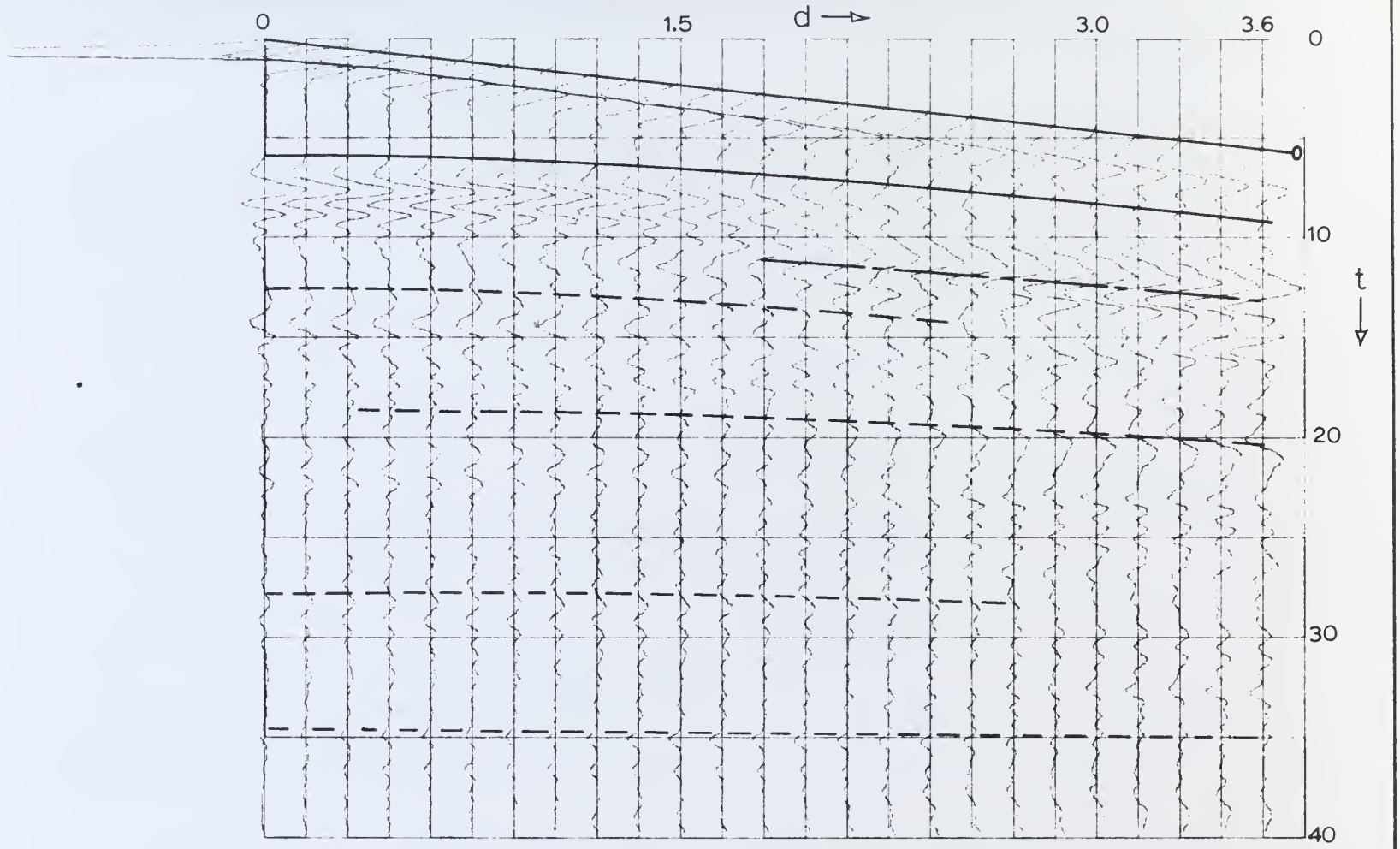

Figure 32A. Reflection Seismogram CA F5A B3 L2: Dilatational Stress

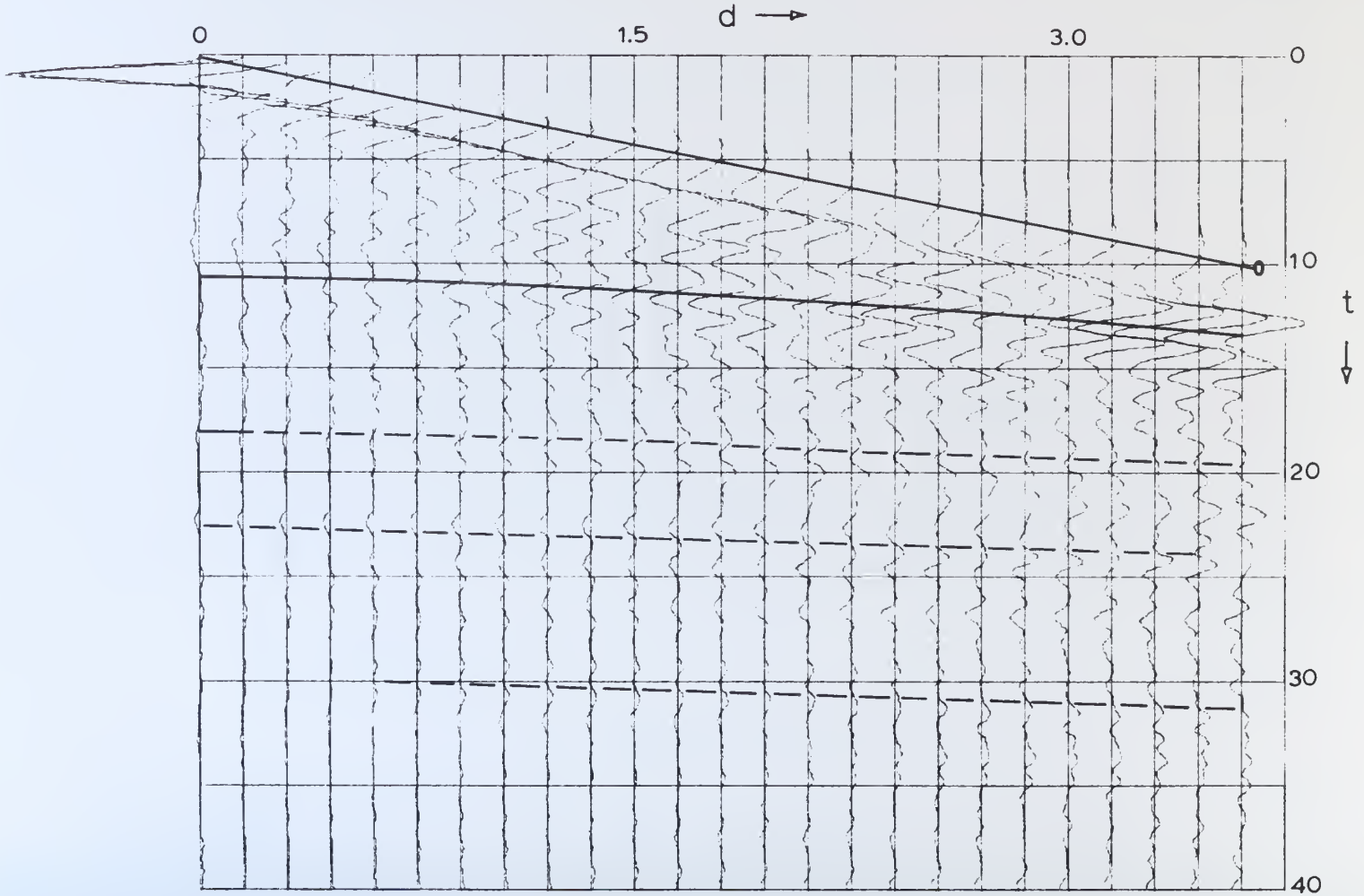

Figure 32B. Reflection Seismogram CA F5A B3 L2: Shear stress

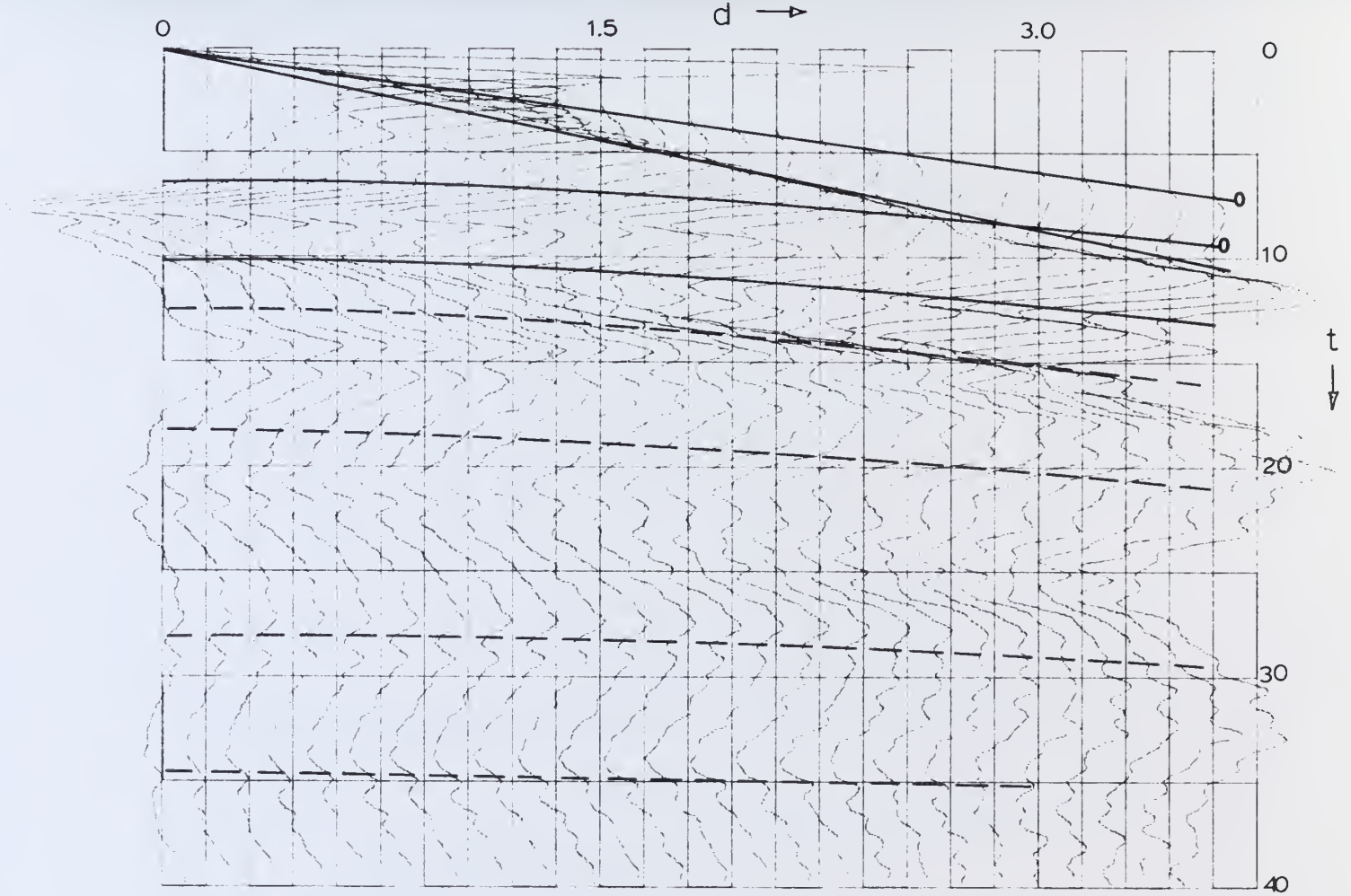

Figure 32C. Reflection Seismogram CA F5A B3 L2: Vertical Displacement

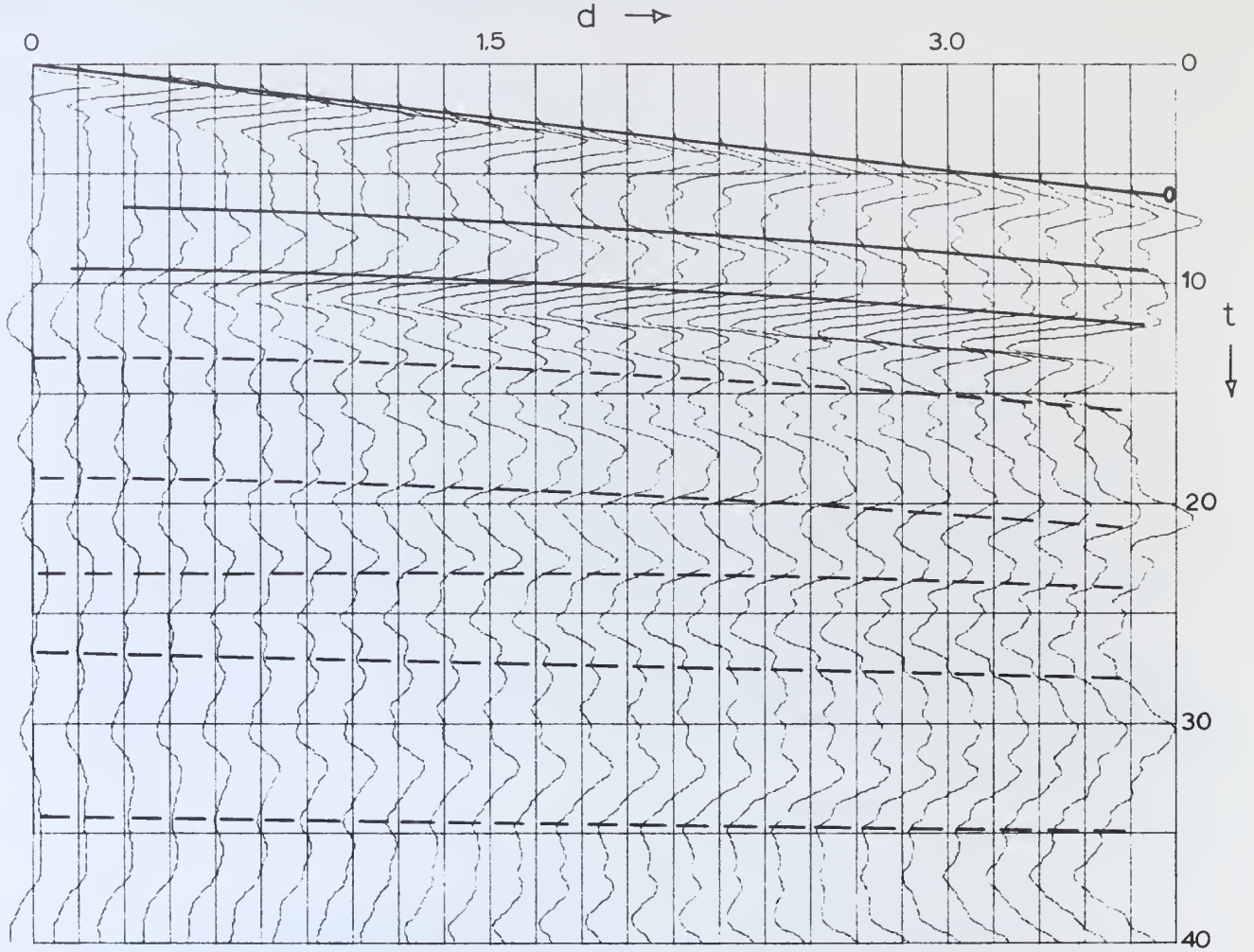

Figure 32D: Reflection Seismogram CA F5A B3 L2: Horizontal Displacement

Figure 33

Refraction seismogram CA F5A B3 L2

Shear stress

DX: 0.10 DY: 0.15 DT: 0.05

L: 71 M: 81 N: 800

IA: 2 ID: 1 JB: 22 JJ: 2

Horizontal distance (d)

versus

time (t)

————o Direct wave arrivals

———— First reflections

—— - —— Refracted arrivals

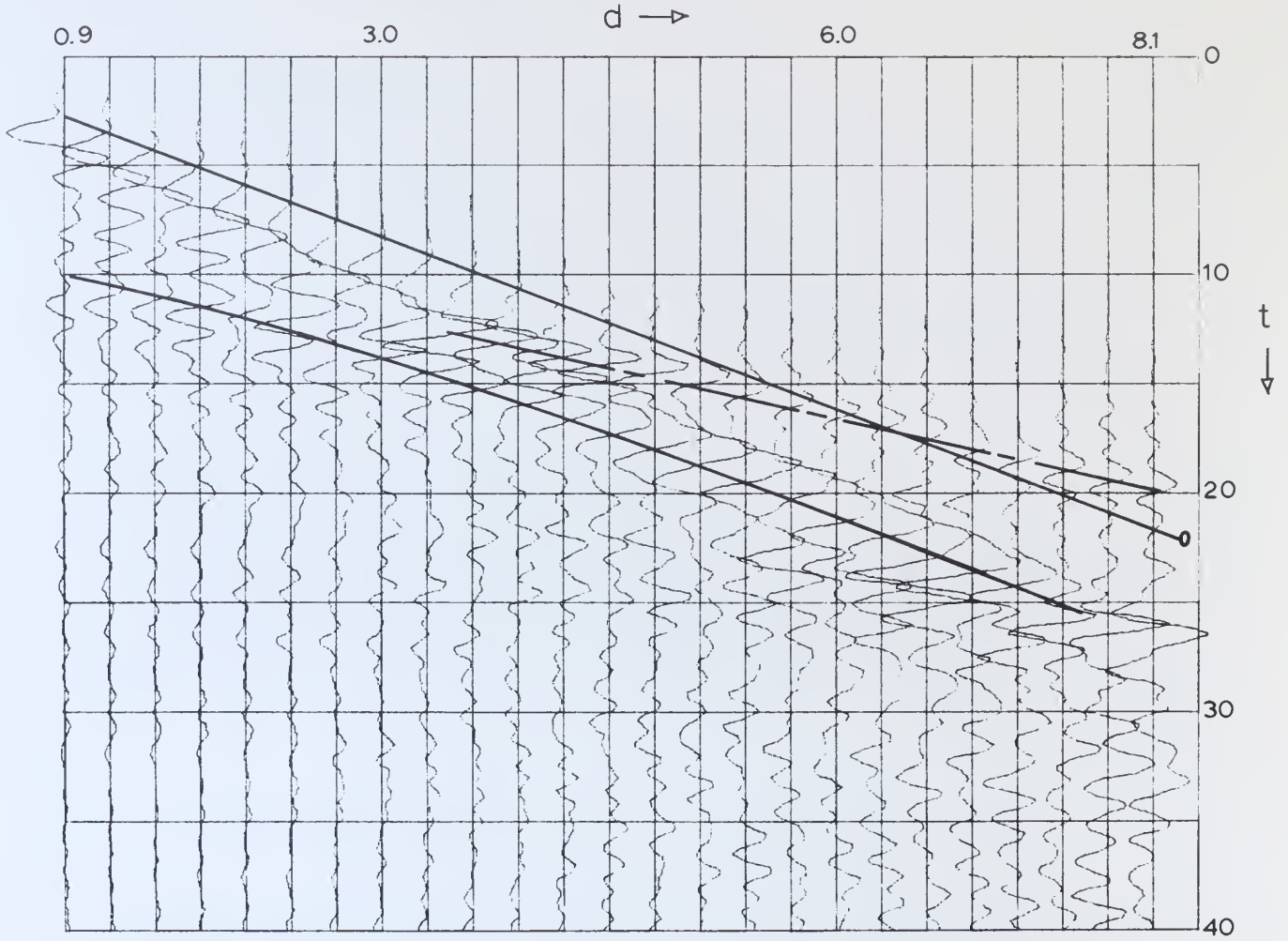

Figure 33. Refraction Seismogram CA F5A B3 L2: Shear Stress

Figure 34

Reflection seismogram CB F5A B3 L2

Dilatational stress

DX: 0.10 DY: 0.15 DT: 0.05

L: 71 M: 81 N: 800

IA: 2 ID: 1 JB: 16 JJ: 1

Horizontal distance (d)

versus

time (t)

————o Direct wave arrivals

———— First reflections

— — — Multiple reflections

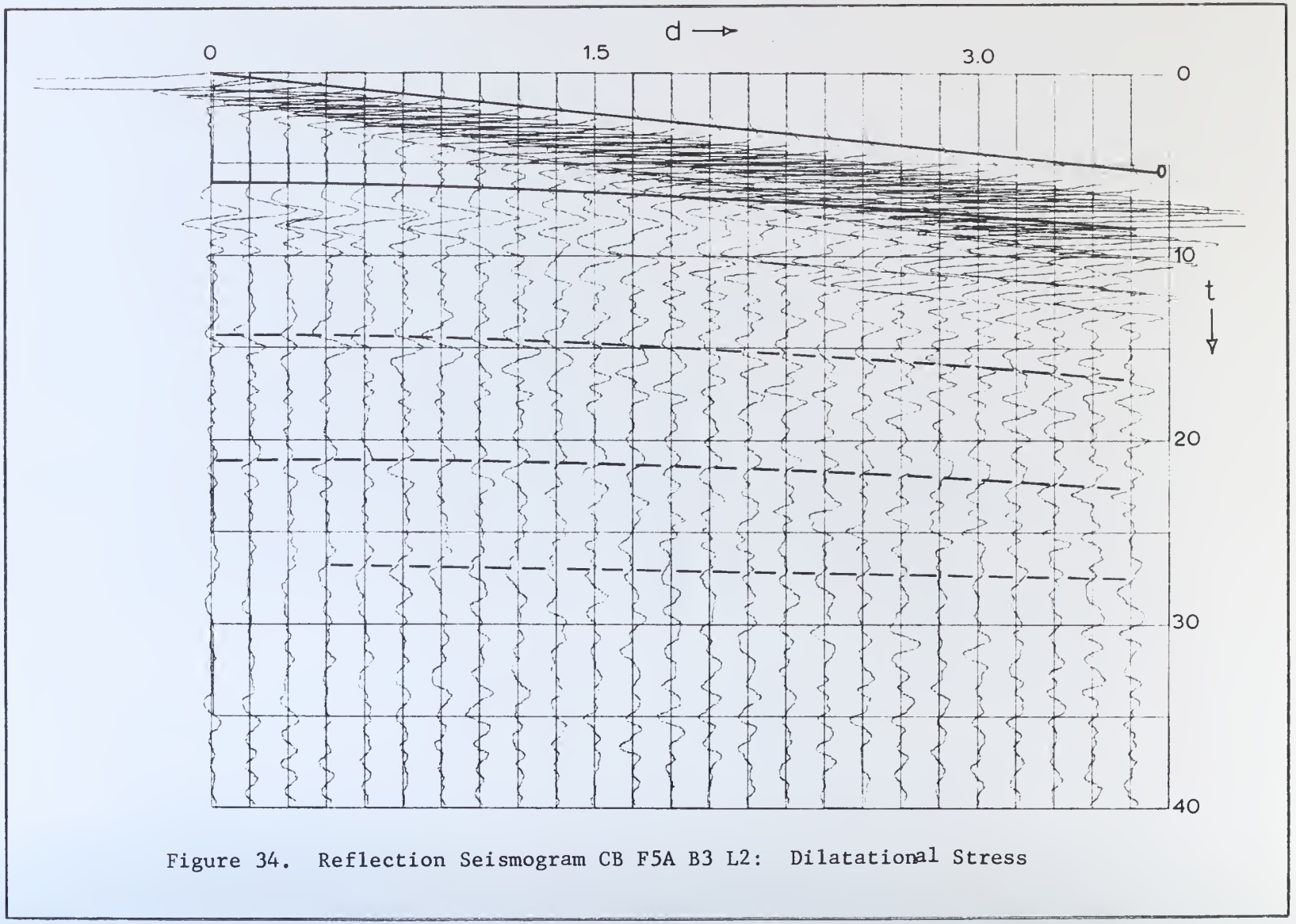

Figure 34. Reflection Seismogram CB F5A B3 L2: Dilatational Stress

Figure 35

Bottom detector seismogram CB F5A B3 L2

Dilatational stress

DX: 0.10 DY: 0.15 DT: 0.05

L: 71 M: 81 N: 800

IA: 20 ID: 20 JB: 16 JJ: 2

Horizontal distance (d)

versus

time (t)

————o Direct wave arrivals

— — — Surface reflected multiples

— - — Interface wave conversion

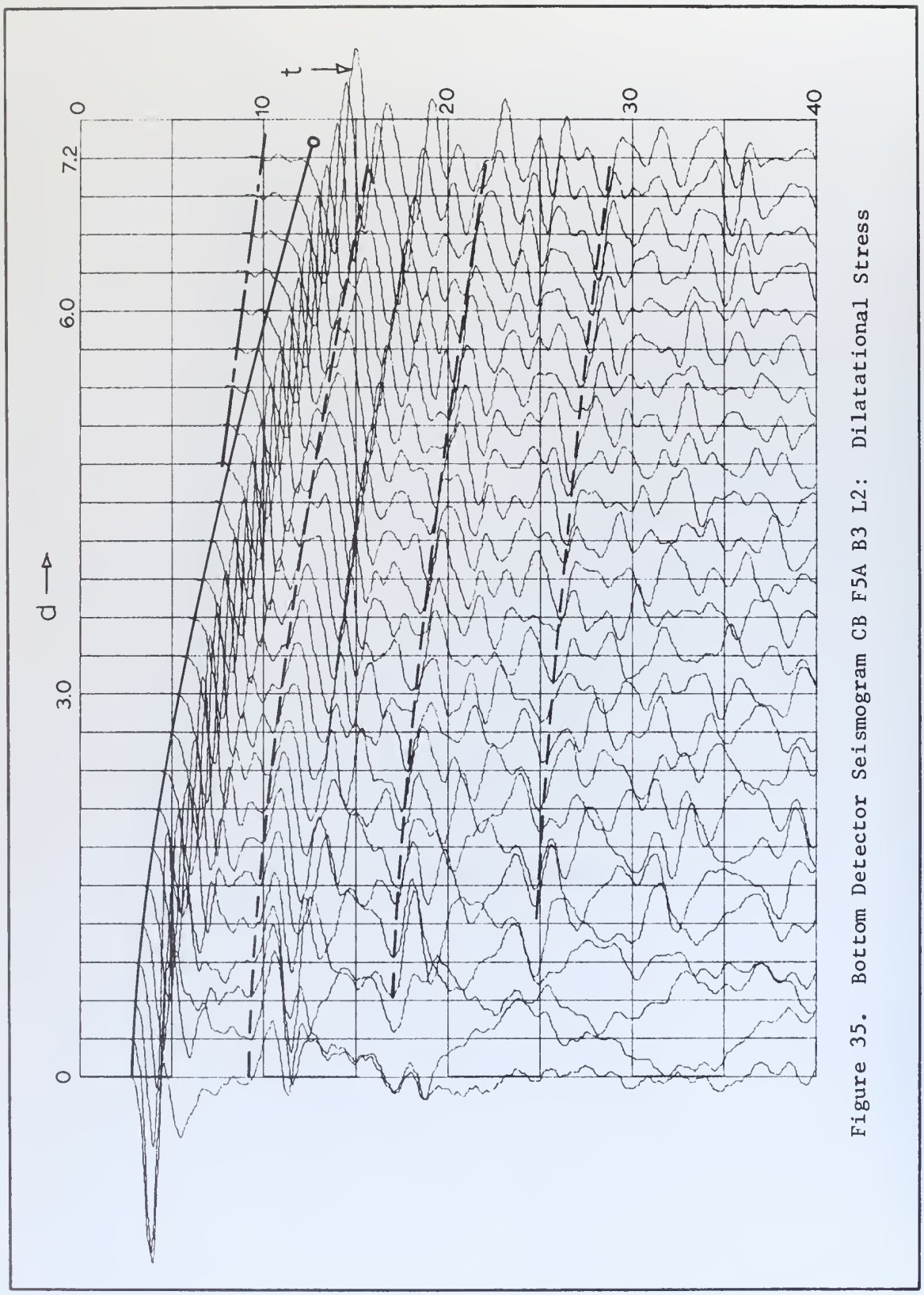

Figure 35. Bottom Detector Seismogram CB F5A B3 L2: Dilatational Stress

Figure 36

Reflection seismogram CC F5A B3 L2

Dilatational stress

DX: 0.10 DY: 0.15 DT: 0.05

L: 71 M: 81 N: 800

IA: 2 ID: 1 JB: 16 JJ: 1

Horizontal distance (d)

versus

time (t)

————o Direct wave arrivals

———— First reflections

— — — Multiple reflections

——-—— Shear wave conversion

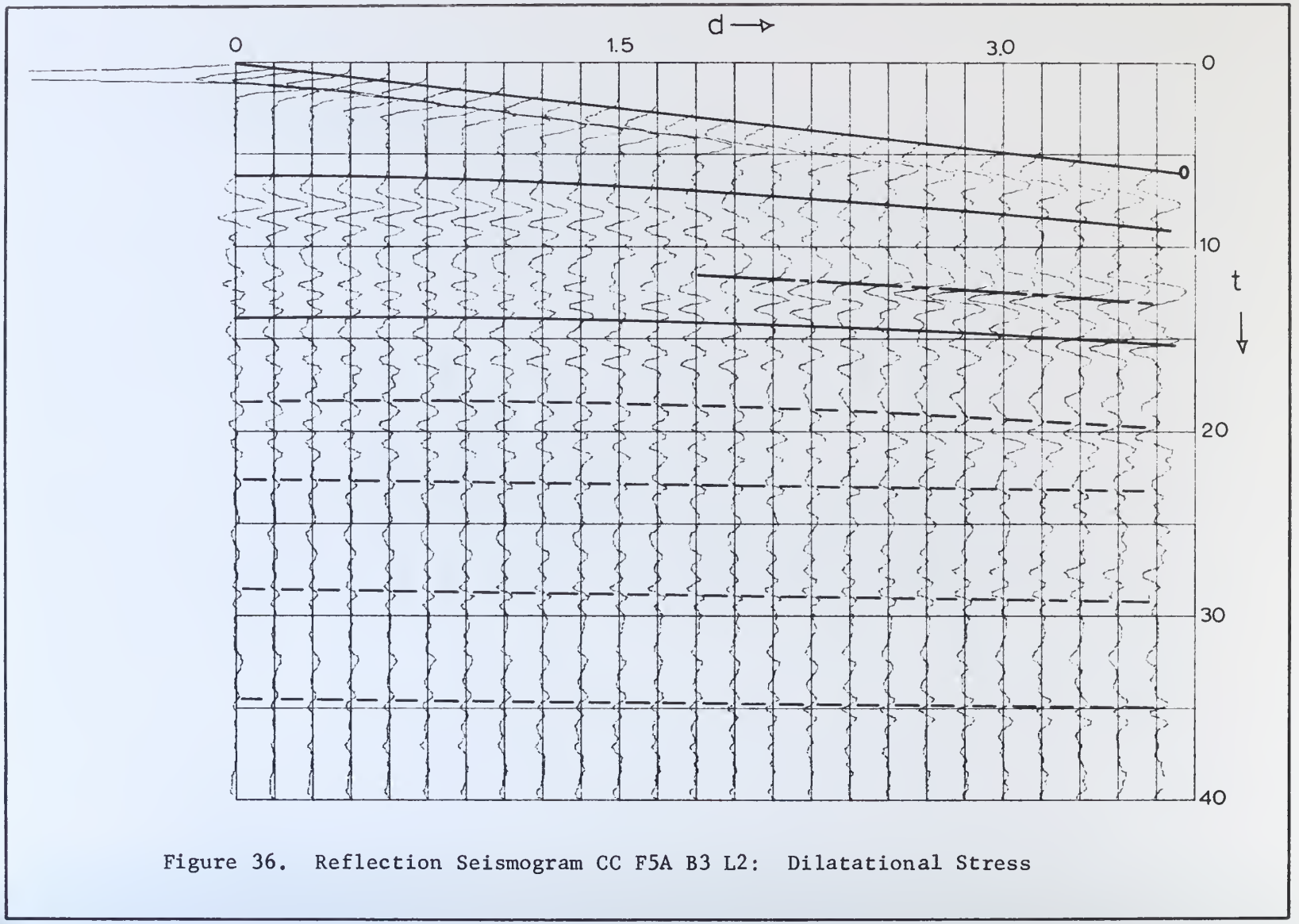

Figure 36. Reflection Seismogram CC F5A B3 L2: Dilatational Stress

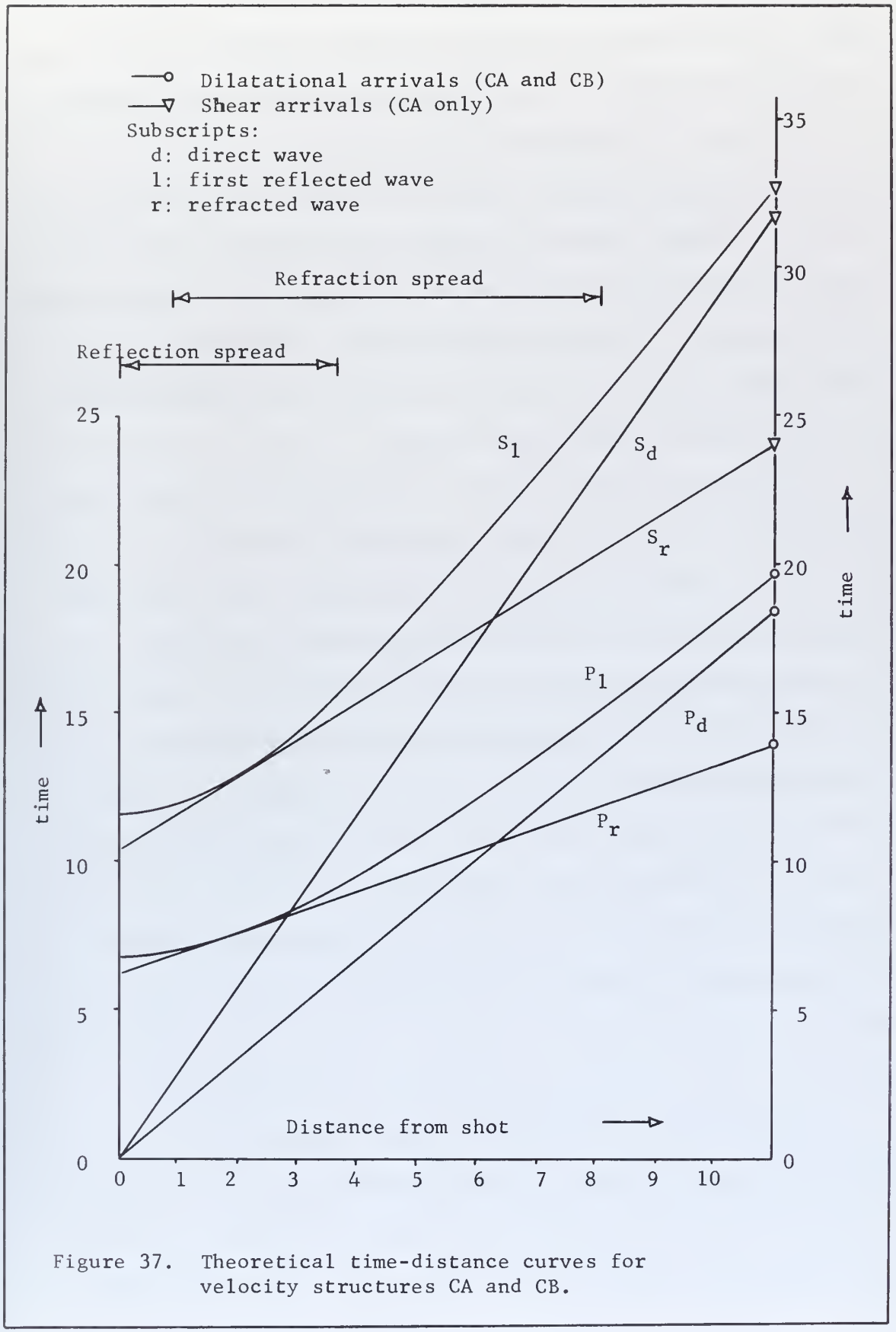

Figure 37. Theoretical time-distance curves for velocity structures CA and CB.

Elastic rebound is present, causing the development of a cyclic wave train. Phase reversal is observed for events reflected from the free surface on all records. These features are particularly apparent in the contour plots discussed in the next section.

Although no refracted arrivals are shown on any of the records of Fig. 32, a close examination of the traces revealed their presence after a refraction record was obtained. Figure 33 is the shear stress refraction record for velocity structure CA. The surface detector spread (shown in Fig. 27) extended across most of the solution space into the attenuation region on the right.

In addition to the arrival of the refracted shear wave, Fig. 33 shows the development of a small shear stress in advance of the first shear arrival. This is generated by the passage of the dilatational wave across the mesh, a result of the coarseness of the mesh relative to the wave velocity. As the dilatational wave passes a mesh point at an oblique angle relative to the x or y axis, shear strains are set up between mesh points. In fact, it is just this effect which causes the generation of the initial shear wave at the forcing function application point, or, more precisely, between one application point (where the applied dilatational stress causes some displacement) and the neighboring mesh point where displacements are different. The shear wave is then generated from two centers. For shot point location L2, these centers are (fictitious) mesh points ($\frac{1}{2}$, $14\frac{1}{2}$) and ($\frac{1}{2}$, $16\frac{1}{2}$).

Figure 34 is the dilatational stress reflection record for velocity structure CB. This structure (shown in Fig. 28) is identical to CA except that, in the upper layer, shear wave velocity (and hence, Lame's constant μ) was set to zero. The record is, of course, very

similar to that obtained from structure CA except that the amplitudes of the first arrivals are somewhat greater. This is caused by the lack of rigidity in the upper layer leading to a loss of the attenuation effect of shear strains on dilatational strains.

An example of a seismogram obtained with a spread of detectors on the bottom of a water layer is shown in Fig. 35. Because of the relationship between shot point location and detector location, the only lineations available for correlation, except for the direct wave, are multiple reflections between the bottom and the surface, and refracted waves. An additional effect observed on this record is the generation of a head wave in advance of the direct wave. This wave is generated at the interface between the two layers by the dilatational wave travelling through the lower medium at a high velocity.

A three-layer reflection seismogram is shown in Fig. 36. The main feature of this record, not seen in the two-layer seismogram, is the mutual interference between the first multiple from the first transition zone and the reflected wave from the second transition zone. As these two waves are out of phase with one another, the initial effect is one of destructive interference. As distance from the shot point is increased, the waves arrive from somewhat different directions, altering the phase relationships, leading eventually to constructive interference.

2. The Contour Output

An on-line printer contour plotting subroutine was developed so that the reflection and transmission of elastic waves might be observed in a qualitative manner. At chosen intervals, the values of horizontal or vertical displacement, dilatational or shear stress or vorticity are

computed for each mesh point, converted to an alphabetic representation and printed as a rectangular contour plot. Figures 38 and 39 show portions of such plots, dilatational stress plotted for the problem CB F5A B4 L2 at time mesh levels K=16 and 91 respectively. Figure 38 shows the generation of the initial dilatational wave by the forcing function. Figure 39 shows the progress of the dilatational wave as it is reflected and transmitted at the transition zone. Some minor modification of the main two-dimensional program was necessary to produce this form of output. Examination of the subroutine shows what additional parameters were necessary. Table X shows the scaled values represented by the plotted characters.

An animated motion picture was made of dilatational and shear stress for this problem. This presentation enables the progress of wave fronts throughout the solution space to be readily observed, including phase changes where they occur. This output allowed the efficacy of the attenuation parameter to be determined quite easily during the development phase of the model. A copy of this motion picture on Super 8mm film is on file at the Naval Postgraduate School, Department of Oceanography (Code 58Ad), and is available to interested investigators on a loan basis.

Some effects were noted on the contour outputs before they were identified on the seismograms. The dilatational plots first showed the development of a head wave in the upper layer (Fig. 40). Other presentations clearly show the development of a shear wave in the lower medium due to the incidence of a dilatational wave against an elastic transition zone (Fig. 41) and the generation of an interface wave travelling along the fluid-elastic boundary in advance of the shear wave (Fig. 42).

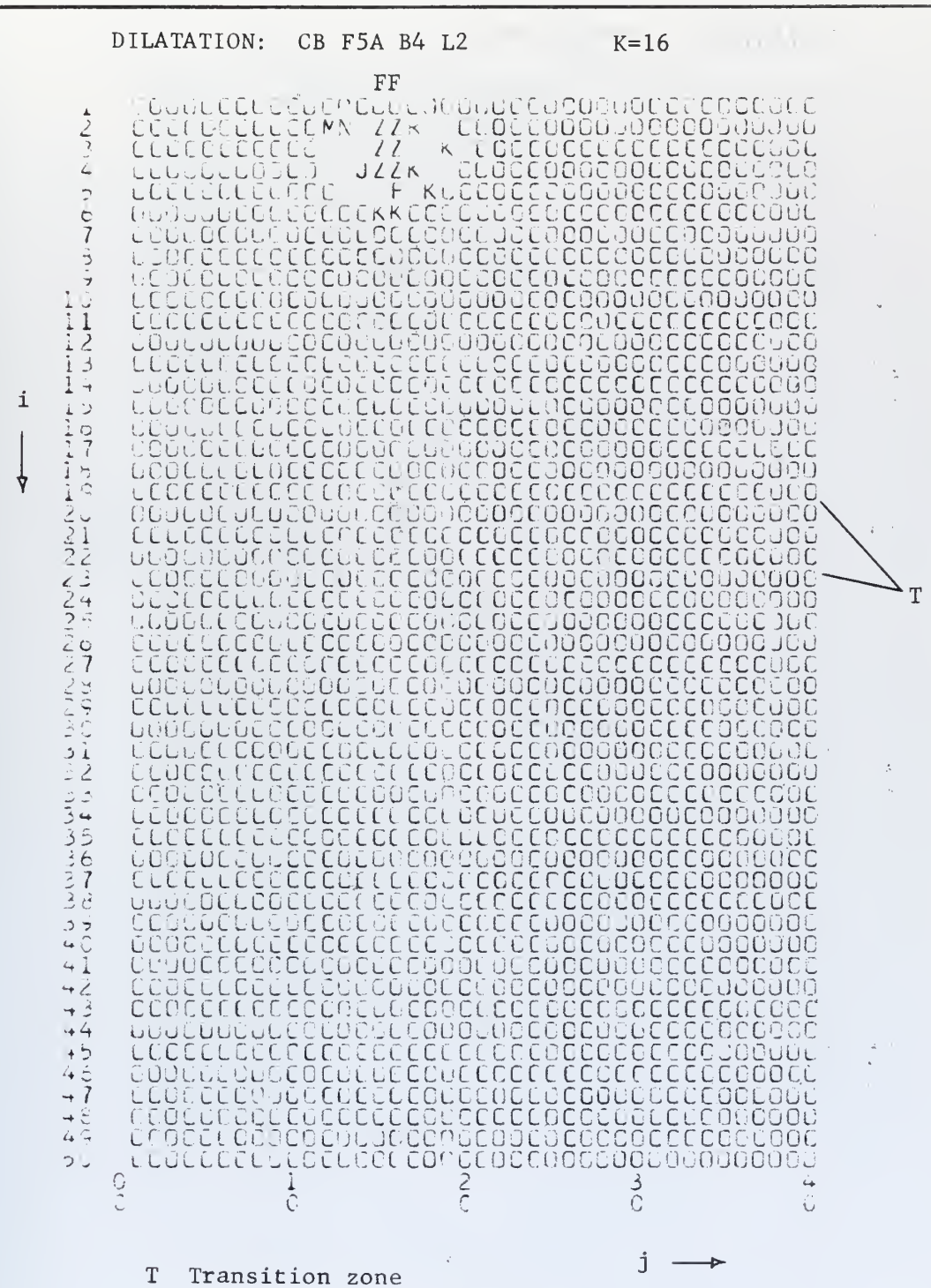

Figure 38. Portion of the printer contour plot showing generation of the dilatational wave. (see Table X for scaled values)

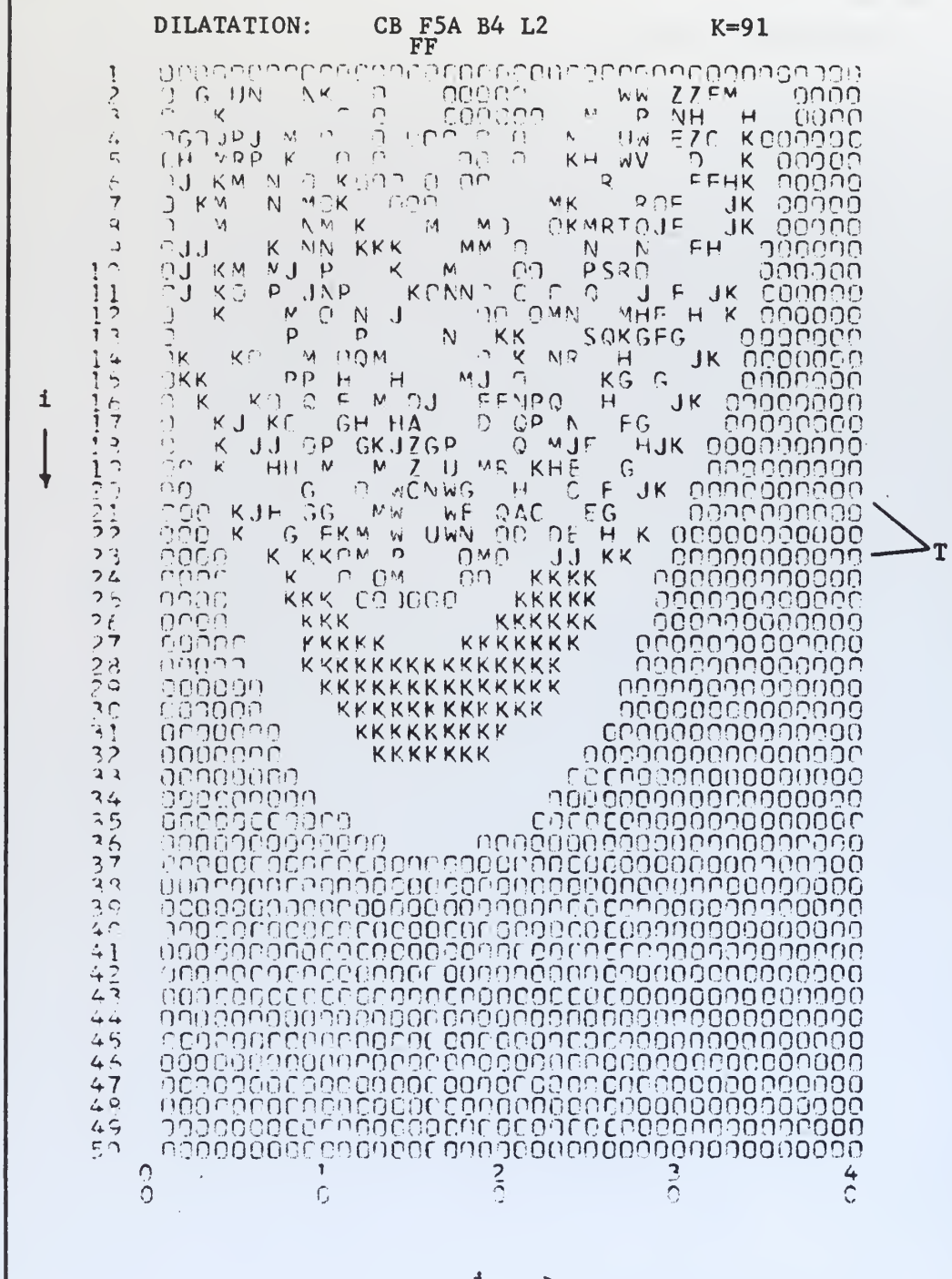

T Transition zone
F Forcing function application point

Figure 39. Portion of the printer contour plot showing transmission of the dilatational wave into the lower media
(see Table X for scaled values)

Table X.

SCALE OF CONTOURED QUANTITY

I	SYM(I)	VALUE
1	A	-0.0085417
2		-0.0081250
3	B	-0.0077083
4		-0.0072917
5	C	-0.0068750
6		-0.0064583
7	D	-0.0060417
8		-0.0056250
9	E	-0.0052083
10		-0.0047917
11	F	-0.0043750
12		-0.0039583
13	G	-0.0035417
14		-0.0031250
15	H	-0.0027083
16		-0.0022917
17	J	-0.0018750
18		-0.0014583
19	K	-0.0010417
20		-0.0006250
21	O	-0.0002083
22		0.0002083
23	M	0.0006250
24		0.0010417
25	N	0.0014583
26		0.0018750
27	P	0.0022917
28		0.0027083
29	Q	0.0031250
30		0.0035417
31	R	0.0039583
32		0.0043750
33	S	0.0047917
34		0.0052083
35	T	0.0056250
36		0.0060417
37	U	0.0064583
38		0.0068750
39	V	0.0072917
40		0.0077083
41	W	OVERSCALE
42	Z	UNDERSCALE

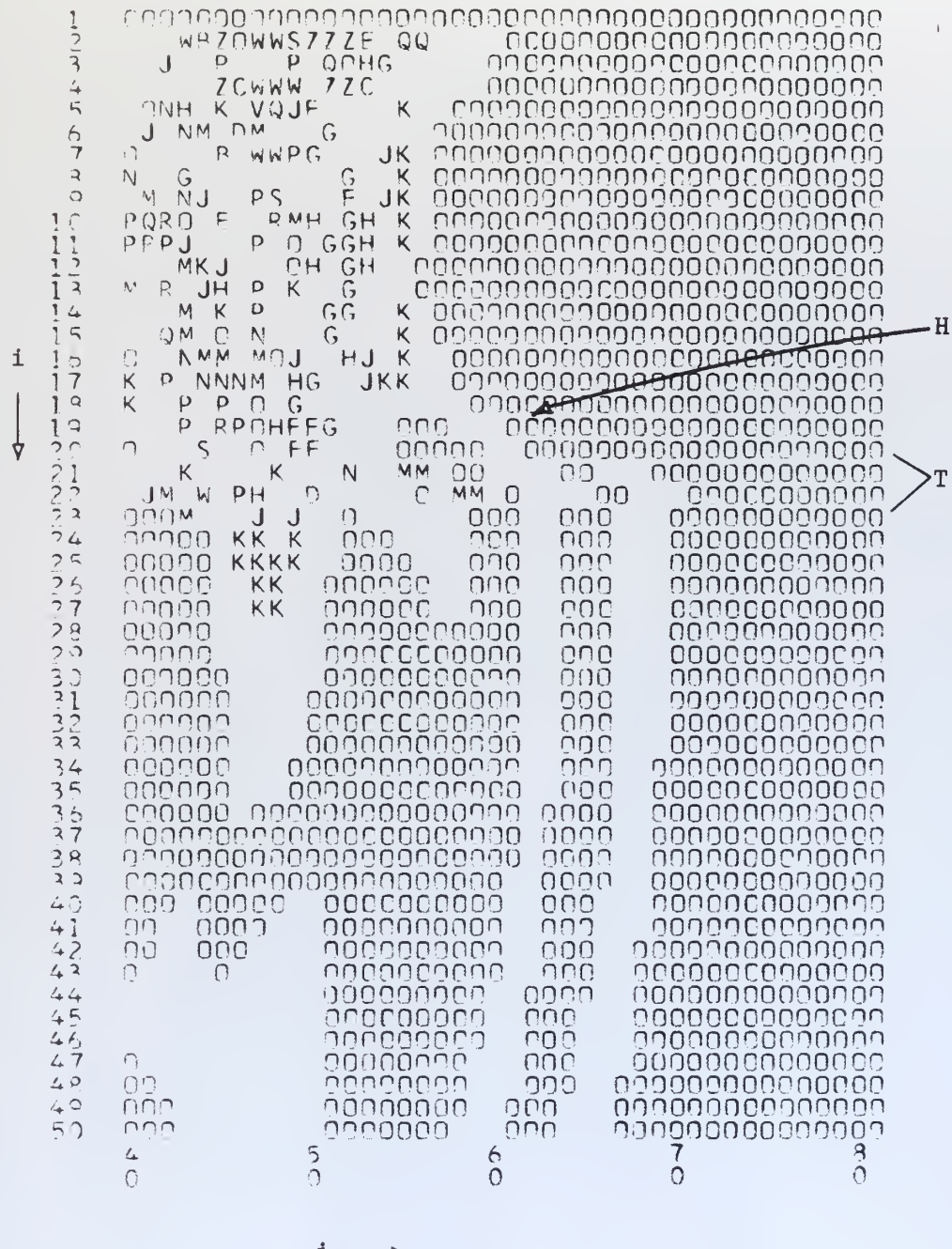

T Transition zone
H Head wave

Figure 40. Portion of the printer contour plot showing the development of a dilatational head wave.
(see Table X for scaled values)

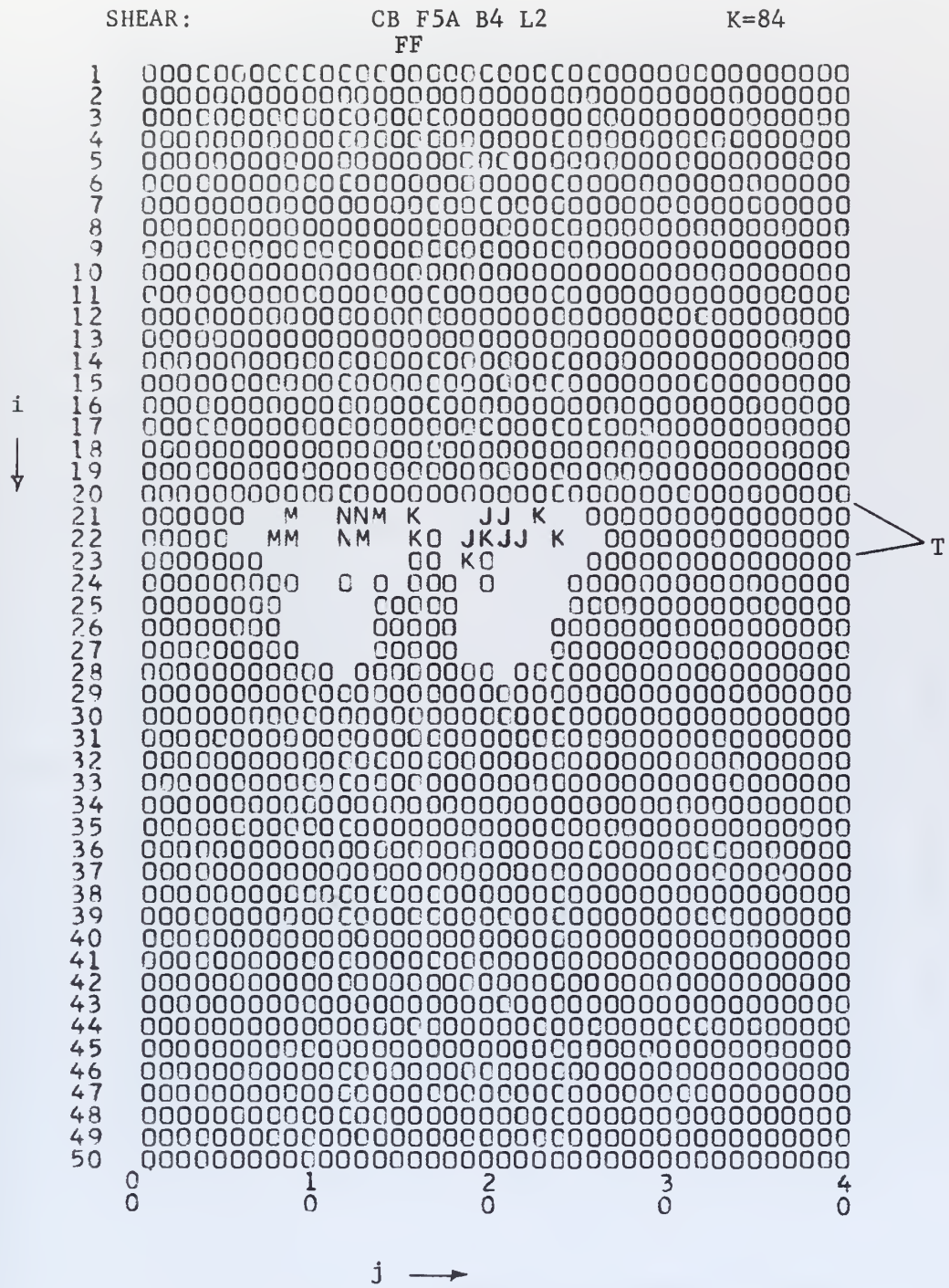

T Transition zone
F Forcing function application point

Figure 41. Portion of the printer contour plot showing generation of a shear wave at the transition zone by the dilatational wave.
(see Table X for scaled values)

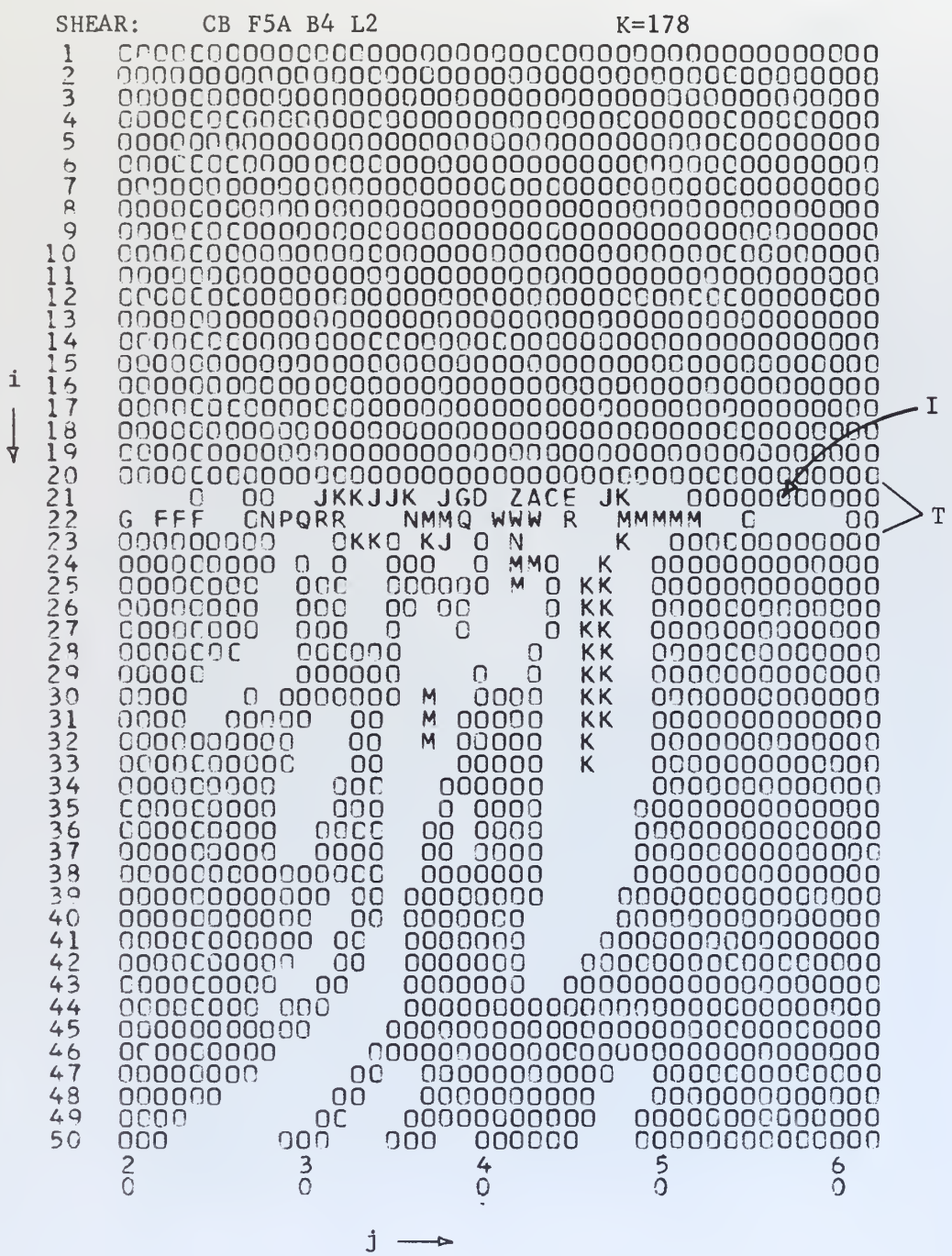

T Transition zone
I Interface wave

Figure 42. Portion of the printer contour plot showing development of an interface shear wave.
(see Table X for scaled values)

V. SUMMARY

The two seismic models presented here were developed primarily as tools to assist in marine geophysical field exploration. The models produce synthetic seismograms similar in format to that of actual field records in order to facilitate direct comparison. Although both models present two-dimensional records (horizontal distance versus time), the reflection profiling model is made up of a series of one-dimensional model solutions. The complete solution simulates a moving source of vertically incident pulses where the velocity structure is slightly altered between transmissions. In contrast, the reflection/refraction model treats the propagation of energy in two dimensions. Each complete solution simulates a single pulse travelling through the solution space. The synthetic seismograms are produced as records from a series of detectors in a horizontal array.

The models are based on numerical solutions to the wave equations in one and two dimensions in bounded domains. The equations are expressed in unsimplified forms which are not amenable to direct analytical solution. The stability of these numerical solutions and their convergence to the analytical solutions was investigated. Stability and convergence criteria were established in terms of mesh ratios and wave velocities.

In order to provide a wide variability of physical simulation, the solution domains are modeled by a number of easily varied non-dimensional parameters. These parameters are used to set the size and subdivision of the solution space as well as the distribution of elastic parameters and the shape and extent of the forcing function.

The structures modeled in this paper were, in general, based upon realistic distributions of the non-dimensional elastic parameters in marine environments. Some of these models have inherent resonance with the type and width of the forcing function used and the mesh sizes. Records are produced with some features which reflect this resonance. In particular, there is some tuning of the pulses in the narrow transition zone in some of the models. Care should be taken when trying to extrapolate features found in these records to cover a more general case.

VI. FUTURE WORK

The applicability of these models to a wide variety of studies was the primary consideration in their design. The interpretation of various velocity structures in this study was limited to a gross overview of simpler problems that might be encountered in field exploration. Although a full presentation of the use of all of the variable parameters was not attempted here, there are areas in both models where improvements could be made which would increase their variability.

A first step in improvement of the one-dimensional model might be the inclusion of a variable depth source. It was felt that this was not warranted in the model due to the complexity of a forcing function at depth that could not be included as part of one boundary condition.

The same improvement might be applied to the two-dimensional model. However, this would involve an additional order of magnitude of complexity and the model could no longer be called "simplified." A more reasonable improvement could be made which would remove the requirement that all transition zones be horizontal. The wave velocities and density could be put into the model as two-dimensional arrays instead of vectors. Terms involving the y-derivative of Lamé's constants and of density would then be retained. This improvement would approximately double the main core storage required (to 550K bytes) and increase the main program run time by about one-third (to 24 min).

Although the attenuation parameters used in both models are considered adequate for the purpose for which they were included (elimination of boundary reflections), they are by no means definitive.

These models could be used to study the effects of various velocity attenuation functions by entering A(x) or B(x,y) as functions of other physical parameters (e.g. overburden pressure, Lame's constants or particle displacement).

Only a single forcing function is presented for each model. Several functions were examined in the development of the models including a flat-topped pulse, spike pulse and "sinc" function. The models could be used to study the reflection and/or refraction of a wide variety of forcing functions, limited only by the size of the time mesh increment (DT).

In Section III, it was noted that an interface wave was observed in shear stress on the contour plot output. This model could certainly be used to study the various classes of such waves under a variety of conditions. Some preliminary work was done in generating particle motion plots from the vertical and horizontal displacement outputs available. Although elliptical particle motions were observed as predicted [Alterman and Rotenberg 1969], limitations of distance from the generating point did not permit identification of the interface phases.

Neither model is by any means limited to the homogeneous layer-transition zone structure presented in this paper. The velocity structure could consist entirely of transition regions of various gradients. This could be applicable to investigation of the effects of the gradients on reverberation.

A collection of records is on file at the Naval Postgraduate School, Department of Oceanography (Code 58Ad).

```
C     SEISMIC REFLECTION PROFILING MODEL
C
C     NUMERICAL METHOD OF ONE DIMENSIONAL SEISMIC MODELING.
C
C     THIS PROGRAM PRODUCES A ONE DIMENSIONAL SEISMIC MODEL FOR THE
C     TRANSMISSION OF A NORMALLY INCIDENT DILATATIONAL WAVE THROUGH
C     TRANSVERSELY ISOTROPIC MEDIA IN WHICH THE DILATATIONAL WAVE
C     VELOCITY AND THE AMOUNT OF VELOCITY ATTENUATION CAN BE
C     DESCRIBED AS COMBINATIONS OF LINEAR FUNCTIONS OF DISTANCE.
C
C          METHOD:
C
C          REPEATED NUMERICAL SOLUTION BY FINITE DIFFERENCES OF THE
C          HYPERBOLIC WAVE EQUATION:
C
C                    (U)TT = (V(U)X)X + A(U)T
C
C          WHERE:
C
C           V IS THE SQUARE OF THE DILATATIONAL WAVE VELOCITY.
C           A IS THE VELOCITY ATTENUATION PARAMETER.
C
C          SUBJECT TO THE FOLLOWING COLLATERAL CONDITIONS:
C
C           B1:  U(L,T) = 0.  LOWER BOUNDARY IS PERFECTLY REFLECTIVE.
C
C           B2:  DU/DX = F(T) ON X=0.  VARIABLE STRESS APPLIED TO
C                                      THE UPPER BOUNDARY.
C
C           I1:  U(X,0) = 0.  INITIAL DISPLACEMENTS ARE ZERO.
C
C           I2:  DU/DT = 0 ON T=0.  INITIAL DISPLACEMENT VELOCITIES
C                                   ARE ZERO.
C     PARAMETER LIST:
C
C          U:   WORKING ARRAY OF DISPLACEMENTS. DIMENSIONED (N,3)
C
C          D:   OUTPUT VECTOR OF DILATATIONAL STRESSES.  DIMENSIONED (M)
C
C          C:   WAVE VELOCITY VECTOR. DIMENSIONED (N).
C
C          A:   ATTENUATION PARAMETER VECTOR.  DIMENSIONED (N)
C
C          F:   FORCING FUNCTION VECTOR. DIMENSIONED (M).
C
C          DX:  MESH SIZE IN THE X DIRECTION.
```

```
C          DT:  MESH SIZE IN THE T DIRECTION.
C
C          DK:  HORIZONTAL DISTANCE BETWEEN SUCCESSIVE SOLUTION
C               STATIONS.
C
C          N:   NUMBER OF X MESH POINTS.  N.LE.251
C
C          M:   NUMBER OF TIME STEPS IN EACH SOLUTION. M.LE.2000
C
C          NC:  NUMBER OF POINTS (CX,CT) DEFINING THE WAVE VELOCITY
C               C(I) POLYGON. NC.LE.20.
C
C          NA:  NUMBER OF POINTS (AX,AT) DEFINING THE DAMPING PARAMETER
C               A(I) POLYGON. NA.LE.20.
C
C          MF:  NUMBER OF POINTS (FT,FX) DEFINING THE FORCING FUNCTION
C               F(I) POLYGON. MF.LE.20.
C
C          IP:  INDEX OF THE X MESH POINT AT WHICH THE OUTPUT STRESS
C               VECTOR IS COMPUTED.
C
C          NG:  NUMBER OF HORIZONTAL STATIONS IN THE VELOCITY ARRAY.
C
C          EX:  VECTOR OF HORIZONTAL STATION LOCATIONS OF THE
C               VELOCITY ARRAY.  DIMENSIONED (NG).
C
C          EE:  ARRAY OF VELOCITIES.  GIVES DEPTH OF A PARTICULAR
C               VELOCITY AT EACH HORIZONTAL STATION.  DIMENSIONED (NG,NC).
C
C          CT:  INITIALIZING VECTOR OF VELOCITY VALUES.  DIMENSIONED (NC).
C
C          EEE: HORIZONTAL DISTANCE TO FIRST SHOT POINT.
C
C          DS:  SCALING FACTOR FOR THE PLOT OF THE STRESS VECTOR.
C
C          TS:  TIME SCALE IN UNITS PER INCH USED IN THE OUTPUT PLOT.
C
C          XSP: SPACING IN INCHES BETWEEN TIME GRID LINES ON THE
C               SYNTHETIC SEISMOGRAM.
C
C          YSP: SPACING IN INCHES BETWEEN TRACES ON THE
C               SYNTHETIC SEISMOGRAM.
C
C     OUTPUT:
C
C               KK SUCCESSIVE GRAPHS OF STRESS VERSUS TIME.
```

```
      DATA GG/'U B2'/
      REAL TA/'TIME'/
      DIMENSION U(251,3),C(251),A(251),F(2000),CX(20),CT(20),AX(20),
     1AT(20),FX(20),FT(20),D(2000),T(2000),X(251),EE(10,13),
     2XG(250),YG(250),GTI(11),EX(10),ET(10),CC(50),CO(50,13),
     3BA(251),BB(251),BC(251),BD(251),BE(251),BF(251)
      READ(5,102)(GTI(I),I=1,11)
      READ(5,103) N,M,NA,NC,NF,NG,LL,IP,NCT,KK
      READ(5,101) DX,DT,DK,DS,TS,EEE
      READ(5,100) XSP,YSP
      READ(5,104)(EX(I),I=1,NG)
C
      WRITE(6,999)
      WRITE(6,211) GTI
      WRITE(6,212) GG
      WRITE(6,213) N,M,NA,NC,NF,NG,LL,IP,NCT,KK
      WRITE(6,214) DX,DT,DK,DS,TS,EEE
      WRITE(6,216) XSP,YSP
      WRITE(6,215)(I,EX(I),I=1,NG)
      NM1=N-1
      MM1=M-1
      MM2=M-2
      R2=(DT/DX)**2
      TP=1.0
      TINC=1.0/TS
      V=M
      ST=V*DT*TS
C
      READ(5,105)((EE(I,J),I=1,NG),CT(J),J=1,NC)
      READ(5,100)(AX(I),AT(I),I=1,NA)
      READ(5,100)(FX(I),FT(I),I=1,NF)
C
      WRITE(6,999)
      WRITE(6,211) GTI
      WRITE(6,206)
      WRITE(6,210)(J,(EE(I,J),I=1,NG),CT(J),J=1,NC)
      WRITE(6,999)
      WRITE(6,200)(I,AX(I),AT(I),I=1,NA)
      WRITE(6,200)(I,FX(I),FT(I),I=1,NF)
C
      CALL POLYG(N,DX,AX,AT,NA,0.0,A,LB)
      DO 13 J=1,M
   13 F(J)=0.0
      CALL POLYG(LL,DT,FX,FT,NF,0.0,F,LC)
C
      WRITE(6,203) LB
      WRITE(6,202)(I,A(I),I=1,N,5)
      WRITE(6,204) LC
```

```
      WRITE(6,202)(J,F(J),J=1,LL)
      WRITE(6,999)
   18 T(1) = 0.0
      X(1) = 0.0
      DO 19 I=1,N
      V=I-1
   19 X(I)=V*DX
      DO 20 J=1,M
      V=J-1
   20 T(J)=V*DT*TS
C
      DO 48 J=1,NC
      DO 49 I=1,NG
      ET(I)=EE(I,J)
   49 CONTINUE
      CALL POLYG(KK,DK,EX,ET,NG,EEE,CC,LF)
      DO 51 I=1,KK
      CO(I,J)=CC(I)
   51 CONTINUE
   48 CONTINUE
      V=KK
      YMAX=V*YSP
      CALL GRID(0.0,ST,0.0,YMAX,XSP,YSP,XG,YG,KA,LO)
      CALL PLOTS
      CALL SYMBOL(1.0,1.0,0.14,GTI,00.0,44)
      CALL SYMBOL(1.0,0.00,0.14,'C D LODGE   BOX 96    B1',0.0,24)
      CALL AXIS(0.0,2.0,TA,NCT,ST,0.0,0.0,TINC)
      CALL PLOT(0.0,2.5,-3)
      CALL LINE(XG,YG,KA,1,1)
C
C
C     SETTING FIRST TWO ROWS TO ZERO:
C
      DO 14 KY=1,KK
      DO 10 I=1,N
      U(I,1)=0.0
      U(I,2)=0.0
   10 CONTINUE
      D(1)=0.0
      D(2)=0.0
      DO 52 I=1,NC
      CX(I)=CO(KY,I)
   52 CONTINUE
C
      VOX=KY-1
      VOX=VOX*DK
      WRITE(6,217) KY,VOX
      WRITE(6,211) GTI
```

```
      WRITE (6,200) (I,CX(I),CT(I),I=1,NC)
      CALL POLYG(N,DX,CX,CT,NC,0.0,C,LA)
C
      DC=C(2)-C(1)
      C2=C(1)**2
      BA(1)=1.0/(1.0-0.5*A(1)*DT)
      BB(1)=(-1.0-0.5*A(1)*DT)*BA(1)
      BC(1)=(2.0-2.0*C2*R2)*BA(1)
      BD(1)=C(1)*R2*DC
      BE(1)=(C2*R2+BD(1))*BA(1)
      BF(1)=(C2*R2-BD(1))*BA(1)
      DO 7 I=2,NM1
      DC=C(I+1)-C(I-1)
      C2=C(I)**2
      BA(I)=1.0/(1.0-0.5*A(I)*DT)
      BB(I)=(-1.0-0.5*A(I)*DT)*BA(I)
      BC(I)=(2.0-2.0*C2*R2)*BA(I)
      BD(I)=0.5*C(I)*R2*DC
      BE(I)=(C2*R2+BD(I))*BA(I)
    7 BF(I)=(C2*R2-BD(I))*BA(I)
CCC
CCC   COMPUTING FIRST AND LAST MEMBERS OF J+1 ROW:
CCC
      NN=1
    9 DO 11 J=3,M
    6 GO TO(1,2,3,5),NN
    1 LI=3
      L=2
      LJ=1
      GO TO 4
    2 LI=1
      L=3
      LJ=2
      GO TO 4
    3 LI=2
      L=1
      LJ=3
      GO TO 4
    5 NN=1
      GO TO 1
    4 U(1,LI)=BC(1)*U(1,L)+(BE(1)+BF(1))*U(2,L)-BF(1)*2.*DX*F(J)
     1+BB(1)*U(1,LJ)
      U(N,LI)  = 0.0
C
CCC   COMPUTING ENTIRE J+1 ROW:
C
      DO 12 I=2,NM1
      U(I,LI)=BC(I)*U(I,L)+BE(I)*U(I+1,L)+BF(I)*U(I-1,L)+BB(I)*U(I,LJ)
```

```
   12 CONTINUE
      NN=NN+1
      D(J)=(0.50/DX)*DS*(U(IP+1,LI)-U(IP-1,LI))
   11 CONTINUE
C
      CALL LINE(T,D,M,1,1)
      CALL PLOT(0.0,YSP,-3)
   14 CONTINUE
      V=10.0
      CALL PLOT(0.0,V,-3)
      CALL PLOTE
      WRITE(6,205)
C
  100 FORMAT(2F10.0)
  101 FORMAT(6F10.0)
  102 FORMAT(11A4)
  103 FORMAT(10I5)
  104 FORMAT(F10.0)
  105 FORMAT(5F10.0)
  200 FORMAT(I7,2F15.5)
  202 FORMAT(I7,F12.5)
  203 FORMAT('1',9X,'LB =',I3//5X,'I',7X,'A(I)'//)
  204 FORMAT('1',9X,'LC =',I3//5X,'J',7X,'F(J)'//)
  205 FORMAT('0'//6X,'END OF GRAM'//)
  206 FORMAT('0',15X,'VELOCITY DEFINING ARRAY'//30X,'DEPTHS',
     122X,'VELO'/)
  210 FORMAT('0',6X,I3,3X,10F5.1)
  211 FORMAT('0',10X,11A4/)
  212 FORMAT(13X,A4/)
  213 FORMAT('0',9X,'N',5X,'M',5X,'NA',4X,'NC',4X,'NF',4X,'NG',4X,
     1'LL',4X,'IP',4X,'NCT',3X,'KK'/6X,10I6)
  214 FORMAT('0',6X,'DX',10X,'DT',10X,'DK',10X,'DS',10X,'TS',10X,
     1'EEE'/6F12.4)
  215 FORMAT('0',10X,'EX(I)'/6(I6,F10.4/))
  216 FORMAT('0',6X,'XSP',9X,'YSP'/2F12.4)
  217 FORMAT('1'//10X,'SHOT NR:',I3,10X,'DIST:',F8.3//)
  999 FORMAT('1')
C
      STOP
      END
```

```
C
C     SEISMIC REFLECTION/REFRACTION MODEL
C
C     NUMERICAL METHOD OF TWO DIMENSIONAL SEISMIC MODELING.
C
C     THIS PROGRAM PRODUCES A TWO DIMENSIONAL SEISMIC MODEL FOR THE
C     TRANSMISSION OF DILATATIONAL AND SHEAR WAVES THROUGH TRANSVERSELY
C     ISOTROPIC HORIZONTALLY LAYERED MEDIA IN WHICH THE WAVE VELOCITIES,
C     DENSITY AND VELOCITY CAN BE DESCRIBED AS COMBINATIONS OF LINEAR
C     FUNCTIONS OF DISTANCE.
C
C     PARAMETER LIST:
C
C      DISTRIBUTION PARAMETERS AND WORKING ARRAYS AND VECTORS:
C
C        U:  WORKING ARRAY OF VERTICAL DISPLACEMENTS. DIMENSIONED (L,M,3).
C
C        V:  WORKING ARRAY OF HORIZONTAL DISPLACEMENTS. DIMENSIONED (L,M,3)
C
C        B:  ARRAY OF ATTENUATION PARAMETERS. DIMENSIONED (L,M).
C
C        C:  VECTOR OF DILATATIONAL VELOCITIES. DIMENSIONED (L).
C
C        S:  VECTOR OF SHEAR VELOCITIES. DIMENSIONED (L).
C
C        RH: VECTOR OF DENSITIES. DIMENSIONED (L).
C
C        F:  ARRAY OF FORCING FUNCTIONS. DIMENSIONED (M,LL)
C
C        FI: FORCING FUNCTION INPUT VECTOR. DIMENSIONED (LL).
C
C        PD,PS,PR,PQ: OUTPUT VECTORS OF DILATATIONAL AND SHEAR STRESSES,
C            VERTICAL AND HORIZONTAL DISPLACEMENTS, EACH DIMENSIONED (KK).
C
C      NUMERICAL PARAMETERS:
C        DX: MESH SIZE IN THE X DIRECTION.
C
C        DY: MESH SIZE IN THE Y DIRECTION.
C
C        DT: MESH SIZE IN THE T DIRECTION.
C
C        L:  NUMBER OF X MESH POINTS.  L.LE.71
C
C        M:  NUMBER OF Y MESH POINTS.  M.LE.81
C
C        N:  NUMBER OF T MESH POINTS.  N.LE.800
C
C        NC: NUMBER OF POINTS DEFINING THE WAVE VELOCITY AND DENSITY
C            POLYGONS. NC.LE.20
```

```
C
C       NBA:NUMBER OF POINTS DEFINING THE VERTICAL ATTENUATION
C           PARAMETER. NBA.LE.20
C
C       NBB:NUMBER OF POINTS DEFINING THE HORIZONTAL ATTENUATION
C           PARAMETER. NBB.LE.20
C
C       NF: NUMBER OF POINTS DEFINING THE FORCING FUNCTION POLYGON. NF.LE.20
C
C       IA: INDEX OF THE X MESH POINT AT WHICH OUTPUT STRESSES ARE
C           TO BE COMPUTED.
C
C       ID: INDEX OF THE X MESH POINT AT WHICH OUTPUT DISPLACEMENTS
C           ARE TO BE COMPUTED.
C
C       KK: NUMBER OF OUTPUT STATIONS (DETECTORS) KK.LE.40
C
C       JB: INDEX OF THE Y MESH POINT OF THE FIRST DETECTOR LOCATION.
C
C       JJ: MESH POINT INCREMENT BETWEEN DETECTORS.
C
C       MA,MB: INCLUSIVE INDICES OF THE FORCING FUNCTION APPLICATION AREA.
C
C       SS: SCALING FACTOR FOR THE OUTPUT VALUES
C
C   OUTPUT:
C
C       THE VALUES OF THE FOUR QUANTITIES (PD,PS,PR,PQ) ARE WRITTEN
C       ON A STORAGE DEVICE (TAPE,DISK OR DRUM) FOR LATER RETREIVAL
C       AND PLOTTING.
C
      DATA GG/'UV11'/
      DIMENSION U(71,81,3),V(71,81,3),AX(20),AT(20),C(71),BA(71),
     1BB(81),FI(100),X(71),Y(81),T(800),B(71,81),F(81,100),S(71),
     2PD(40),PS(40),PR(40),GTI(11),AA(71),AB(71),AC(71),AD(71),
     3AE(71),AF(71),AH(71),AI(71),AJ(71),AK(71),AL(71),RH(71),
     4PQ(40)
      CALL CANCEL(2)
      READ(5,108)(GTI(I),I=1,11)
      READ(5,106) L,M,N,NC,NBA,NBB,NF,IA,LL,KK,JB,JJ,MA,MB,ID
      READ(5,107) DX,DY,DT,SS,TS
      WRITE(6,200)(GTI(I),I=1,11),GG,L,M,N,NC,NBA,NBB,NF,IA,
     1LL,KK,JB,JJ,MA,MB,ID
      WRITE(6,201) DX,DY,DT,SS,TS
      WRITE(1)(GTI(I),I=1,11),GG,L,M,N,NC,NBA,NBB,NF,IA,LL,
     1KK,JB,JJ,MA,MB,ID
      WRITE(1) DX,DY,DT,SS,TS
      NM1=N-1
```

```
      NM2=N-2
      LM1=L-1
      RA=(DT/DX)**2
      RB=0.25*(DT**2)/(DX*DY)
      RC=(DT/DY)**2
      READ(5,100)(AX(I),AT(I),I=1,NC)
      CALL POLYG(L,DX,AX,AT,NC,0.0,RH,KR)
      WRITE(6,110)(I,AX(I),AT(I),I=1,NC)
      READ(5,100)(AX(I),AT(I),I=1,NC)
      CALL POLYG(L,DX,AX,AT,NC,0.0,S,KS)
      WRITE(6,110)(I,AX(I),AT(I),I=1,NC)
      READ(5,100)(AX(I),AT(I),I=1,NC)
      CALL POLYG(L,DX,AX,AT,NC,0.0,C,KC)
      WRITE(6,110)(I,AX(I),AT(I),I=1,NC)
      READ(5,100)(AX(I),AT(I),I=1,NBA)
      CALL POLYG(L,DX,AX,AT,NBA,0.0,BA,KB)
      XL=AX(2)
      READ(5,100)(AX(I),AT(I),I=1,NBB)
      CALL POLYG(M,DY,AX,AT,NBB,0.0,BB,KZ)
      READ(5,100)(AX(I),AT(I),I=1,NF)
      CALL POLYG(100,DT,AX,AT,NF,0.0,FI,KF)
      DO 1 I=1,L
      Z=I-1
      X(I)=Z*DX
      IF(X(I).GT.XL) GO TO 3
      DO 2 J=1,M
    2 B(I,J)=BB(J)
      GO TO 1
    3 DO 4 J=1,M
      IF(BA(I).GT.BB(J)) GO TO 5
      B(I,J)=BB(J)
      GO TO 4
    5 B(I,J)=BA(I)
    4 CONTINUE
    1 CONTINUE
      WRITE(6,101)KC
      WRITE(6,102)(I,X(I),C(I),I=1,L)
      WRITE(6,120) KS
      WRITE(6,102)(I,X(I),S(I),I=1,L)
      WRITE(6,121) KR
      WRITE(6,102)(I,X(I),RH(I),I=1,L)
      WRITE(6,103)KB
      WRITE(6,102)(I,X(I),BA(I),I=1,L)
      DO 6 J=1,M
      Z=J-1
      Y(J)=Z*DY
      DO 7 K=1,LL
      IF(J.LT.MA.OR.J.GT.MB) GO TO 8
```

```
      F(J,K)=FI(K)
      GO TO 7
    8 F(J,K)=0.0
    7 CONTINUE
    6 CONTINUE
      TM=RH(IA)*(S(IA)**2)
      TL=RH(IA)*(C(IA)**2)-2.0*TM
      TK=TL+(2.0*TM)/3.0
      C2=C(1)**2
      S2=S(1)**2
      AAA=C2*RA
      AAB=S2*RC
      AAC=2.0*C(1)*(C(2)-C(1))
      AAD=2.0*S(1)*(S(2)-S(1))
      AAE=C2*RC
      AAF=S2*RA
      DM=(2.0*AAD+S2)*RH(1)
      DL=(2.0*AAC+C2)*RH(1)-2.0*DM
      AA(1)=2.0*(1.0-AAA-AAB)
      AB(1)=AAA+0.25*(DL+2.0*DM)*RA
      AC(1)=AAA-0.25*(DL+2.0*DM)*RA
      AD(1)=AAB
      AE(1)=DL*RB
      AF(1)=(C2-S2)*RB
      AH(1)=2.0*(1.0-AAE-AAF)
      AI(1)=AAF+0.25*DM*RA
      AJ(1)=AAF-0.25*DM*RA
      AK(1)=AAE
      AL(1)=DM*RB
      DO 17 I=2,LM1
      C2=C(I)**2
      S2=S(I)**2
      AAA=C2*RA
      AAB=S2*RC
      AAC=C(I)*(C(I+1)-C(I-1))
      AAD=S(I)*(S(I+1)-S(I-1))
      AAE=C2*RC
      AAF=S2*RA
      AAG=RH(I+1)-RH(I-1)
      DM=2.0*RH(I)*AAD+S2*AAG
      DL=2.0*RH(I)*AAC+C2*AAG-2.0*DM
      AA(I)=2.0*(1.0-AAA-AAB)
      AB(I)=AAA+0.25*(DL+2.0*DM)*RA
      AC(I)=AAA-0.25*(DL+2.0*DM)*RA
      AD(I)=AAB
      AE(I)=DL*RB
      AF(I)=(C2-S2)*RB
      AH(I)=2.0*(1.0-AAE-AAF)
```

```
      AI(I)=AAF+0.25*DM*RA
      AJ(I)=AAF-0.25*DM*RA
      AK(I)=AAF
   17 AL(I)=DM*RB
      DO 10 K=1,3
      DO 10 I=1,L
      DO 10 J=1,M
      U(I,J,K)=0.0
   10 V(I,J,K)=0.0
      LOS=10
      NN=1
      DO 20 J=1,KK
      PD(J)=0.0
      PS(J)=0.0
      PQ(J)=0.0
   20 PR(J)=0.0
      DO 21 I=1,2
      DO 21 J=1,KK
   21 WRITE(1) PD(J),PS(J),PQ(J),PR(J)
   11 DO 12 K=3,N
  606 GO TO(601,602,603,604),NN
  601 LI=3
      LJ=2
      LK=1
      GO TO 605
  602 LI=1
      LJ=3
      LK=2
      GO TO 605
  603 LI=2
      LJ=1
      LK=3
      GO TO 605
  604 NN=1
      GO TO 606
  605 DO 13 J=1,M
      IF(J.EQ.1.OR.J.EQ.M) GO TO 15
      IF(K.GT.LL) GO TO 600
      UA=2.0*DX*(F(J+1,K)-F(J-1,K))
      AG=2.0*DX*F(J,K)
      GO TO 607
  600 UA=0.0
      AG=0.0
  607 BP=0.50*B(1,J)*DT
      BM=1.-BP
      BP=1.+BP
      U(1,J,LI)=(U(1,J,LJ)*AA(1)+U(2,J,LJ)*(AB(1)+AC(1))-AG*AC(1)
     1+(U(1,J+1,LJ)+U(1,J-1,LJ))*AD(1)+(V(1,J+1,LJ)-V(1,J-1,LJ))*AE(1)
```

```
     2-U(1,J,LK)*BP)/BM
      V(1,J,LI)=(V(1,J,LJ)*AH(1)+V(2,J,LJ)*(AI(1)+AJ(1))
     1+(V(1,J+1,LJ)+V(1,J-1,LJ))*AK(1)+(U(1,J+1,LJ)-U(1,J-1,LJ))*AL(1)
     2+UA*AF(1)-V(1,J,LK)*BP)/BM
      DO 14 I=2,LCS
      BP=0.50*B(I,J)*DT
      BM=1.-BP
      BP=1.+BP
      UA=U(I+1,J+1,LJ)+U(I-1,J-1,LJ)-U(I-1,J+1,LJ)-U(I+1,J-1,LJ)
      VA=V(I+1,J+1,LJ)+V(I-1,J-1,LJ)-V(I-1,J+1,LJ)-V(I+1,J-1,LJ)
      U(I,J,LI)=(U(I,J,LJ)*AA(I)+U(I+1,J,LJ)*AB(I)+U(I-1,J,LJ)*AC(I)
     1+(U(I,J+1,LJ)+U(I,J-1,LJ))*AD(I)+(V(I,J+1,LJ)-V(I,J-1,LJ))*AE(I)
     2+VA*AF(I)-U(I,J,LK)*BP)/BM
      V(I,J,LI)=(V(I,J,LJ)*AH(I)+V(I+1,J,LJ)*AI(I)+V(I-1,J,LJ)*AJ(I)
     1+(V(I,J+1,LJ)+V(I,J-1,LJ))*AK(I)+(U(I,J+1,LJ)-U(I,J-1,LJ))*AL(I)
     2+UA*AF(I)-V(I,J,LK)*BP)/BM
  14 CONTINUE
      U(L,J,LI)=0.0
      V(L,J,LI)=0.0
      GO TO 13
  15 DO 16 I=1,L
      U(I,J,LI)=0.0
  16 V(I,J,LI)=0.0
  13 CONTINUE
      JA=JB
      DO 28 J=1,KK
      PXX=(U(IA+1,JA,LI)-U(IA-1,JA,LI))*(0.5/DX)
      PXY=(U(IA,JA+1,LI)-U(IA,JA-1,LI))*(0.5/DY)
      PYY=(V(IA,JA+1,LI)-V(IA,JA-1,LI))*(0.5/DY)
      PYX=(V(IA+1,JA,LI)-V(IA-1,JA,LI))*(0.5/DX)
      PD(J)=(PXX+PYY)*SS*TK
      PS(J)=(PYX+PXY)*SS*TM
      PQ(J)=U(ID,JA,LI)*SS
      PR(J)=V(ID,JA,LI)*SS
      WRITE(1) PD(J),PS(J),PQ(J),PR(J)
  28 JA=JA+JJ
      NN=NN+1
      IF(LOS.EQ.LM1) GO TO 12
      LCS=LOS+1
  12 CONTINUE
  25 DO 26 K=1,N
      Z=K-1
  26 T(K)=Z*DT*TS
      WRITE(6,104)KZ
      WRITE(6,102)(J,Y(J),BB(J),J=1,M)
      WRITE(6,105)KF
      WRITE(6,102)(K,T(K),FI(K),K=1,LL)
 100 FORMAT(2F10.0)
```

```
101 FORMAT(1H1,6X,'KC=',I7//)
102 FORMAT(10X,I4,2F15.5)
103 FORMAT(1H1,6X,'KB=',I7//)
104 FORMAT(1H1,6X,'KZ=',I7//)
105 FORMAT(1H1,6X,'KF=',I7//)
106 FORMAT(15I5)
107 FORMAT(5F10.0)
108 FORMAT(11A4)
110 FORMAT('0',10X,I4,2F10.3/)
120 FORMAT(1H1,6X,'KS=',I7//)
121 FORMAT('1',6X,'KR=',I7//)
200 FORMAT('1',10X,11A4,6X, A4//20X,'L:',I5/20X,'M:',I5/20X,'N:',I5/
   120X,'NC:',I4/20X,'NBA:',I3/20X,'NBB:',I3/20X,'NF:',I4/20X,'IA:',
   2I4/20X,'LL:',I4/20X,'KK:',I4/20X,'JB:',I4/20X,'JJ:',I4/20X,
   3'MA:',I4/20X,'MB:',I4/20X,'ID:',I4//)
201 FORMAT(20X,'DX:',F10.5/20X,'DY:',F10.5/20X,'DT:',F10.5/20X,
   1'SS:',F8.3/20X,'TS:',F8.3//)
    STOP
    END
```

```
C      SEISMOGRAM PLOTTING PROGRAM
CCCCC  THIS PROGRAM IS USED IN CONJUNCTION WITH THE TWO DIMENSIONAL
CCCCC  SEISMIC MODEL TO PRODUCE THE SYNTHETIC SEISMOGRAMS. THE DATA
CCCCC  IS READ FROM THE STORAGE DEVICE (TAPE, DISK OR DRUM) CONVERTED
CCCCC  TO VECTOR FORMAT AND PLOTTED ON THE CALCOMP 765 PLOTTER.
CCCCC
CCCCC  PARAMETER LIST:
CCCCCCC
CCCCCCC      PS:  SCALING FACTOR FOR THE PLOTTED VALUES.
CCCCCCC
CCCCCCC      BT:  SPACE IN INCHES BETWEEN SEPARATE SEISMOGRAMS.
CCCCCCC
CCCCCCC      TT:  TIME AXIS SCALE IN UNITS PER INCH.
CCCCCCC
CCCCCCC      YSP: SPACING IN INCHES BETWEEN INDIVIDUAL TRACES.
CCCCCCC
CCCCCCC      XSP: SPACING IN INCHES BETWEEN TIME GRID LINES.
CCCCCCC
CCCCCCC      TID,TIS,TIQ,TIR: TITLES FOR THE FOUR SEISMOGRAMS, LIMITED
CCCCCCC      TO 24 CHARACTERS. ADDITIONALLY, THE TITLE GTI FROM THE
CCCCCCC      MAIN PROGRAM IS WRITTEN ON THE TRACES.
      DATA TI/'TIME'/
      DIMENSION D(25,800),GTI(11),T(800),P(800),
     1TID(6),TIS(6),TIR(6),XG(100),YG(100),TIQ(6)
      READ(1)(GTI(I),I=1,11),GG,L,M,N,NC,NBA,NBB,NF,IA,LL,
     1KK,JB,JJ,MA,MB,ID
      READ(1)DX,DY,DT,SS,TS
      READ(5,100) PS,BT,TT,YSP,XSP
      READ(5,101)(TID(I),I=1,6)
      READ(5,101)(TIS(I),I=1,6)
      READ(5,101)(TIQ(I),I=1,6)
      READ(5,101)(TIR(I),I=1,6)
      WRITE(6,200)(GTI(I),I=1,11),GG,L,M,N,NC,NBA,NBB,NF,IA,
     1LL,KK,JB,JJ,MA,MB,ID
      WRITE(6,201) DX,DY,DT,SS,TS
      WRITE(6,202) PS,BT,TT,YSP,XSP
      DO 1 K=1,N
      DO 2 J=1,KK
    2 READ(1) D(J,K),DD,DD,DD
    1 CONTINUE
      REWIND 1
      NN=1
      DO 3 K=1,N,2
      V=K-1
      T(NN)=V*DT*TT
    3 NN=NN+1
      V=KK
```

```
      YLG=V*YSP
      V=N
      XLG=V*DT*TT
      XPP=XLG+0.40
      XPO=XPP+0.50
      TINC=1.0/TT
      CALL GRID(0.0,XLG,0.0,YLG,XSP,YSP,XG,YG,KA,LO)
      WRITE(6,220) KA
      WRITE(6,221)(I,XG(I),YG(I),I=1,KA)
      CALL PLOTS
      CALL SYMBOL(1.0,-.2,.14,'C.D.LODGE  BOX 96 QT',0.0,20)
      CALL PLOT(0.0,1.0,-3)
      CALL LINE(XG,YG,KA,1,1)
      CALL SYMBOL(XPP,0.0,0.14,TID,90.0,24)
      CALL SYMBOL(XPP,3.,.14,GTI,90.,44)
      CALL SYMBOL(XPO,0.1,0.14,GG,90.0,4)
      DO 5 J=1,KK
      NN=1
      DO 6 K=1,N,2
      P(NN)=D(J,K)*PS
      IF(ABS(P(NN)).LT.1.0) GO TO 6
      WRITE(6,225) P(NN)
      P(NN)=1.0
      WRITE(6,224) TID,K,NN,J
    6 NN=NN+1
      NN=NN-1
      CALL LINE(T,P,NN,1,1)
    5 CALL PLOT(0.0,YSP,-3)
      CALL PLOT(0.0,BT,-3)
      CALL PLOTE
      WRITE(6,603) TID
   31 READ(1)(GTI(I),I=1,11),GG,L,M,N,NC,NBA,NBB,NF,IA,LL,
     1KK,JB,JJ,MA,MB,ID
      READ(1)DX,DY,DT,SS,TS
      DO 13 K=1,N
      DO 14 J=1,KK
   14 READ(1) DD,D(J,K),DD,DD
   13 CONTINUE
      REWIND 1
      CALL PLOTS
      CALL SYMBOL(1.0,-.2,.14,'C.D.LODGE  BOX 96 QT',0.0,20)
      CALL PLOT(0.0,1.0,-3)
      CALL LINE(XG,YG,KA,1,1)
      CALL SYMBOL(XPP,0.0,0.14,TIS,90.0,24)
      CALL SYMBOL(XPP,3.,.14,GTI,90.,44)
      CALL SYMBOL(XPO,0.1,0.14,GG,90.0,4)
      DO 7 J=1,KK
      NN=1
```

```
      DO 8 K=1,N,2
      P(NN)=D(J,K)*PS
      IF(ABS(P(NN)).LT.1.0) GO TO 8
      WRITE(6,225) P(NN)
      P(NN)=1.0
      WRITE(6,224) TIS,K,NN,J
    8 NN=NN+1
      NN=NN-1
      CALL LINE(T,P,NN,1,1)
    7 CALL PLOT(0.0,YSP,-3)
      CALL PLOT(0.0,BT,-3)
      CALL PLOTE
      WRITE(6,603) TIS
      READ(1)(GTI(I),I=1,11),GG,L,M,N,NC,NBA,NBB,NF,IA,LL,
     1KK,JB,JJ,MA,MB,ID
      READ(1)DX,DY,DT,SS,TS
      DO 15 K=1,N
      DO 16 J=1,KK
   16 READ(1) DD,DD,D(J,K),DD
   15 CONTINUE
      REWIND 1
      CALL PLOTS
      CALL SYMBOL(1.0,-.2,.14,'C.D.LODGE  BOX 96 QT',0.0,20)
      CALL PLOT(0.0,1.0,-3)
      CALL LINE(XG,YG,KA,1,1)
      CALL SYMBOL(XPP,0.0,0.14,TIQ,90.0,24)
      CALL SYMBOL(XPP,3.,.14,GTI,90.,44)
      CALL SYMBOL(XPO,0.1,0.14,GG,90.0,4)
      DO 9 J=1,KK
      NN=1
      DO 10 K=1,N,2
      P(NN)=D(J,K)*0.5*PS
      IF(P(NN).LT.10.0) GO TO 10
      WRITE(6,225) P(NN)
      P(NN)=0.0
      WRITE(6,224) TIQ,K,NN,J
   10 NN=NN+1
      NN=NN-1
      CALL LINE(T,P,NN,1,1)
    9 CALL PLOT(0.0,YSP,-3)
      CALL PLOT(0.0,BT,-3)
      CALL PLOTE
      WRITE(6,603) TIQ
      READ(1)(GTI(I),I=1,11),GG,L,M,N,NC,NBA,NBB,NF,IA,LL,
     1KK,JB,JJ,MA,MB,ID
      READ(1)DX,DY,DT,SS,TS
      DO 17 K=1,N
      DO 18 J=1,KK
```

```
   18 READ(1) DD,DD,DD,D(J,K)
   17 CONTINUE
      REWIND 1
      CALL PLOTS
      CALL SYMBOL(1.0,-.2,.14,'C.D.LODGE  BOX 96 QT',0.0,20)
      CALL PLOT(0.0,1.0,-3)
      CALL LINE(XG,YG,KA,1,1)
      CALL SYMBOL(XPP,0.0,0.14,TIR,90.0,24)
      CALL SYMBOL(XPP,3.,.14,GTI,90.,44)
      CALL SYMBOL(XPO,0.1,0.14,GG,90.0,4)
      DO 11 J=1,KK
      NN=1
      DO 12 K=1,N,2
      P(NN)=D(J,K)*0.5*PS
      IF(P(NN).LT.10.0) GO TO 12
      WRITE(6,225) P(NN)
      P(NN)=0.0
      WRITE(6,224) TIR,K,NN,J
   12 NN=NN+1
      NN=NN-1
      CALL LINE(T,P,NN,1,1)
   11 CALL PLOT(0.0,YSP,-3)
      CALL PLOT(0.0,BT,-3)
      CALL PLOTE
      WRITE(6,603) TIR
  100 FORMAT(5F10.0)
  101 FORMAT(6A4)
  200 FORMAT('1',10X,11A4,6X, A4//20X,'L:',I5/20X,'M:',I5/20X,'N:',I5/
     120X,'NC:',I4/20X,'NBA:',I3/20X,'NBB:',I3/20X,'NF:',I4/20X,'IA:',
     2I4/20X,'LL:',I4/20X,'KK:',I4/20X,'JB:',I4/20X,'JJ:',I4/20X,
     3'MA:',I4/20X,'MB:',I4/20X,'ID:',I4//)
  201 FORMAT(20X,'DX:',F10.5/20X,'DY:',F10.5/20X,'DT:',F10.5/20X,
     1'SS:',F8.3/20X,'TS:',F8.3)
  202 FORMAT(20X,'PS:',F8.3/20X,'BT:',F8.3/20X,'TT:',F8.3/20X,
     1'YSP:',F7.3/20X,'XSP:',F7.3/)
  220 FORMAT('0',6X,'KA=',I4//)
  221 FORMAT(I6,2F12.5)
  224 FORMAT(10X,6A4,3I7)
  225 FORMAT(3X,F20.3)
  600 FORMAT(1X,'D',I4,2X,12F10.5)
  601 FORMAT(1X,'S',I4,2X,12F10.5)
  602 FORMAT(1X,'R',I4,2X,12F10.5)
  603 FORMAT('0'//6X,6A4,'GRAM COMPLETE'/)
      STOP
      END
```

```
C     SUBROUTINE POLYG(N,DX,F,G,NS,XI,P,L)
CCCCC
CCCCC PURPOSE
CCCCC     TO EVALUATE A FUNCTION APPROXIMATED BY A POLYGON OF 20 OR
CCCCC     LESS STRAIGHT LINE SEGMENTS
CCCCC
CCCCC     THE ORDINATES ARE GENERATED BY ADDING MULTIPLES OF AN
CCCCC     INCREMENT DX TO A BASE VALUE XI.
CCCCC
CCCCC     THE OUTPUT ARRAY OF ABCISSAE IS GENERATED BY REPEATED
CCCCC     SOLUTION OF :  P = AX + B.
CCCCC
CCCCC DESCRIPTION OF PARAMETERS:
CCCCC
CCCCC    N:    NUMBER OF POINTS AT WHICH P IS TO BE DETERMINED.  N.LE.900.
CCCCC
CCCCC    DX:   SIZE OF X INCREMENT.
CCCCC
CCCCC    F:    ARRAY OF X-COORDINATES OF THE POINTS THROUGH WHICH THE
CCCCC          APPROXIMATING POLYGON PASSES.
CCCCC
CCCCC    G:    ARRAY OF Y-COORDINATES OF THE POINTS THROUGH WHICH THE
CCCCC          APPROXIMATING POLYGON PASSES.
CCCCC
CCCCC    NS:   NUMBER OF POLYGONAL POINTS.  NS.LE.20.
CCCCC
CCCCC    XI:   INITIAL X-COORDINATE.  XI.GE.F(1).
CCCCC
CCCCC    P:    OUTPUT ARRAY OF Y-COORDINATES ON THE POLYGON CORRESPONDING
CCCCC          TO X-COORDINATES OF I*DX;  WHERE   I = 1,N
CCCCC
CCCCC    L:    OUTPUT PARAMETER INDICATING SUCCESS OF COMPLETION OF THE
CCCCC          SUBROUTINE
CCCCC            L=0  SUBROUTINE SUCCESSFULLY COMPLETED.
CCCCC            L=1  SUBROUTINE TERMINATED PRIOR TO COMPLETION.
CCCCC


      SUBROUTINE POLYG(N,DX,F,G,NS,XI,P,L)
      DIMENSION A(20),B(20),F(20),G(20),X(900),P(900),C(20),D(20)
      L=0
      NSM = NS-1
      EPS=0.001
      IF(XI.LT.F(1)) GO TO 2
      IF (N.GT.900) GO TO 2
      II=0
      DO 1 I=1,NSM
```

```
      GG=F(I+1)-F(I)
      IF(ABS(GG).LT.EPS) GO TO 1
      II=II+1
      C(II)=F(I)
      D(II)=G(I)
    1 CONTINUE
      C(II+1)=F(NS)
      D(II+1)=G(NS)
      DO 5 I=1,II
      GG=C(I+1)-C(I)
      GM=D(I+1)-D(I)
      A(I)=GM/GG
    5 B(I)=(C(I+1)*D(I)-C(I)*D(I+1))/GG
      DO 11 I=1,N
      Z = I-1
      X(I)=XI+Z*DX
   11 CONTINUE
      K = 1
      DO 3 I=1,II
    4 IF(X(K).GT.C(I+1)) GO TO 3
      P(K)=A(I)*X(K)+B(I)
      K= K + 1
      IF(K.GT.N) GO TO 6
      GO TO 4
    3 CONTINUE
    6 RETURN
    2 L = 1
      RETURN
      END
```

```
      SUBROUTINE GRID(XMIN,XMAX,YMIN,YMAX,GX,GY,X,Y,KA,L)
C
C      THIS SUBROUTINE GENERATES A SEQUENCE OF POINTS (X,Y)
C     WHICH MAY BE USED TO PLOT A GRID ON A CALCOMP PLOTTER
C     GRAPH
C
C     DESCRIPTION OF PARAMETERS:
C
C        INPUT PARAMETERS:
C
C          XMIN:  MINIMUM VALUE OF THE X COORDINATE TO BE
C                 GRIDDED.  IN INCHES.
C
C          XMAX:  MAXIMUM VALUE OF THE X COORDINATE TO BE
C                 GRIDDED.  IN INCHES.
C
C          YMIN:  MINIMUM VALUE OF THE Y COORDINATE TO BE
C                 GRIDDED.  IN INCHES.
C
C          YMAX:  MAXIMUM VALUE OF THE Y COORDINATE TO BE
C                 GRIDDED.  IN INCHES.
C
C          GX:    HORIZONTAL (X) GRID SPACING.  IN INCHES.
C
C          GY:    VERTICAL (Y) GRID SPACING.  IN INCHES.
C
C        OUTPUT PARAMETERS:
C
C          X:     VECTOR OF ORDINATES.  DIMENSIONED .LE.500.
C
C          Y:     VECTOR OF ABCISSAE.  DIMENSIONED .LE.500.
C
C          KA:    NUMBER OF GRID POINTS (X,Y PAIRS) GENERATED.
C                 KA.LE.500.
C
C          L:     PARAMETER INDICATING SUCCESS OF SUBROUTINE:
C
C                   L=0  SUBROUTINE SUCCESSFULLY COMPLETED.
C                   L=1  SUBROUTINE NOT FULLY COMPLETED.
C                   L=2  KA OUT OF RANGE.
C
C     NOTE:  A 6 BY 10 INCH GRID OF ONE INCH SQUARES REQUIRES
C            36 POINTS.
C            AN 8 BY 60 INCH GRID OF HALF INCH SQUARES REQUIRES
C            280 POINTS.
C
```

```
      SUBROUTINE GRID(XMIN,XMAX,YMIN,YMAX,GX,GY,X,Y,KA,L)
      DIMENSION X(500),Y(500)
      L=1
      A = 0.0
      I = 1
    1 X(I) = XMIN
      Y(I) = YMIN + A*GY
      X(I+1) = XMAX
      Y(I+1) = YMIN + A*GY
      KA = I + 2
      IF(KA.GT.500) GO TO 5
      IF(Y(I+1).GE.YMAX) GO TO 2
      X(I+2) = XMAX
      Y(I+2) = YMIN + (A+1.0)*GY
      X(I+3) = XMIN
      Y(I+3) = YMIN + (A+1.0)*GY
      KA = I + 4
      IF(KA.GT.500) GO TO 5
      IF(Y(I+3).GE.YMAX) GO TO 2
      I = I + 4
      A = A + 2.0
      GO TO 1
    2 A = 0.0
      I = KA
    3 X(I) = XMIN + A*GX
      Y(I) = YMAX
      X(I+1) = XMIN + A*GX
      Y(I+1) = YMIN
      KA = I + 1
      IF(KA.GT.500) GO TO 5
      IF(X(I+1).GE.XMAX) GO TO 4
      X(I+2) = XMIN + (A+1.0)*GX
      Y(I+2) = YMIN
      X(I+3) = XMIN + (A+1.0)*GX
      Y(I+3) = YMAX
      KA = I + 3
      IF(KA.GT.500) GO TO 5
      IF(X(I+3).GE.XMAX) GO TO 4
      I = I + 4
      A = A + 2.0
      GO TO 3
    4 L=0
      RETURN
    5 L=2
      RETURN
      END
```

```
C      SUBROUTINE CONPLT(L,M,K,NH,DX,DY,GS)
CCCCCC
CCCCCC THIS SUBROUTINE IS USED IN COMMON WITH THE TWO DIMENSIONAL
CCCCCC SEISMIC MODEL TO GENERATE A PRINTER CONTOUR PLOT OF A SELECTED
CCCCCC VARIABLE OVER THE ENTRIRE MESH. THE CALLING PROGRAM MUST PROVIDE
CCCCCC PRINTER PAGINATION AND TITLE IF DESIRED. THE SUBROUTINE ACCEPTS
CCCCCC HORIZONTAL AND VERTICAL DISPLACEMENT VALUES AND COMPUTES VALUES
CCCCCC AS REQUIRED. WHEN STRESSES OR VORTICITY ARE DESIRED, THE SUBROUTINE
CCCCCC REDUCES THE MATRIX BY ONE ROW AND COLUMN AND PRINTS 0'S ALONG THE
CCCCCC TOP AND LEFT BORDERS OF THE MATRIX.
CCCCCC
CCCCCC PARAMETER LIST:
CCCCCC
CCCCCC K:       MATRIX LEVEL TO BE CONTOURED (K=1,2 OR 3).
CCCCCC
CCCCCC SYM:     VECTOR OF 42 ALPHA-NUMERIC CHARACTERS TO BE USED TO
CCCCCC          REPRESENT THE VALUES CONTOURED.
CCCCCC
CCCCCC GS:      SCALING FACTOR TO BE APPLIED TO THE CONTOURED QUANTITY.
CCCCCC
CCCCCC NH:      INPUT PARAMETER SPECIFYING THE OUTPUT VARIABLE
CCCCCC            ZZ WHICH IS PLOTTED BY THE SUBROUTINE.
CCCCCC
CCCCCC               NH=1:  VERTICAL DISPLACEMENT.
CCCCCC               NH=2:  HORIZONTAL DISPLACEMENT.
CCCCCC               NH=3:  DILATATION.
CCCCCC               NH=4:  SHEAR.
CCCCCC               NH=5:  ROTATION.
CCCCCC
CCCCCC ALL OTHER PARAMETERS ARE DISCUSSED IN THE CALLING PROGRAM.
C


      SUBROUTINE CONPLT(L,M,K,NH,DX,DY,GS)
C
      COMMON U,V,SYM,ZZ,C,S,RH
      DIMENSION U(71,81,3),V(71,81,3),SYM(42),ZZ(81),RH(71),
     1C(71),S(71)
      DO 500 I=1,L
      TM=RH(I)*(S(I)**2)
      TL=RH(I)*(C(I)**2)-2.0*TM
      TK=TL+(2.0*TM)/3.0
      DO 501 J=1,M
      GO TO (505,511,506,507,512),NH
  505 KO=(U(I,J,K)*GS+2.05)*10.0+1.0
  509 IF(KO.LT.1) GO TO 502
      IF(KO.GT.41) GO TO 503
      GO TO 504
```

```
506 IF(I.EQ.1.OR.J.EQ.1) GO TO 510
    D=((U(I,J,K)-U(I-1,J,K))/DX+(V(I,J,K)-V(I,J-1,K))/DY)*TK
    KC=(D*GS+2.05)*10.0+1.0
    GO TO 509
510 KC=21
    GO TO 504
511 KC=(V(I,J,K)*GS+2.05)*10.0+1.0
    GO TO 509
507 IF(I.EQ.1.OR.J.EQ.1) GO TO 508
    D=((V(I,J,K)-V(I-1,J,K))/DX+(U(I,J,K)-U(I,J-1,K))/DY)*TM
    KC=(D*GS+2.05)*10.0+1.0
    GO TO 509
508 KC=21
    GO TO 504
512 IF(I.EQ.1.OR.J.EQ.1) GO TO 513
    D=((V(I,J,K)-V(I-1,J,K))/DX-(U(I,J,K)-U(I,J-1,K))/DY)*TM
    KC=(D*GS+2.05)*10.0+1.0
    GO TO 509
513 KC=21
    GO TO 504
502 ZZ(J)=SYM(42)
    GO TO 501
503 ZZ(J)=SYM(41)
    GO TO 501
504 ZZ(J)=SYM(KC)
501 CONTINUE
    WRITE(6,402)(I,(ZZ(J),J=1,M))
500 CONTINUE
    WRITE(6,410)
    WRITE(6,411)
402 FORMAT(10X,I2,2X,81A1)
410 FORMAT(' ',12X,'0',9X,'1',9X,'2',9X,'3',9X,'4',9X,'5',9X,
   1'6',9X,'7',9X,'8')
411 FORMAT(13X,'0',8(9X,'0'))
    RETURN
    END
```

LIST OF REFERENCES

Alterman, Z.S. and Karal, F.C., 1968, Propagation of Elastic Waves in Layered Media by Finite Difference Methods, Bulletin of the Seismological Society of America, v. 58, n. 1, pp. 367-398.

Alterman, Z.S. and Rotenberg, A., 1969, Seismic Waves in a Quarter Plane, Bulletin of the Seismological Society of America, v. 59, n. 1, pp. 347-368.

Bullen, K.E., 1959, An Introduction to the Theory of Seismology, Cambridge University Press.

Constantino, C.J., 1969, Two Dimensional Wave Propagation through Nonlinear Media, Journal of Computational Physics, v. 4, n. 3, pp. 147-170.

Dobrin, M.B., 1960, Introduction to Geophysical Prospecting, McGraw-Hill.

Forsythe, G.E. and Wasow, W.R., 1967, Finite Difference Methods for Partial Differential Equations, John Wiley.

Fox, L., and others, 1962, Numerical Solution of Ordinary and Partial Differential Equations, Pergamon Press.

Grant, F.S. and West, G.F., 1965, Interpretation Theory in Applied Geophysics, McGraw-Hill.

Gupta, R.N., 1966a, Reflection of Elastic Waves from a Linear Transition Layer, Bulletion of the Seismological Society of America, v. 56, n. 2, pp. 511-526.

_____, 1966b, Reflection of Plane Elastic Waves from Transition Layers with Arbitrary Variation of Velocity and Density, Bulletin of the Seismological Society of America, v. 56, n. 3, pp. 633-642.

Officer, C.B., 1958, Introduction to the Theory of Sound Transmission, McGraw-Hill.

Sengbush, R..L., Lawrence, P.L. and McDonal, F.J., 1961, Interpretation of Synthetic Seismograms, Geophysics, v. 26, n. 2, pp. 138-157.

Smith, G.D., 1965, Numerical Solution of Partial Differential Equations, Oxford University Press.

Takeuchi, H., 1966, Theory of the Earth's Interior, Blaisdell.

Tooley, R.D., Spencer, T.W. and Sagoci, H.F., 1965, Reflection and Transmission of Plane Compressional Waves, Geophysics, v. 30, n. 4, pp. 552-570.

United States Naval Postgraduate School Computer Facility, 1969, Technical Note 0211-03, Plotting Package for NPGS IBM 360/67, by P. C. Johnson.

Wolf, A., 1937, The Reflection of Elastic Waves from Transition Layers of Variable Velocity, Geophysics, v. 2, n. 4, pp. 357-363.

INITIAL DISTRIBUTION LIST

		No. Copies
1.	Defense Documentation Center Cameron Station Alexandria, Virginia 22314	20
2.	Library, Code 0212 Naval Postgraduate School Monterey, California 93940	2
3.	Professor R. S. Andrews Department of Oceanography Naval Postgraduate School Monterey, California 93940	5
4.	Department of Oceanography Naval Postgraduate School Monterey, California 93940	3
5.	Oceanographer of the Navy The Madison Building 732 N. Washington Street Alexandria, Virginia 22314	1
6.	LCDR C. D. Lodge P.O. Box 274 Pebble Beach, California 93953	2
7.	Professor J. J. von Schwind Department of Oceanography Naval Postgraduate School Monterey, California 93940	1

DOCUMENT CONTROL DATA - R & D

Security classification of title, body of abstract and indexing annotation must be entered when the overall report is classified)

ORIGINATING ACTIVITY (Corporate author)	2a. REPORT SECURITY CLASSIFICATION
Naval Postgraduate School Monterey, California 93940	Unclassified
	2b. GROUP

REPORT TITLE

Simplified Numerical Models for the Generation of Synthetic Reflection Profiling Seismograms and Synthetic Reflection/Refraction Seismograms

DESCRIPTIVE NOTES *(Type of report and inclusive dates)*

Master's Thesis; (April 1970)

AUTHOR(S) *(First name, middle initial, last name)*

Charles David Lodge

REPORT DATE	7a. TOTAL NO. OF PAGES	7b. NO. OF REFS
April 1970	128	17

a. CONTRACT OR GRANT NO.	9a. ORIGINATOR'S REPORT NUMBER(S)
b. PROJECT NO	
c.	9b. OTHER REPORT NO(S) *(Any other numbers that may be assigned this report)*
d.	

0 DISTRIBUTION STATEMENT

This document has been approved for public release and sale; its distribution is unlimited.

1 SUPPLEMENTARY NOTES	12. SPONSORING MILITARY ACTIVITY
	Naval Postgraduate School Monterey, California 93940

3. ABSTRACT

Two numerical models were developed which generate synthetic seismograms in formats similar to those of records obtained in field exploration. The models solve the hyperbolic wave equations in one and two dimensions by finite difference approximations in initially undeformed solution domains of transversely-isotropic layered media subjected to a time varying, dilatational forcing stress applied at the surface. A velocity attenuation term was included in the models to inhibit strong boundary reflections.

The one-dimensional model produces synthetic reflection profiling seismograms for arbitrary horizontal or dipping layers. The two-dimensional model generates synthetic reflection/refraction seismograms for horizontal layered media with arbitrary distribution of wave velocities, Poisson's ratio and density. Several sample records were produced for some representative velocity structures. The synthetic seismograms were interpreted and gross correlation was carried out as if they were actual field records.

D FORM 1 NOV 65 1473 (PAGE 1)

N 0101-807-6811

14 KEY WORDS	LINK A		LINK B		LINK C	
	ROLE	WT	ROLE	WT	ROLE	WT
Numerical						
Seismic						
Model						

Thesis
L7912
c.1

117688

Lodge
Simplified numerical models for the generation of synthetic reflection profiling seismograms and synthetic reflection/ refraction seismograms.